Charge symmetry at the partonic level

J. T. Londergan*

Department of Physics and Nuclear Theory Center, Indiana University, Bloomington, Indiana 47404, USA

J. C. Peng

Department of Physics, University of Illinois at Urbana–Champaign, Urbana, Illinois 61801, USA

A. W. Thomas

Thomas Jefferson National Laboratory, 12000 Jefferson Avenue, Newport News, Virginia 23606, USA
and CSSM, School of Chemistry and Physics, University of Adelaide, Adelaide, South Australia 5005, Australia

(Published 12 July 2010)

This review article discusses the experimental and theoretical status of partonic charge symmetry. It is shown how the partonic content of various structure functions gets redefined when the assumption of charge symmetry is relaxed. Various theoretical and phenomenological models for charge-symmetry violation in parton distribution functions are reviewed. After summarizing the current experimental upper limits on charge-symmetry violation in parton distributions, a series of new experiments are proposed, which might reveal partonic charge-symmetry violation or alternatively might lower the current upper limits on parton charge-symmetry violation.

DOI: 10.1103/RevModPhys.82.2009 PACS number(s): 11.30.Hv, 13.40.Ks, 13.85.Qk

CONTENTS

I. Charge Symmetry and Parton Distributions 2009
II. Relations Between High-Energy Cross Sections and Parton Distributions 2011
A. General form of high-energy cross sections 2011
B. Charge symmetry and parton distribution functions 2013
C. Structure functions in terms of parton distribution functions 2014
D. Relations between structure functions 2015
III. Charge Symmetry in Valence Quark Distributions 2016
A. Phenomenological estimates of valence quark CSV 2016
B. Theoretical estimates of valence quark CSV 2017
1. QED splitting: Another source of parton CSV 2021
C. Experimental limits on valence quark charge symmetry 2023
1. The charge ratio: Comparison of F_2 structure functions in reactions of muons and neutrinos 2023
2. Charge symmetry and determination of the weak mixing angle 2026
D. Isospin-dependent nuclear effects 2030
E. Dedicated experiments sensitive to valence quark charge symmetry 2031
1. Drell-Yan processes initiated by charged pions 2031
2. Parity-violating asymmetry in electron scattering 2033
3. Charged pion leptoproduction from isoscalar targets 2035
4. Test of weak current relation $F_2^{W^+N_0}(x) = F_2^{W^-N_0}(x)$ 2037
IV. Charge-Symmetry Violation for Sea Quarks 2038
A. Estimates of sea quark CSV 2038
B. Limits on sea quark CSV 2039
1. W production asymmetry at a hadron collider 2040
2. Limits on charge-symmetry violation for gluon distributions 2040
C. Charge-symmetry contributions to DIS sum rules 2041
1. Gottfried sum rule: Sea quark flavor and charge symmetry 2042
2. Adler sum rule 2044
3. Gross–Llewellyn Smith sum rule 2045
4. A charge-symmetry sum rule 2047
V. Summary and Outlook 2048
Acknowledgments 2050
References 2050

I. CHARGE SYMMETRY AND PARTON DISTRIBUTIONS

The notion of isotopic spin was introduced to account for the strong similarity between the proton and neutron. In this picture the proton and neutron are defined as two components of a single object, the *nucleon*. If the strong interaction H_s does not distinguish between the proton and neutron, then H_s will commute with the isospin vector $\mathbf{T}$ such that

*tlonderg@indiana.edu

 ©2010 The American Physical Society

$$[H_s, \mathbf{T}] = 0. \tag{1}$$

A strong interaction satisfying Eq. (1) is said to satisfy charge independence. *Charge symmetry* is a specific operation involving the isospin vector. It is defined as a rotation of 180° about the 2 axis in isospin space. Thus the charge-symmetry operator P_{CS} is defined as

$$P_{CS} = e^{i\pi T_2}. \tag{2}$$

Charge symmetry involves interchanging a proton and neutron. When operating on light quarks, the charge-symmetry operator interchanges up and down quarks, namely,

$$P_{CS}|u\rangle = -|d\rangle, \quad P_{CS}|d\rangle = |u\rangle. \tag{3}$$

In nucleon isospin space, the operation of charge symmetry thus interchanges up and down quarks (also up and down antiquarks), while interchanging proton and neutron labels.

As is well understood, inclusive processes at high energies can be described in terms of a small number of structure functions, and these structure functions can be characterized in terms of parton distribution functions (PDFs) that describe the probability of finding a given flavor quark or antiquark with a fraction x of the nucleon's momentum. Over the last 30 years, increasingly precise measurements have been made of the PDFs and their dependence on x and Q^2. If we assume that charge symmetry is obeyed at the level of parton distributions, this implies

$$\begin{aligned} u^p(x,Q^2) &= d^n(x,Q^2), \\ d^p(x,Q^2) &= u^n(x,Q^2), \\ s^p(x,Q^2) &= s^n(x,Q^2) \equiv s(x,Q^2), \\ c^p(x,Q^2) &= c^n(x,Q^2) \equiv c(x,Q^2). \end{aligned} \tag{4}$$

In Eq. (4), the superscript describes the target nucleon, and the quantities u, d, s, and c represent the flavor of the struck quark. Relations analogous to Eq. (4) are obtained by replacing all quark distributions by antiquarks.

Until recently, all quark-parton phenomenological models assumed the validity of charge symmetry at the outset. This was a sensible assumption for several reasons. First, charge symmetry is obeyed to a high precision at low energies; whereas in many nuclear reactions isospin symmetry is obeyed only to the level of a few percent, in most cases charge symmetry is valid to better than 1% (Henley and Miller, 1979; Miller *et al.*, 1990). Recent precise measurements of charge-symmetry violation (CSV) in single-pion production in few-body systems (Opper *et al.*, 2003; Stephenson *et al.*, 2003) have led to better understanding of charge symmetry at low energies (Frankfurt *et al.*, 1989; Henley and Miller, 1990; Niskanen, 1999; van Kolck *et al.*, 2000; Miller *et al.*, 2006). The high precision of charge symmetry at low energies makes it natural to assume that charge symmetry is valid at high energies; indeed, it is difficult to imagine a scenario with large charge-symmetry violation at the partonic level, which would lead to very small CSV at low energies. Second, the assumption of charge symmetry reduces by a factor of 2 the number of independent quark PDFs that must be determined. Third, early measurements of high-energy structure functions showed that the requirements of charge symmetry were at least qualitatively obeyed (Macfarlane *et al.*, 1984; Meyers *et al.*, 1986; Benvenuti *et al.*, 1987, 1990; Whitlow *et al.*, 1990, 1992).

In 1998 the current situation regarding parton charge symmetry was reviewed (Londergan and Thomas, 1998). Since then there have been several developments that warrant an updated review. At that time, comparison of the F_2 structure functions from charged lepton deep inelastic scattering (DIS) and neutrino charge-changing DIS (Seligman, 1997; Seligman *et al.*, 1997) suggested substantial CSV contributions in the nucleon sea (Boros *et al.*, 1998a; Boros, Londergan, and Thomas, 1999). However, reanalysis of the neutrino reactions (Boros, Steffens, *et al.*, 1999; Yang *et al.*, 2001) removed the discrepancies that appeared at that time to indicate the possibility of surprisingly large CSV effects (Boros *et al.*, 1998a).

In the last few years CSV terms have for the first time been included in global fits to high-energy data (Martin *et al.*, 2004). Although these global fits contain some model dependence, nonetheless such fits allow one to set phenomenological limits on CSV contributions to PDFs. In addition, another mechanism for isospin violation in PDFs (quantum electromagnetic or "QED splitting" effects) has now been included in calculations of PDFs (Glück *et al.*, 2005; Martin *et al.*, 2005) through modification of what is termed the Dokshitzer-Gribov-Lipatov-Altarelli-Parisi (DGLAP) evolution (Gribov and Lipatov, 1972; Altarelli and Parisi, 1977; Dokshitzer, 1977). Inclusion of these QED splitting terms also leads to CSV effects in parton distribution functions.

The phenomenological limits for PDFs obtained from global fits to high-energy data provide effective upper limits for the magnitude of CSV effects. As we shall see, these limits are somewhat larger than those obtained from theoretical estimates of partonic CSV contributions. Using these phenomenological estimates provides limits to the size of CSV effects that might reasonably be observed in certain experiments. We use the phenomenological limits obtained from global fits to estimate the maximum value of CSV effects that might be seen in dedicated experiments. This will provide at least qualitative estimates of the size of effects that could be observed in various experiments. It will also provide guidance as to the most promising experiments that could tighten the existing upper limits on parton CSV.

Since the publication of the previous review on parton CSV (Londergan and Thomas, 1998), the NuTeV group has measured total cross sections for ν and $\bar{\nu}$ charged-current and neutral-current reactions on an iron target (Zeller *et al.*, 2002a, 2002b). These measurements allow them to extract an independent measurement of the weak mixing angle. Their measurement differs by 3σ

from the extremely precise values for the weak mixing angle measured at the Z^0 mass (Abbaneo *et al.*, 2001). The publication of the NuTeV measurement has led to investigation of effects that might explain this result. We review various "QCD corrections" to the NuTeV result (i.e., corrections within the standard model) and in particular we summarize the potential corrections to the NuTeV measurement from parton CSV.

Our review is organized as follows. In Sec. II.A we review the general form of high-energy cross sections in terms of structure functions. In Sec. II.B we define parton distributions when charge-symmetry violation is included. In Sec. II.C we review the definitions of structure functions in terms of quark-parton distributions. We list the general form of structure functions when one relaxes the assumption of charge symmetry. In Sec. II.D we give relations between leading-order structure functions and show how the possible presence of parton CSV affects those relations.

Section III reviews both the experimental and theoretical situations regarding CSV in valence quark PDFs. In Sec. III.A we summarize recent global fits of PDFs that allow for charge-symmetry violation. Section III.B reviews various theoretical estimates of CSV in valence quark distributions. We argue that one can make reasonably model-independent estimates of the magnitude and sign of valence parton CSV. In Sec. III.B.1 we summarize the phenomenon of QED splitting, a new source of partonic CSV that results from inclusion of terms where a quark radiates a photon; this is the electromagnetic analog of the familiar terms where quarks radiate gluons.

In Sec. III.C we summarize the experimental limits on valence parton CSV. The most rigorous upper limits on partonic CSV come from the "charge ratio," which compares the F_2 structure functions measured in charge-changing reactions induced by neutrinos and antineutrinos, with the F_2 structure function from charged lepton DIS, in principle both measured on isoscalar targets. This is reviewed in Sec. III.C.1. In Sec. III.C.2 we review the NuTeV measurements of ν and $\bar{\nu}$ reactions on iron targets and the resulting extraction of the weak mixing angle. We particularly examine potential contributions to this result from partonic CSV.

A new nuclear effect has been proposed that will mimic the effects of partonic charge-symmetry violation. This nuclear isospin-dependent effect is defined in Sec. III.D. We show that these nuclear isospin-dependent effects could make significant contributions to the analyses of the NuTeV experiment. We also discuss how this effect could be observed by measuring the nuclear dependence of the European Muon Collaboration (EMC) effect.

Existing and proposed new experimental facilities offer several opportunities for dedicated precision experiments that could significantly improve our chances of observing partonic CSV effects or alternatively of lowering the current upper limits on such effects. In Sec. III.E we summarize four such experiments. We show the size of the effects that are compatible with the current limits on partonic CSV, and we discuss those experimental facilities that would be best suited to such measurements.

In Sec. IV we review the situation regarding sea quark CSV. In contrast to valence quark CSV, where there are reliable and rather model-independent estimates of the magnitude and sign of such effects, it is substantially more difficult either to make theoretical predictions of sea quark CSV or to conceive of experiments to measure such effects. In Sec. IV.A we review theoretical and phenomenological estimates of sea quark CSV. Perhaps surprisingly, the phenomenological fit by Martin, Roberts, Stirling, and Thorne (MRST) (Martin *et al.*, 2004) found evidence for a rather large sea quark CSV effect. One potentially promising way to test sea quark CSV effects involves partonic sum rules. The most popular QCD sum rules involve the first moment of some combination of structure functions. For the purposes of this review, we define the nth moment of a parton distribution $q(x)$ as

$$\int_0^1 x^{n-1} q(x) dx. \tag{5}$$

The first moment of valence quark CSV effects is necessarily zero in order to preserve valence quark normalization. Thus the only CSV effects to survive in this integration are from sea quark CSV. In Sec. IV.C we review the contributions of partonic CSV to the Gottfried, Adler, and Gross–Llewellyn Smith sum rules. In Sec. IV.C.4 we review a new sum rule proposed by Ma (1992). Such a sum rule would be uniquely sensitive to sea quark CSV effects. In Sec. V we provide a summary and outlook.

II. RELATIONS BETWEEN HIGH-ENERGY CROSS SECTIONS AND PARTON DISTRIBUTIONS

A. General form of high-energy cross sections

We can write the cross sections for deep inelastic scattering in terms of a set of structure functions, which depend on the relativistic kinematics of the reaction. Through the quark-parton model, these structure functions can in turn be written in terms of quark-parton distributions (Leader and Predazzi, 1996). For simplicity, we write the cross sections in leading order (LO) in QCD. By now, all phenomenological analyses of high-energy reactions and structure functions work in next to leading order (NLO) or higher (Pumplin *et al.*, 2002; Martin *et al.*, 2007). At sufficiently high energies, quark mass effects are small and can be accounted for with quite good precision. Current issues in partonic analyses involve data, particularly in neutrino experiments, in the region where the charm quark mass cannot be neglected. One way to deal with these issues is to work in a variable flavor number scheme (VFNS), where one increases the number of active quark flavors at various matching points (Aivazis, Olness, and Tung, 1994). Recently the Coordinated Theoretical-Experimental

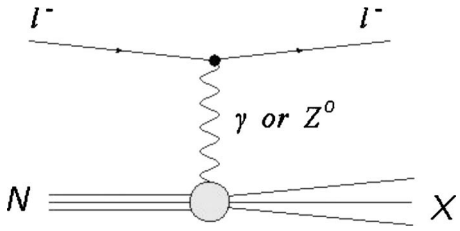

FIG. 1. Schematic of deep inelastic scattering of charged leptons from a nucleon. Neutral-current electroweak interactions involve exchange of a photon or Z^0.

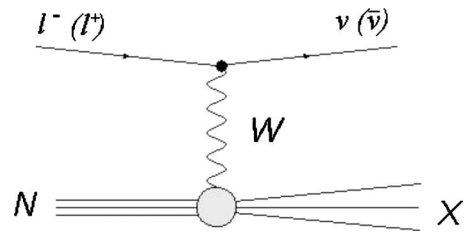

FIG. 2. Schematic of deep inelastic scattering involving the charged-current weak interaction initiated by charged leptons. An intermediate W is exchanged between the leptons and the nucleon.

Project in QCD (CTEQ) group has examined the effects of quark masses in global fit analyses, particularly in extracting the strong coupling constant α_S from such global fits (Tung *et al.*, 2007). The MRST group has produced a new set of parton distributions at next to next to leading order (NNLO) (Martin *et al.*, 2007). In their VFNS scheme they introduce discontinuities into their coefficient functions that counter the discontinuities that arise in their parton distributions at the matching points.

The cross section for scattering of a left- (L) or right- (R) handed charged lepton in neutral current (NC) deep inelastic-scattering reactions has the form

$$\begin{aligned}\frac{d^2\sigma_{\rm NC}^{L,R}}{dx\,dy} = \frac{4\pi\alpha^2 s}{Q^4}\Bigg(&[xy^2F_1^\gamma(x,Q^2)+f_1(x,y)F_2^\gamma(x,Q^2)]\\ &-\frac{Q^2}{(Q^2+M_Z^2)}\frac{v_\ell \pm a_\ell}{2\sin\theta_W\cos\theta_W}\\ &\times[xy^2F_1^{\gamma Z}(x,Q^2)+f_1(x,y)F_2^{\gamma Z}(x,Q^2)\\ &\pm f_2(y)xF_3^{\gamma Z}(x,Q^2)]+\left(\frac{Q^2}{Q^2+M_Z^2}\right)^2\\ &\times\frac{v_\ell \pm a_\ell}{2\sin\theta_W\cos\theta_W}[xy^2F_1^Z(x,Q^2)\\ &+f_1(x,y)F_2^Z(x,Q^2)\pm f_2(y)xF_3^Z(x,Q^2)]\Bigg).\end{aligned} \tag{6}$$

In Eq. (6), the + sign is associated with the left-handed (L) charged lepton and the − with the right-handed (R) lepton.

This process is shown schematically in Fig. 1. In Eq. (6) α is the electromagnetic coupling, M_Z is the mass of the Z^0 boson, and θ_W is the weak mixing angle. We define the quantities

$$\begin{aligned} f_1(x,y) &\equiv 1-y-\frac{xyM^2}{s},\\ f_2(y) &\equiv y-\frac{y^2}{2}.\end{aligned} \tag{7}$$

In Eq. (7), M is the nucleon mass. These equations are usually evaluated at very high energies where $xyM^2 \ll s$, so we generally neglect this term; in this case for the remainder of this paper we assume $f_1(x,y)\approx f_1(y)=1-y$.

Either a photon or Z boson can be exchanged in this process. The relativistic invariants in Eq. (6) are $Q^2=-q^2$, the square of the four momentum transfer for the reaction, and x and y. For four momentum k (p) for the initial-state lepton (nucleon), we have

$$x=\frac{Q^2}{2p\cdot q},\quad y=\frac{p\cdot q}{p\cdot k},\quad s=(k+p)^2. \tag{8}$$

Explicit expressions for the various structure functions F_i^X in terms of parton distribution functions are given in Sec. II.C.

In Eq. (6), we have

$$\begin{aligned} v_\ell &= \frac{-1+4\sin^2\theta_W}{4\sin\theta_W\cos\theta_W},\\ a_\ell &= \frac{-1}{4\sin\theta_W\cos\theta_W}.\end{aligned} \tag{9}$$

The most general form of the cross section for charged-current (CC) interactions initiated by charged leptons on nucleons can be written as

$$\begin{aligned}\frac{d^2\sigma_{\rm CC}^{l^+(l^-)}}{dx\,dy} = \frac{\pi s}{2}\left(\frac{\alpha}{2\sin^2\theta_W(M_W^2+Q^2)}\right)^2&[xy^2F_1^{W^\pm}(x,Q^2)\\ &+f_1(y)F_2^{W^\pm}(x,Q^2)\mp f_2(y)xF_3^{W^\pm}(x,Q^2)].\end{aligned} \tag{10}$$

This process is shown schematically in Fig. 2. It involves a charged virtual $W^\pm$ of momentum q being interchanged between the lepton-neutrino vertex and the hadronic vertex. In Eq. (10), M_W is the mass of the charged weak vector boson.

Similarly, the cross section for charged-current interactions initiated by neutrinos or antineutrinos on nucleons has the form

$$\begin{aligned}\frac{d^2\sigma_{\rm CC}^{\nu(\bar\nu)}}{dx\,dy} = \pi s\left(\frac{\alpha}{2\sin^2\theta_W(M_W^2+Q^2)}\right)^2&[xy^2F_1^{W^\pm}(x,Q^2)\\ &+f_1(y)F_2^{W^\pm}(x,Q^2)\pm f_2(y)xF_3^{W^\pm}(x,Q^2)].\end{aligned} \tag{11}$$

This process is obtained by interchanging the initial- and final-state leptons in Fig. 2.

Finally, NC reactions initiated by neutrinos or antineutrinos have the form

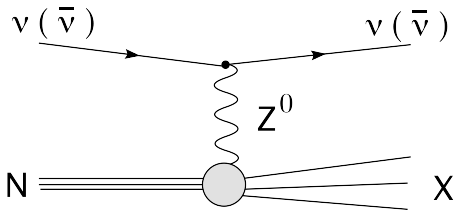

FIG. 3. Schematic of deep inelastic scattering of neutrinos through neutral-current interactions mediated by Z^0 exchange.

$$\frac{d^2\sigma_{\rm NC}^{\nu(\bar{\nu})}}{dxdy} = \pi s\left(\frac{\alpha}{2\sin^2\theta_W\cos^2\theta_W(M_Z^2+Q^2)}\right)^2 \times[xy^2F_1^Z(x,Q^2)+f_1(y)F_2^Z(x,Q^2) \pm f_2(y)xF_3^Z(x,Q^2)]. \tag{12}$$

This process is shown schematically in Fig. 3.

B. Charge symmetry and parton distribution functions

To obtain the charge-symmetry violating parton distributions, we introduce the CSV parton distributions for up and down quarks via

$$d^n(x) \equiv u^p(x) - \delta u(x), \quad u^n(x) \equiv d^p(x) - \delta d(x) \tag{13}$$

and analogous relations for the antiquark distributions. If the quantities $\delta u(x)$ and $\delta d(x)$ vanish, then charge symmetry is exact. We assume that the strange quark distributions are the same in both the proton and neutron, as are the antistrange distributions. There is no theoretical or experimental reason to expect strange or charm distributions to vary significantly from proton to neutron. Except at low x, the strange and charm distributions are also rather small.

It is useful to divide light quark parton distributions into valence quark and sea quark parts. For a given flavor q, the valence quark distributions in a nucleon are defined by

$$u_v(x) \equiv u(x) - \bar{u}(x), \qquad d_v(x) \equiv d(x) - \bar{d}(x). \tag{14}$$

We also use a capital letter to denote the second moment of a parton distribution, i.e.,

$$U_v \equiv \int_0^1 dx\, xu_v(x). \tag{15}$$

The quantity U_v in Eq. (15) gives the fraction of the total momentum carried by up valence quarks in a nucleon.

For heavy quarks and sea quarks, these often appear as linear combinations of the sum and difference of quark and antiquark distributions. For these we use the notation

$$q^{\pm}(x) \equiv q(x) \pm \bar{q}(x). \tag{16}$$

From Eq. (16) it is obvious that $u_v(x)=u^-(x)$. However, as we examine in detail features of the up and down valence quark PDFs, in this review we use the notation of Eq. (14) for the light valence quarks.

The first moments of the valence quark distributions obey the quark normalization conditions

$$\frac{1}{2}\int_0^1 u_v^p(x)dx = \frac{1}{2}\int_0^1 d_v^n(x)dx = \int_0^1 d_v^p(x)dx = \int_0^1 u_v^n(x)dx = 1, \qquad \int_0^1 s^-(x)dx = \int_0^1 c^-(x)dx = 0. \tag{17}$$

The CSV quantities defined in Eq. (13) can also be decomposed into valence and sea pieces. From the definitions of valence quark CSV and the valence quark normalization from Eq. (17), it is straightforward to show that the first moment of the valence quark CSV distributions must vanish, i.e.,

$$\int_0^1 \delta u_v(x)dx = \int_0^1 \delta d_v(x)dx = 0. \tag{18}$$

If Eq. (18) was not true, this would mean that the valence quark normalization conditions of Eq. (17) could not be satisfied. A consequence of Eq. (18) is that

$$\int_0^1 \delta u(x)dx = \int_0^1 \delta\bar{u}(x)dx$$

and

$$\int_0^1 \delta d(x)dx = \int_0^1 \delta\bar{d}(x)dx. \tag{19}$$

The most precise limits on sea quark CSV are derived from QCD sum rules, which involve various moments of the structure functions integrated over all x. Some observables will involve the first moment of sea quark parton CSV distributions. Thus we can distinguish two different types of partonic charge symmetry. The first or "strong form" of charge symmetry is the statement that charge-symmetry violating parton distributions vanish at all x. The "weak form" of charge symmetry corresponds to the assumption that the first moment of the CSV sea quark parton distributions is zero, i.e.,

$$\int_0^1 \delta\bar{u}(x)dx = \int_0^1 \delta\bar{d}(x)dx = 0, \tag{20}$$

even if the parton CSV distributions themselves do not necessarily vanish.

Note that valence quark normalization requires that the first moments of heavy quark and antiquark distributions must be identical. From Eq. (17) we see that

$$\int_0^1 s(x)dx = \int_0^1 \bar{s}(x)dx \tag{21}$$

with an analogous relation for charm quarks. This simply reflects the statement that the nucleon contains no

net strangeness or charm. From Eq. (21), it is tempting to conclude that the strange quark and antiquark distributions should be equal for all values of x, e.g.,

$$s^-(x) \equiv s(x) - \bar{s}(x) = 0, \tag{22}$$

with an identical relation to Eq. (22) for the charm and anticharm distributions. If all strange quarks arise from gluon radiation, Eq. (22) would be satisfied since s and $\bar{s}$ would always be produced in pairs. However, there is no compelling theoretical reason why strange quarks cannot arise from other sources. For example, in "meson-cloud" models (Signal and Thomas, 1987; Ji and Tang, 1995; Brodsky and Ma, 1996; Glück *et al.*, 1996; Holtmann *et al.*, 1996; Melnitchouk and Malheiro, 1997; Speth and Thomas, 1997), which include virtual transitions of a nucleon into a baryon and meson, the quark resides in the nucleon and the antiquark in the meson. Such models naturally lead to differences between quark and antiquark PDFs. We return to this issue in Sec. III.C.2, where it will be relevant in interpreting the "NuTeV anomaly" in the determination of the weak mixing angle.

Eventually, we would expect partonic charge-symmetry violation to be calculated directly from lattice gauge theory. This would require two additional inputs into current lattice calculations. The first would be to input different up and down current quark masses. The second will be to include electromagnetic interactions into lattice calculations. The first of these should be straightforward. As far as electromagnetic interactions are concerned, there are presently lattice calculations that include electromagnetic effects. For example, Blum *et al.* estimated light quark masses by including electromagnetic interactions and calculating pion and kaon mass splittings (Blum *et al.*, 2007) using two flavors of domain-wall quarks. However, for the purpose of testing partonic charge symmetry, one must include electromagnetic interactions to sufficient accuracy to account for all of the major effects in the nucleon. A good test would be the degree to which the inclusion of electromagnetic effects on the lattice can reproduce the experimental neutron-proton mass difference of 1.3 MeV.

C. Structure functions in terms of parton distribution functions

Introducing the CSV parton distributions from Eq. (13), we can write the leading order expressions for structure functions without assuming charge symmetry. Most tests of charge symmetry involve deep inelastic scattering on isoscalar targets, which we label as N_0, e.g., $F_1^{\gamma N_0}$ represents the F_1 structure function per nucleon for electromagnetic interactions on an isoscalar target. Such reactions involve contributions from equal numbers of protons and neutrons. So we write the electromagnetic and weak structure functions per nucleon on an isoscalar target. These expressions are true under the following conditions. First, we have neglected contributions from small components of the Cabibbo-Kobayashi-Maskawa (CKM) quark mixing matrix (Cabibbo, 1963; Kobayashi and Maskawa, 1973). Second, we have not included effects of quark masses in the kinematics or on particle-production thresholds (this assumption may be inappropriate for the charm quark mass, particularly in the case of charged-current interactions initiated by neutrinos). These expressions neglect higher-twist contributions to the structure functions. The PDFs depend on the starting scale μ^2 at which they are evaluated; in the following equations we do not explicitly include the dependence on the starting scale.

First we provide expressions for the structure functions relevant to NC reactions induced by charged leptons, given in Eq. (6),

$$36F_1^{\gamma N_0}(x,Q^2) = 5[u^+(x) + d^+(x)] + 2s^+(x) + 8c^+(x) - 4\delta d^+(x) - \delta u^+(x). \tag{23}$$

In the lowest-order quark-parton model, the structure function $F_2^{\gamma p}$ is related to the structure function $F_1^{\gamma p}$ by

$$F_2^{\gamma p}(x,Q^2) = \frac{1 + R(x,Q^2)}{1 + 4M^2x^2/Q^2} 2xF_1^{\gamma p}(x,Q^2). \tag{24}$$

In Eq. (24), $R = \sigma_L/\sigma_T$ is the ratio of the cross section for longitudinally to transversely polarized photons. An empirical relation fit to the world's available data on R has been made by Whitlow *et al.* (1990). This fit covers the kinematic region $x > 0.1$ and $Q^2 < 125$ GeV^2.

For momentum transfers which are sufficiently small (relative to M_Z^2) and for parity-conserving interactions, we can neglect the contribution from Z bosons, in which case the scattering is a function only of the two electromagnetic structure functions F_1^γ and F_2^γ, respectively. The cross terms involving Z bosons are important either at very large values of Q^2 or alternatively for parity-violating (PV) lepton scattering where the leading terms cancel. The structure functions involving photon-Z interference have the form

$$\begin{aligned} 6F_1^{\gamma Z;N_0}(x,Q^2) &= (2g_V^u - g_V^d)[u^+(x) + d^+(x)] \\ &\quad + 2g_V^u[2c^+(x) - \delta d^+(x)] \\ &\quad - g_V^d[2s^+(x) - \delta u^+(x)], \\ 2F_3^{\gamma Z;N_0}(x,Q^2) &= (g_V^u - g_V^d)[u_v(x) + d_v(x)] \\ &\quad - g_V^u\delta d_v(x) + g_V^d\delta u_v(x). \end{aligned} \tag{25}$$

The structure functions corresponding to Z^0 exchange can be written as

$$\begin{aligned} 4F_1^{ZN_0}(x,Q^2) &= (G_u^2 + G_d^2)[u^+(x) + d^+(x)] \\ &\quad + G_d^2[2s^+(x) - \delta u^+(x)] \\ &\quad + G_u^2[2c^+(x) - \delta d^+(x)], \\ 2F_3^{ZN_0}(x,Q^2) &= (g_V^u - g_V^d)[u_v(x) + d_v(x)] \\ &\quad + g_V^u[2c^-(x) - \delta d_v(x)] \\ &\quad - g_V^d[2s^-(x) - \delta u_v(x)]. \end{aligned} \tag{26}$$

In Eqs. (25) and (26) we have introduced

$$g_V^u = \tfrac{1}{2} - \tfrac{4}{3}\sin^2\theta_W, \quad G_u^2 = (g_V^u)^2 + \tfrac{1}{4},$$
$$g_V^d = \tfrac{2}{3}\sin^2\theta_W - \tfrac{1}{2}, \quad G_d^2 = (g_V^d)^2 + \tfrac{1}{4}. \tag{27}$$

For charged-current interactions initiated either by charged leptons or by neutrinos, for sufficiently low values of Q^2 one must take account of the masses of heavy quarks. We do not include bottom and top quark effects in this review; however, one must account in some way for the nonzero charm quark mass. In this case the charged-current structure functions will depend on the CKM matrix elements (Cabibbo, 1963; Kobayashi and Maskawa, 1973). Expressions for the charged-current structure functions that take into account effects of heavy quark masses and CKM matrix elements can be found in the literature (Leader and Predazzi, 1996). However, for sufficiently large values of Q^2, the structure functions in Eqs. (10) and (11) will to a good approximation simplify to the form

$$\begin{aligned}
2F_1^{W^+N_0}(x,Q^2) &\to u^+(x) + d^+(x) + 2s(x) + 2\bar{c}(x) \\
&\quad - \delta u(x) - \delta\bar{d}(x), \\
2F_1^{W^-N_0}(x,Q^2) &\to u^+(x) + d^+(x) + 2\bar{s}(x) + 2c(x) \\
&\quad - \delta d(x) - \delta\bar{u}(x), \\
F_3^{W^+N_0}(x,Q^2) &\to u_v(x) + d_v(x) + 2s(x) - 2\bar{c}(x) \\
&\quad - \delta u(x) + \delta\bar{d}(x), \\
F_3^{W^-N_0}(x,Q^2) &\to u_v(x) + d_v(x) - 2\bar{s}(x) + 2c(x) \\
&\quad - \delta d(x) + \delta\bar{u}(x).
\end{aligned} \tag{28}$$

In Eq. (23) and subsequent equations, we have suppressed the nucleon index on the parton distributions. Since we have explicitly introduced the parton CSV amplitudes, the remaining PDFs are now understood to be those for the proton. The relation between the F_1 and F_2 structure functions for neutrinos is given by an equation analogous to Eq. (24), where R is now the longitudinal to transverse ratio that holds for CC and NC neutrino reactions. For the CC reactions initiated by neutrinos, the experimental values for R^ν are summarized by Conrad *et al.* (1998). For NC reactions, the value of R is essentially unknown. This provides some uncertainty in extracting parton distribution functions from neutrino NC reactions.

We have written the nuclear structure functions in terms of the parton distributions for free nucleons. However, as is well known, parton distributions are modified in nuclei. At small x there are shadowing corrections, at intermediate x there are "EMC effects," (Ashman *et al.*, 1988, 1989; Geesaman *et al.*, 1995), and at large x Fermi-motion effects dominate. Nuclear modifications of PDFs have been reviewed recently by Kumano and collaborators (Kumano, 2002; Hirai *et al.*, 2004, 2005) and also by Kulagin and Petti (2006, 2007a, 2007b). Consequently, in any precision experiments these effects must be accounted for if we compare to parton distributions taken from free protons [there should even be small modifications arising in the deuteron (Frankfurt and Strikman, 1978, 1981; Melnitchouk and Thomas, 1993, 1996; Melnitchouk *et al.*, 1994b)]. We discuss these effects later as they arise.

D. Relations between structure functions

Using the relation between leading-order high-energy structure functions given in Eqs. (23) and (28), we obtain the following relation between the structure functions, including charge-symmetry violating effects:

$$\begin{aligned}
\frac{5}{18}\bar{F}_2^{WN_0}(x) - F_2^{\gamma N_0}(x) &= \frac{1}{12}[xF_3^{W^+N_0}(x) - xF_3^{W^-N_0}(x)] \\
&\approx \frac{x}{12}\{2[s^+(x) - c^+(x)] \\
&\quad + \delta d^+(x) - \delta u^+(x)\}.
\end{aligned} \tag{29}$$

Equation (29), sometimes called the "5/18 rule," relates the F_2 structure function from charged-current neutrino reactions to the F_2 structure function from interactions of charged leptons, with both quantities measured on isoscalar targets. In Eq. (29) we have for simplicity neglected the longitudinal to transverse correction factors R given in Eq. (24). However, these correction factors were included when the F_2 structure functions were extracted from experimental cross sections.

In Eq. (29), $\bar{F}_2^{WN_0}$ is the average of the CC cross sections induced by ν and $\bar{\nu}$,

$$\bar{F}_2^{WN_0}(x) = \tfrac{1}{2}[F_2^{W^+N_0}(x) + F_2^{W^-N_0}(x)]. \tag{30}$$

The right-hand side of Eq. (29) includes contributions from strange and charmed quarks and is correct to lowest order in CSV terms. Although the light quark contributions cancel in this expression, there is a residual contribution from strange and charm quarks. At small x one has contributions from both the CSV and heavy quark PDFs. However, at larger values of x the strange and charm contributions should be extremely small, and in this region the only significant contribution to the right-hand side of Eq. (29) should come from valence quark CSV terms. Furthermore, if the heavy quark contributions are known, Eq. (29) may be used to investigate the charge-symmetry violating quark distributions for the light quarks.

The strange quark PDFs have been determined from the production of opposite-charge muon pairs in neutrino-induced reactions (Foudas *et al.*, 1990; Rabinowitz *et al.*, 1993; Bazarko *et al.*, 1995; Sterman *et al.*, 1995; Goncharov *et al.*, 2001; Kretzer *et al.*, 2004; Mason *et al.*, 2007). Thus comparison of these two F_2 structure functions, combined with our knowledge of strange and charm PDFs, has the potential to measure (or to place strong upper limits on) parton CSV probabilities. The current experimental and theoretical situation will be reviewed in Sec. III.C.1. From Eq. (28), we

note that in principle we could obtain the same information as in Eq. (29) by measuring the difference between the xF_3 structure functions from charge-changing ν and $\bar{\nu}$ interactions on isoscalar targets.

We can obtain another relation between structure functions by measuring the F_2 structure function from ν and $\bar{\nu}$ CC reactions on isoscalar targets. Using Eq. (28) we obtain

$$F_2^{W^+N_0}(x) - F_2^{W^-N_0}(x) = x\{2[s^-(x) - c^-(x)] + \delta d_v(x) - \delta u_v(x)\}. \tag{31}$$

The right-hand side of Eq. (31) contains "valence" contributions (the difference between quark and antiquark probabilities) for strange and charm quarks, as well as contributions from valence quark CSV terms. In Sec. III.E.4, we discuss the experimental possibilities for measuring this quantity, and we show theoretical predictions and phenomenological limits on this quantity.

Another relation for structure functions can be obtained by comparing the F_2 structure functions obtained from charge-changing interactions of antineutrinos and neutrinos on proton targets. If one takes the difference between these structure functions and divides by $2x$, one obtains

$$\frac{F_2^{W^-p}(x) - F_2^{W^+p}(x)}{2x} = u_v(x) - d_v(x) - s^-(x) + c^-(x). \tag{32}$$

Since the first moment of the strange and charmed valence contributions must vanish, the difference between these two F_2 structure functions, divided by $2x$ and integrated over all x, should be equal to the difference between the up and down valence quark occupation numbers in the proton or 1. This is the Adler sum rule (Adler, 1966), which will be reviewed in Sec. IV.C.2.

If the F_3 structure functions for neutrino and antineutrino charge-changing reactions are measured on isoscalar targets, then from Eq. (28) the sum of these structure functions gives

$$\frac{xF_3^{W^+N_0}(x) + xF_3^{W^-N_0}(x)}{2x} = u_v(x) + d_v(x) + s^-(x) + c^-(x) - \frac{\delta d_v(x) + \delta u_v(x)}{2}. \tag{33}$$

The sum of these structure functions includes only valence quark probabilities plus valence CSV contributions. Consequently integrating Eq. (33) over all x and applying valence quark normalization from Eqs. (17) and (18) give (modulo QCD corrections) just the sum of valence up and down probabilities in the nucleon or 3. This is the Gross–Llewellyn Smith sum rule (Gross and Llewellyn Smith, 1969), reviewed in Sec. IV.C.3.

One final relation can be obtained by comparing the F_2 structure function from charged lepton DIS on protons with that for neutrons. One obtains

$$\frac{F_2^{\gamma p}(x) - F_2^{\gamma n}(x)}{x} = \frac{u^+(x) - d^+(x)}{3} + \frac{4\delta d^+(x) + \delta u^+(x)}{9}. \tag{34}$$

If the quantity in Eq. (34) is integrated over all x then one obtains the Gottfried sum rule (Gottfried, 1967). The experimental and theoretical implications of this sum rule are discussed in Sec. IV.C.1.

III. CHARGE SYMMETRY IN VALENCE QUARK DISTRIBUTIONS

In this section, we review both theory and experiment regarding charge symmetry in valence quark distributions. First, we review phenomenological estimates of CSV for valence quarks. Next, we review theoretical estimates of valence CSV, and then we review the experimental upper limits. Finally, we suggest new experiments that could provide strong constraints on valence quark CSV.

A. Phenomenological estimates of valence quark CSV

Recently, the MRST group (Martin *et al.*, 2004) has evaluated uncertainties in parton distributions arising from a number of factors, including isospin violation. They chose a specific model for valence quark charge-symmetry violating PDFs, adopting a function of the form

$$\delta u_v(x) = -\delta d_v(x) = \kappa f(x), \qquad f(x) = (1-x)^4 x^{-0.5}(x - 0.0909). \tag{35}$$

The quantity $f(x)$ in Eq. (35) was chosen so that its x dependence had roughly the same form as the MRST valence quark parton distribution functions (at the starting scale for QCD evolution) in both the limits $x \to 0$ and $x \to 1$. The first moment of $f(x)$ was fixed to be zero, in agreement with the valence quark normalization constraint of Eqs. (17) and (18). The valence quark normalization condition requires that the CSV function $f(x)$ has at least one node.

Inclusion of valence quark CSV can in principle change the momentum carried by valence quarks in the neutron from those in the proton since the total momentum carried by valence quarks is given by the second moment of the distribution. The total momentum carried by valence (up plus down) quarks in the neutron is determined experimentally to within about 2%, so MRST chose a functional form that ensured that equal momentum was carried by valence quarks in the proton and neutron. For this reason, they insisted that the valence CSV terms δd_v and δu_v be equal and opposite. With this constraint it is straightforward to show that

$$u_v^p(x) + d_v^p(x) = u_v^n(x) + d_v^n(x). \tag{36}$$

Multiplying both sides of Eq. (36) by x shows that the momentum carried by valence quarks is identical for proton and neutron. The overall coefficient κ in Eq. (35)

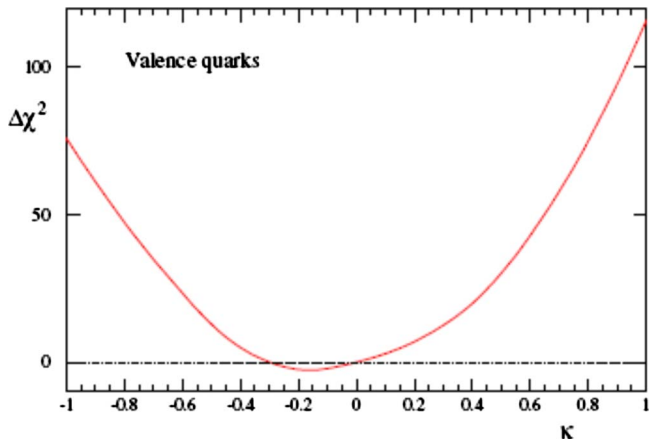

FIG. 4. (Color online) The χ^2 obtained by MRST, for a global fit to high-energy data of parton distribution functions including valence quark CSV with the functional form defined in Eq. (35). χ^2 is plotted vs the free parameter κ. From Martin *et al.*, 2004.

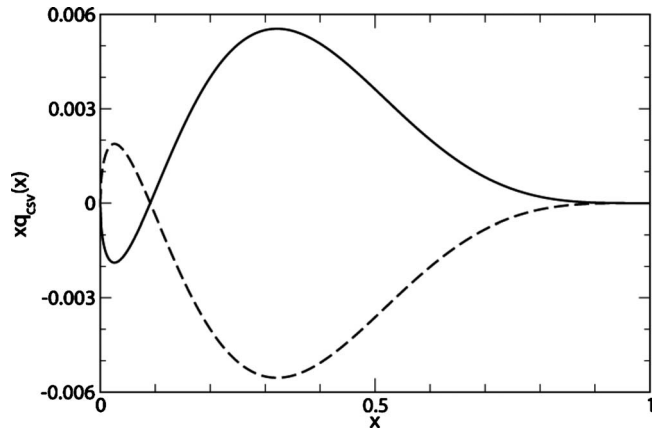

FIG. 5. The phenomenological valence quark CSV function from MRST, corresponding to best-fit value $\kappa=-0.2$ defined in Eq. (35). Solid curve, $x\delta d_v$; dashed curve, $x\delta u_v$. From Martin *et al.*, 2004.

was varied in a global fit to a wide range of high-energy data. For simplicity, MRST neglected the Q^2 dependence of the CSV term in their global fit. Later, when we use these charge-symmetry-violating PDFs to estimate potential effects of partonic CSV, this will introduce some uncertainty. To lowest order in QCD, typical CSV effects will have a form approximately proportional to

$$\frac{\delta u(x) - \delta d(x)}{u(x) + d(x)}. \tag{37}$$

If we use the MRST CSV PDFs obtained using Eq. (35), for a given Q^2 we will be using parton distributions where the denominator has been evolved in Q^2 but the numerator is not evolved.

Including valence quark CSV in their global fit to high-energy data, MRST obtained a very shallow minimum in χ^2 with a best-fit value $\kappa=-0.2$ and a 90% confidence level for the range $-0.8\leqslant\kappa\leqslant+0.65$. The χ^2 for their fit versus the parameter κ is shown in Fig. 4. Since MRST chose a specific functional form for valence quark CSV, their results could have a substantial model dependence. The MRST global fit guarantees that CSV distributions with this shape and with values of κ within the 90% confidence range will give reasonable agreement with all of the high-energy data used to extract quark and gluon PDFs.

Since the MRST functional form for valence CSV PDFs requires that δd_v be equal in magnitude to δu_v, this implies that at large x the fractional charge-symmetry violation is substantially larger for the "minority valence quark" distribution d_v than for u_v since $d_v \ll u_v$ in this region. Similar results have been obtained for valence CSV distributions within a number of theoretical models, as discussed in the following section.

In Fig. 5 we show the phenomenological valence quark CSV distributions obtained by MRST using the function $f(x)$ from Eq. (35) with the parameter $\kappa=-0.2$, which represents the best fit to the high-energy data. The solid curve corresponds to $x\delta d_v(x)$ and the dashed curve corresponds to $x\delta u_v(x)$. These valence CSV PDFs reach a maximum value of approximately 0.006 at a value $x\sim 0.3$, and [by inspection of Eq. (35)] they have a zero crossing at $x=0.0909$.

B. Theoretical estimates of valence quark CSV

The phenomenological MRST results of Sec. III.A can be compared with theoretical estimates of valence quark CSV. In a valence quark approximation, the nucleon can be considered as consisting of three valence quarks, with proton and neutron described as

$$|p\rangle \sim [uud], \quad |n\rangle \sim [udd]. \tag{38}$$

In quark models evaluated on the light cone, the valence quark distribution can be expressed as (Jaffe, 1983; Signal and Thomas, 1989; Schreiber *et al.*, 1991)

$$q_v(x,\mu^2) = M\sum_X \left| \langle X|\frac{1+\alpha_3}{2}\psi(0)|N\rangle \right|^2 \times \delta(M(1-x) - p_X^+). \tag{39}$$

In Eq. (39) $\alpha_3=\gamma^0\gamma^3$; this relation denotes the process where a valence quark is removed from a nucleon $|N\rangle$, and the result is summed over all final states $|X\rangle$. The quantity p_X^+ is the energy of the state following removal of a valence quark with momentum k. The quantity μ^2 represents the starting value for the Q^2 evolution of the parton distribution. Equation (39) treats only the quark longitudinal momentum and neglects transverse quark momentum.

There are several potential sources of charge-symmetry violation in Eq. (39). First, there is possible charge-symmetry violation in the quark wave functions. Second, there are mass differences in the spectator multiquark system. Finally, there are additional electromagnetic effects that break charge symmetry. Now, model quark wave functions are found to be almost invariant

under the small mass changes typical of CSV (Rodionov *et al.*, 1994), so we do not discuss these effects further. Electromagnetic effects are of order α, where α is the electromagnetic coupling constant; hence such effects are expected to be at the 1% level. At the large values of Q^2 characteristic of high-energy reactions, typically 1 to many GeV^2, such effects should be small.

We consider two quantities that break partonic charge symmetry. Each of these arises from different combinations of the sources of CSV. The first is the *n-p* mass difference $\delta M \equiv M_n - M_p = 1.3$ MeV. A second quantity is the difference in diquark masses arising from the current quark mass difference between up and down quarks. We define the quantity

$$\delta\tilde{m} = m_{dd} - m_{uu}. \tag{40}$$

One has a robust estimate for this mass difference, $\delta\tilde{m} \sim 4$ MeV (Bickerstaff and Thomas, 1989). Since the two quantities δM and $\delta\tilde{m}$ arise from different combinations of mass differences and EM effects, we can consider them as independent quantities. We can determine charge-symmetry violating valence parton distributions by calculating their variation with respect to each of these quantities, i.e.,

$$\delta q_v \approx \frac{\partial q_v}{\partial(\delta\tilde{m})}\delta\tilde{m} + \frac{\partial q_v}{\partial(\delta M)}\delta M. \tag{41}$$

From Eq. (41) the valence charge-symmetry violating parton distributions are obtained by taking variations with respect to diquark and nucleon masses on valence parton distributions from quark models.

If we take the simple valence quark picture of the nucleon as given by Eq. (38), then we can consider diquark mass differences following the removal of one quark from the nucleon. If we remove a "majority" valence quark (a u quark in the proton or d quark in the neutron), then for both proton and neutron one is left with a ud diquark. Thus for the majority quark distribution, there is no quark mass asymmetry for the residual diquark. For removal of a "minority" quark (a d quark in the proton or u quark in the neutron), the remainders are a uu diquark in the proton and a dd diquark in the neutron. Thus the diquark mass asymmetry is given by the quantity $\delta\tilde{m}$ in Eq. (40).

This technique was used by Sather (1992), who investigated these effects in a static quark model. Sather obtained an analytic approximation relating valence quark CSV to derivatives of the valence PDFs,

$$\delta d_v(x) = -\frac{\delta M}{M}\frac{d}{dx}[x d_v(x)] - \frac{\delta\tilde{m}}{M}\frac{d}{dx}d_v(x),$$
$$\delta u_v(x) = \frac{\delta M}{M}\left(-\frac{d}{dx}[x u_v(x)] + \frac{d}{dx}u_v(x)\right). \tag{42}$$

Note that Sather's equations agree with our earlier arguments. The majority quark CSV distributions $\delta u_v(x) = u_v^p(x) - d_v^n(x)$ are functions only of δM and do not depend on $\delta\tilde{m}$, while the minority valence quark CSV distributions $\delta d_v(x)$ depend on both δM and $\delta\tilde{m}$.

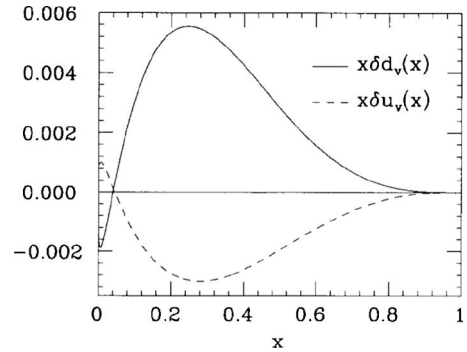

FIG. 6. Theoretical valence CSV PDFs from Sather (1992) and Eq. (42). Solid curve, $x\delta d_v$; dashed curve, $x\delta u_v$. The valence PDFs were preliminary fits to CCFR Tevatron structure functions evolved to $Q^2 = 12.6$ GeV^2.

In Fig. 6 we plot the CSV valence parton distributions of Sather (1992). The valence parton distributions used by Sather were from preliminary fits to the Tevatron structure functions obtained by the Columbia-Chicago-Fermilab-Rochester (CCFR) group (Seligman *et al.*, 1992). The solid curve is $x\delta d_v(x)$ vs x, while the dashed curve plots $x\delta u_v(x)$. The PDFs have been evolved to $Q^2 = 12.6$ GeV^2. The qualitative features of these charge-symmetry violating valence PDFs are similar for all models that we review. Since the first moment of the valence CSV parton distributions has to vanish (in order to maintain valence quark normalization), the valence CSV PDFs must change sign at least once. For Sather's model this occurs at $x \sim 0.05$. In general, if one calculates the CSV valence PDFs by inserting phenomenological parton distribution functions into Eq. (42) or other analytic formulas, the resulting CSV parton distributions will not obey the valence quark normalization condition. However, Sather obtained his PDFs from moments of the quark distributions; for his valence CSV parton distributions Sather set the first moment to zero, thus guaranteeing valence quark normalization.

For larger values of x, $\delta d_v(x)$ is positive while $\delta u_v(x)$ is negative. The distributions peak at $x \sim 0.3$. In Sather's model $\delta d_v(x)$ is roughly 50% larger in magnitude than $\delta u_v(x)$. By observing the quark model wave functions we can understand these qualitative features of the valence quark CSV distributions. The minority valence quark CSV term is defined by $\delta d_v = d_v^p - u_v^n$. Removing a minority valence quark from a nucleon with three valence quarks leaves a diquark system that is uu for the proton and dd for the neutron. Simple theoretical arguments (Rodionov *et al.*, 1994) suggest that the down quark distribution in the proton will be shifted to higher x and the up quark distribution in the neutron will be shifted to lower x. This predicts that, at large x, δd_v should be positive.

Conversely for the majority valence quark CSV term $\delta u_v = u_v^p - d_v^n$, removing a majority quark leaves intermediate states with the same quark configuration (ud) for both neutron and proton. From Eq. (42) the majority

valence CSV term should depend only on the n-p mass difference, and one expects that δu_v should be negative at large x. These qualitative predictions agree with the quark model CSV valence distributions shown in Fig. 6, and they also are in agreement with the phenomenological best-fit CSV PDFs shown in Fig. 5. Although the down valence distribution in the proton is less than half the up valence distribution, these qualitative arguments suggest that

$$\delta d_v(x) > |\delta u_v(x)| \tag{43}$$

at large x. This is observed in the theoretical model calculations by Sather, however, Eq. (43) is not satisfied by the phenomenological MRST parametrization of Eq. (35), which requires by definition that $\delta d_v(x)$ and $\delta u_v(x)$ should be equal in magnitude and opposite in sign.

There is another way to understand the qualitative features of these valence CSV distributions. It was pointed out by Londergan and Thomas (2003b) that from Sather's expression (42) one can obtain an analytic expression for the second moment of the CSV parton distributions,

$$\delta U_v = \frac{\delta M}{M}(U_v - 2),$$

$$\delta D_v = \frac{\delta M}{M} D_v + \frac{\delta \tilde{m}}{M}, \tag{44}$$

$$\delta D_v \approx \frac{\delta M}{M}(D_v + 3).$$

In Eq. (44), U_v and D_v are the total momentum carried by up and down valence quarks, respectively. The final line of Eq. (44) follows from the fact that $\delta\tilde{m} \sim 3\delta M$. Since the valence CSV distributions are required by valence quark normalization to have zero first moment [see Eq. (18)], the valence CSV distributions must change sign at least once. Equation (44) predicts that, at large x, δu_v will be negative and δd_v will be positive. The sign of the valence CSV distributions is the same for all parton distributions derived from quark models. Furthermore, from the relative magnitude of δU_v and δD_v, we expect the maximum of δd_v to be larger than that for δu_v.

Benesh and Londergan (1998) also considered parton charge-symmetry violation from quark models using Eq. (39). They related the change in PDFs due to charge-symmetry violation in minority valence quark distributions (the term proportional to the diquark mass difference $\delta\tilde{m}$) to the color hyperfine splitting between N and Δ states in quark models of baryons that initially assume SU(4) spin-flavor symmetry (these arise from diquark spin splittings). Using the work of Close and Thomas (1988), they obtained

$$\delta d_v(x) = \frac{\delta\tilde{m}}{\delta_{\rm hf}}\left[\frac{u_v(x) - 2d_v(x)}{6}\right] - \frac{\delta M}{M}\frac{d}{dx}d_v(x), \tag{45}$$

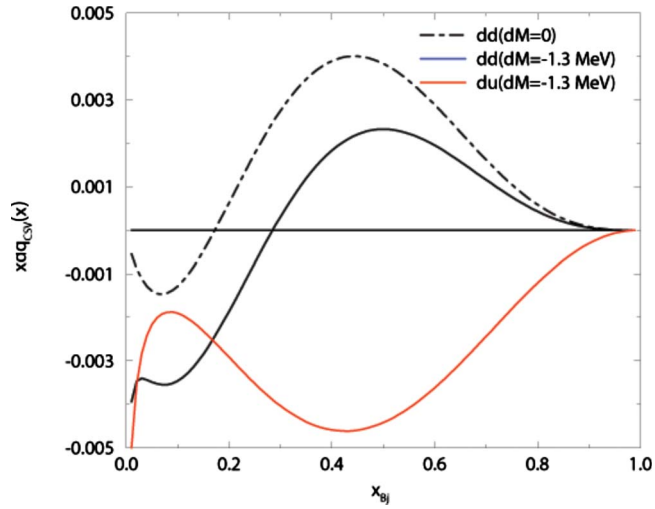

FIG. 7. (Color online) Theoretical valence CSV PDFs (Benesh and Londergan, 1998) given in Eq. (45). Thick solid line, $x\delta d_v$; thin solid line, $x\delta u_v$. Dash-dotted line, $x\delta d_v$ when the n-p mass difference is set to zero. The PDFs were the CTEQ LQ parton distributions (Lai *et al.*, 1997), evaluated at the low momentum starting scale $Q^2 = 0.49$ GeV^2.

$$\delta u_v(x) = -\frac{\delta M}{M}\frac{d}{dx}u_v(x).$$

In Eq. (45), $\delta_{\rm hf} = 50$ MeV is the $S=1$ color hyperfine splitting in the SU(4) limit. These equations also differ from Sather's result of Eq. (42) in that Benesh and Londergan considered variations of the nucleon mass M while keeping the quantity Mx constant, following arguments by Benesh and Goldman (1997).

In Fig. 7 we plot the theoretical valence CSV parton distributions calculated by Benesh and Londergan (1998) using Eq. (45). The PDFs used were the phenomenological CTEQ low Q (LQ) parton distributions from the CTEQ group (Lai *et al.*, 1997) evaluated at the low momentum starting scale $Q^2 = 0.49$ GeV^2.

As mentioned [see Eq. (18)], valence parton CSV distributions should respect valence quark normalization, and hence $\langle\delta d_v\rangle = \langle\delta u_v\rangle = 0$. By inspection of Fig. 7, the valence CSV PDFs of Benesh and Londergan do not satisfy the quark normalization condition. Although the sign of the CSV PDFs obtained by Benesh and Londergan agrees with that of Sather and also with the predictions of Eq. (44), the magnitudes are somewhat different. Here the magnitude of δu_v is larger than δd_v, a result opposite from Sather and in disagreement with Eq. (44). The difference between these theoretical PDFs is likely related to the fact that Benesh and Londergan used an additional approximation to relate quark CSV terms to mass splittings in SU(4) symmetric quark models. Note that the Benesh-Londergan PDFs are evaluated at a considerably lower value of Q^2 than for Sather. One could evolve these CSV PDFs to higher Q^2 by inserting these parton distributions into the QCD evolution equations.

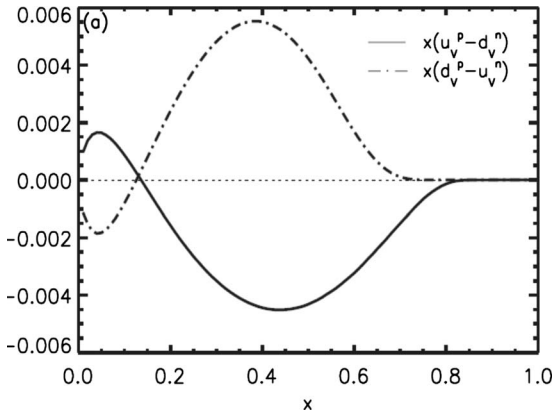

FIG. 8. Theoretical CSV parton distributions. Solid line, $x\delta u_v$; dash-dotted line, $x\delta d_v$. The PDFs have been evolved to $Q^2 = 10\ \mathrm{GeV}^2$. From Rodionov *et al.*, 1994.

Rodionov, Thomas, and Londergan (1994) also calculated charge-symmetry violating parton distributions using Eq. (39). They included the relativistic diquark recoil energy (if one ignores this the resulting parton distributions do not have the correct support; the PDFs are then defined on the range $0 \leqslant x < \infty$ rather than from $0 \leqslant x \leqslant 1$). Rodionov *et al.* also evaluated Eq. (39) including the effects of quark transverse momentum. In this case one can no longer obtain analytic expressions for the CSV valence parton distributions.

Figure 8 plots the theoretical quark model calculations of valence CSV by Rodionov *et al.* (1994). The dash-dotted curve in Fig. 8 represents the quantity $x\delta d_v(x)$, while the solid curve is $x\delta u_v(x)$. The curves were initially calculated at the low Q^2 appropriate for quark models and evaluated at $Q^2 = 10\ \mathrm{GeV}^2$ through DGLAP evolution (Gribov and Lipatov, 1972; Altarelli and Parisi, 1977; Dokshitzer, 1977). The valence CSV parton distributions obtained by Rodionov *et al.* (1994) are quite similar to those of Sather (1992), as seen by comparison of Figs. 6 and 8. The sign and magnitude of both $\delta d_v(x)$ and $\delta u_v(x)$ are very similar, and the second moments of both distributions agree to within about 20%. The zero crossing in Sather's model appears at a smaller value of x than that for Rodionov.

We can also compare the theoretical valence CSV distributions with the phenomenological valence CSV distributions obtained by MRST from their global fit to high-energy data. These are plotted in Fig. 5 for the best-fit value $\kappa = -0.2$ in Eq. (35). The solid (dashed) curve in Fig. 5 represents $x\delta d_v(x)$ $[x\delta u_v(x)]$. The sign and relative magnitude of both δd_v and δu_v, and the point where they cross zero, are remarkably similar in both the MRST phenomenological CSV PDFs, and the results obtained by Rodionov *et al.* are shown in Fig. 8. The second moments of the Rodionov quark model CSV PDFs are both equal to the moments of the corresponding MRST values to better than 10%.

The valence CSV parton distributions δu_v obtained by Benesh and Londergan (1998) and shown in Fig. 7 are quite similar to those of Sather and Rodionov, while the CSV valence distribution δd_v is roughly a factor of 2 smaller than the others. Benesh and Goldman (1997) calculated parton CSV distributions from a quark potential model, and their CSV PDFs have the same sign and a similar shape to those derived by Sather and Rodionov, but the Benesh-Goldman CSV PDFs are roughly a factor of 2 smaller in magnitude.

The qualitative agreement between the phenomenological valence quark PDFs obtained by MRST, using the best value $\kappa = -0.2$ from their global fit and shown in Fig. 5, and the theoretical CSV PDFs obtained by Rodionov *et al.* and shown in Fig. 8 is rather remarkable, especially considering that the theoretical results were obtained some ten years earlier and used relatively simple bag model quark wave functions. The excellent agreement with the phenomenological results provides some theoretical support for the functional form chosen by MRST. However, within the 90% confidence region for the global fit, the valence quark CSV PDFs either could be four times as large as those predicted by Sather and Rodionov or they could be three times as large with the opposite sign.

One feature of the theoretical CSV distributions is the prediction that for moderately large values of x (i.e., for x above the zero crossings)

$$|\delta u_v(x) + \delta d_v(x)| \ll |\delta u_v(x) - \delta d_v(x)|. \tag{46}$$

Consequently, valence quark CSV observables that depend on the difference between the minority and majority CSV terms should be substantially larger than those that depend on the sum of these terms. Equation (46) is satisfied trivially for the MRST phenomenological valence CSV distributions of Eq. (35) since by definition their sum is zero.

Cao and Signal (2000) calculated partonic charge-symmetry violation assuming that partonic CSV arises through mesonic fluctuations of the nucleon. They used a meson-cloud model to estimate partonic CSV (Speth and Thomas, 1997; Kumano, 1998). In the meson-cloud model, mass splittings in the baryon and meson multiplets lead to charge-symmetry violating parton distributions. The resulting CSV distributions obtained by Cao and Signal are substantially smaller than those obtained by Sather (1992) or Rodionov *et al.* (1994) and peak at substantially smaller values $x \sim 0.1$. This could be expected from the splitting functions for baryons in meson-cloud models.

Cao and Signal break up the parton distributions into three parts: a bare part, a perturbative part, and a nonperturbative part. The first two of these are assumed to be charge symmetric. The perturbative part is assumed to arise from gluon splitting. In Sec. III.B.1 we show that there is an additional perturbative part arising from photon splitting. This additional part will contribute to parton charge-symmetry violation since the photons couple differently to up and down quarks by virtue of their different charges.

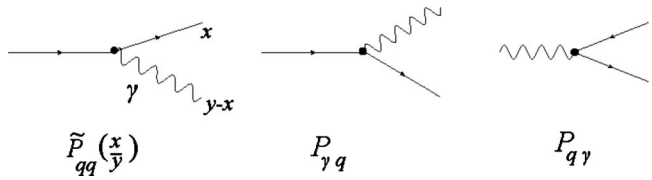

FIG. 9. Schematic of quarks coupling to photons. Replacing a gluon line by a photon everywhere (except for the gluon self-coupling) produces the electromagnetic coupling of photons to partons. This gives the origin of QED splitting that produces additional CSV effects in parton distribution functions.

1. QED splitting: Another source of parton CSV

Recently, another source of parton charge-symmetry violation has been included in calculations of PDFs by both MRST (Martin *et al.*, 2005) and Glück *et al.* (2005). The most important terms in the usual QCD evolution involve gluon radiation, where a quark radiates a gluon leaving a quark with a lower x value. They suggested that one assumes charge symmetry at some initial extremely low-mass scale and includes in the QCD evolution equations the effect of photon radiation. This involves the explicit coupling of quarks to photons, the analog of quark coupling to gluons.

Figure 9 shows schematically the coupling of quarks to photons. The electromagnetic couplings are obtained by replacing gluon lines with photons, except for the gluon self-coupling which is not present for photons, and replacing the gluon splitting functions with the appropriate coupling for photons. This QED coupling changes the parton distribution functions in two distinct ways. First, it introduces an additional source of charge-symmetry violation since the photon couples differently to up and down partons because of their different electromagnetic charges. Second, radiation of the photon produces a "photon parton distribution." This photon PDF must be accounted for in the evolution equations. The photon PDF also makes a contribution to the total momentum carried by the nucleon.

When one includes QED contributions in this way, to lowest order in both the strong coupling α_S and the electromagnetic coupling α, the so-called DGLAP evolution equations due to Dokshitzer (1977), Gribov and Lipatov (1972), and Altarelli and Parisi (1977) are modified. To lowest order in the QED coupling α the evolution equations obtained by MRST have the form

$$\frac{\partial q_i(x,\mu^2)}{\partial \ln \mu^2} = \frac{\alpha_S}{2\pi}[P_{qq} \otimes q_i + P_{qg} \otimes g] + \frac{\alpha}{2\pi}\tilde{P}_{qq} \otimes e_i^2 q_i,$$

$$\frac{\partial g(x,\mu^2)}{\partial \ln \mu^2} = \frac{\alpha_S}{2\pi}\left[P_{gq} \otimes \sum_j q_j + P_{gg} \otimes g\right], \tag{47}$$

$$\frac{\partial \gamma(x,\mu^2)}{\partial \ln \mu^2} = \frac{\alpha}{2\pi}P_{\gamma q} \otimes \sum_j e_j^2 q_j.$$

The convolution integral in Eq. (47) is defined by

$$P \otimes f \equiv \int_x^1 \frac{dy}{y} P(y) f\left(\frac{x}{y}\right). \tag{48}$$

In Eq. (47), the right-hand side of the schematic evolution equations represents a convolution of the splitting functions with the quark and gluon distributions (which have an explicit dependence on the factorization scale parameter μ^2). Inclusion of the electromagnetic contribution to the evolution equations introduces a photon parton distribution $\gamma(x,\mu^2)$ which is coupled to the quark and gluon distributions. The new splitting functions that occur in Eq. (47) are related to the standard QCD splitting functions by

$$\tilde{P}_{qq}(y) = P_{qq}(y)/C_F,$$

$$P_{\gamma q}(y) = P_{gq}(y)/C_F, \tag{49}$$

$$C_F = \frac{N_c^2 - 1}{2N_c}.$$

In Eq. (49), N_c is the number of colors. Conservation of momentum is assured by

$$\int_0^1 dx\, x\left[\sum_i q_i(x,\mu^2) + g(x,\mu^2) + \gamma(x,\mu^2)\right] = 1. \tag{50}$$

It is necessary to simplify Eq. (47). First, since the electromagnetic interaction is not asymptotically free, it is difficult to determine a model-independent method for setting the starting values for the various PDFs that are coupled by these QED effects. In particular, it is not clear where the QED effects should be assumed to vanish. Second, inclusion of the QED couplings could in principle more than double the number of parton distribution functions (one must now differentiate between proton and neutron PDFs, in addition to the new photon PDFs).

Two groups have adopted somewhat different strategies, with similar overall results. Glück *et al.* (2005) adopted the standard convention for DIS reactions of setting the scale $\mu^2 = Q^2$. The most important contribution from the photon coupling occurs in the valence quark PDFs. To lowest order in the electromagnetic coupling α, the convolution equations for the CSV valence quark distributions arising from QED coupling have the form

$$\frac{d\delta u_v(x,Q^2)}{d\ln Q^2} = \frac{\alpha}{2\pi}\int_x^1 \frac{dy}{y} P(y) u_v\left(\frac{x}{y},Q^2\right) = \frac{\alpha}{2\pi} P \otimes u_v,$$

$$\frac{d\delta d_v(x,Q^2)}{d\ln Q^2} = -\frac{\alpha}{2\pi}\int_x^1 \frac{dy}{y} P(y) d_v\left(\frac{x}{y},Q^2\right)$$

$$= -\frac{\alpha}{2\pi} P \otimes d_v, \tag{51}$$

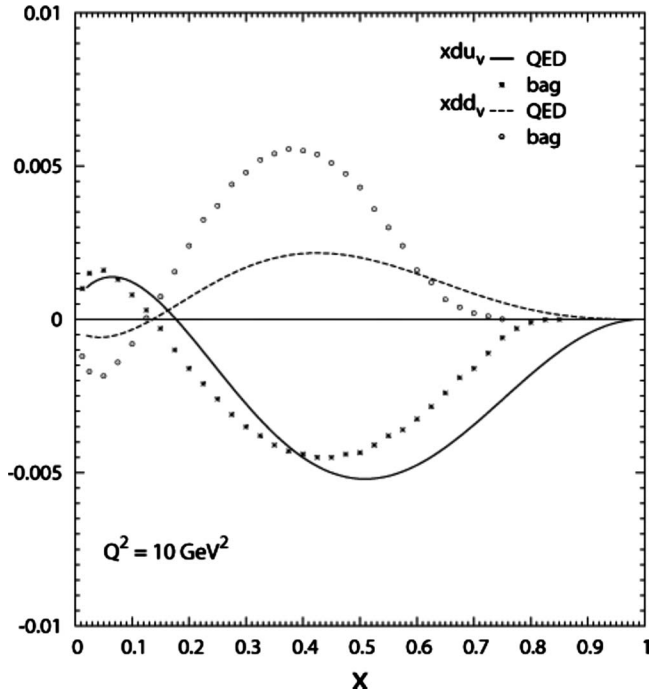

FIG. 10. The isospin-violating majority $x\delta u_v$ (solid curve) and minority $x\delta d_v$ (dashed curve) valence parton distributions (Glück *et al.*, 2005) at $Q^2=10$ GeV^2, assuming QED evolution from a scale set by the current quark mass. These are compared with majority (solid points) and minority (open circles) CSV distributions obtained from theoretical quark model calculations (Rodionov *et al.*, 1994).

$$P(z) = (e_u^2 - e_d^2)\tilde{P}_{qq}(z) = (e_u^2 - e_d^2)\left(\frac{1+z^2}{1-z}\right)_+ .$$

Similar relations hold for the antiquark distributions. Glück *et al.* assumed that the average current quark mass $\bar{m}_q=10$ MeV is the kinematical lower bound for a quark to emit a photon. This is analogous to taking the electron mass as the lower limit for radiation of photons in the earliest calculations of the Lamb shift (before the advent of renormalization group arguments) (Bethe and Salpeter, 1957). Equation (51) is then integrated from $\bar{m}_q^2$ to Q^2. QED evolution effects are evaluated while keeping the QCD effects fixed. The quark distributions appearing on the right-hand side of Eq. (51) are the Glück-Reya-Vogt (GRV) leading-order parton distributions (Glück *et al.*, 1998). In the resulting integrals, in the region $\bar{m}_q^2 \leq q^2 < \mu_{\rm LO}^2 = 0.26$ GeV^2 corresponding to momentum transfers below the input scale for GRV, the PDFs are "frozen," i.e., in this region they are assumed to be equal to their value at the input scale $\mu_{\rm LO}^2$.

The resulting valence isospin asymmetries $x\delta u_v$ and $x\delta d_v$ are plotted in Fig. 10 at $Q^2=10$ GeV^2. For comparison, they are plotted along with the valence quark CSV asymmetries obtained from quark model calculations by Rodionov *et al.* (1994) and Londergan and Thomas (2003a). In the Rodionov calculations CSV distributions arose from diquark mass differences $\delta\tilde{m}=m_{dd}-m_{uu} \approx 4$ MeV (Sather, 1992; Rodionov *et al.*, 1994), and from the target nucleon mass difference $\delta M = M_n - M_p$. While the quantity δu_v is quite similar in both sign and magnitude for both the bag model and the QED calculations, the QED results for δd_v are roughly half as large as the bag model results. This can be understood from the evolution equations of Eq. (51). The coefficients of the QED evolution are equal and opposite for up and down valence quarks, but since u_v is roughly twice d_v, one expects the CSV effects for up quarks to be approximately twice the magnitude and the opposite sign as those for down quarks. As a result, the CSV effects obtained from QED splitting will not obey the relation of Eq. (36) assumed by MRST in their phenomenological fit. As noted previously, the bag model results for valence quark CSV are extremely close to those obtained by MRST using the phenomenological form of Eq. (35) for the best-fit value $\kappa=-0.2$.

The MRST group (Martin *et al.*, 2005) solved the evolution equations of Eq. (47) with assumptions about the parton distributions at the starting scale $Q_0^2=1$ GeV^2. At the starting scale, the sea quark and gluon distributions are assumed to be charge symmetric. The photon PDFs at the starting scale were taken as those due to one-photon radiation from valence quarks in leading-logarithm approximation, evolved from current quark masses $m_u=6$ MeV and $m_d=10$ MeV to Q_0. This produces different photon PDFs for the neutron and proton at the starting scale. Enforcing overall valence parton momentum conservation from Eq. (50) requires valence quark charge asymmetry at the starting scale. MRST assumed a simple phenomenological form chosen to obey the valence quark normalization condition, which produced charge-symmetry violating distributions that resemble the valence PDFs at large and small x and with an overall magnitude chosen to enforce quark momentum conservation. MRST then determined the proton's quark and gluon distributions at the starting scale Q_0^2 by a global fit to an array of high-energy data. The only difference from other MRST global fits is the use of the modified DGLAP evolution equations of Eq. (47). The MRST results for valence quark CSV are quantitatively quite similar to the Glück analysis.

The contribution to CSV arising from QED splitting would occur even if the up and down quark masses and the neutron-proton masses were initially identical. This is different from the CSV terms which were calculated from quark models and described in Sec. III.B. From Eq. (41), it is clear that those CSV terms were proportional to the up-down quark mass difference and the n-p mass difference.

Because the two types of parton charge-symmetry violation tend to arise from different sources and both CSV effects are quite small, we have evaluated them independently and we add them together. Note, however, that the CSV contributions from QED splitting cannot be treated as being completely independent of the quark-model CSV terms. This is because the quark-model calculations used estimates of electromagnetic effects in calculating $m_{dd}-m_{uu}$ as described following Eq. (42).

The quark PDFs calculated using the QED splitting terms in Eq. (47) have explicitly included photon radiation by the quarks. These PDFs are relevant for the quark distribution prior to a hard interaction. Thus, it would be double counting if one included radiative corrections for a quark prior to a hard interaction since these represent the same terms that were included in Eq. (47). Such a procedure corresponds to the "DIS factorization" scheme, which assumes that the $\mathcal{O}(\alpha)$ corrections arising from photon emission from incoming quarks are included in the definition of the quark PDFs. The consistent treatment of partonic radiative corrections has been discussed by Diener *et al.* (2004, 2005).

C. Experimental limits on valence quark charge symmetry

There have been no direct observations of any violation of partonic charge symmetry. As a result we have at present only upper limits on the magnitude of parton CSV. We also have indirect evidence for partonic CSV from the global fits carried out by the MRST group and discussed in Sec. III.A. From Eq. (29) in Sec. II.D, we can obtain a relation between the F_2 structure function in charged-lepton DIS and the average of the F_2 structure functions for neutrinos and antineutrinos, both on isoscalar targets. The difference between these two (appropriately normalized) structure functions is given by two components. The first is a contribution from strange and charmed quarks, and the second is a contribution from partonic CSV.

At small Bjorken x, comparison of these two structure functions will provide a linear combination of heavy quark PDFs and charge-symmetry violating parton distributions. Extracting limits on parton CSV then requires accurate knowledge of heavy quark parton distributions. This is further complicated by the fact that sea quark distributions increase quite rapidly at very small x; so the fractional contribution of partonic CSV is likely to be small in this region.

One has two possibilities for placing stronger experimental limits on partonic CSV. The first is to go to large Bjorken x. Since the heavy quark PDFs are quite small at large x, the relative contribution of charge-symmetry violating parton distributions will be significantly larger. The second possibility is to take the first moment by integrating the parton distributions over all x. One then uses the valence quark normalization condition. This condition, given by Eqs. (17) and (18), requires that the first moment of the valence quark CSV terms vanish. Consequently, if one integrates parton distributions over all x, the valence quark CSV terms must give zero. Following this integration the only remaining contributions will be from the first moment of the sea quark CSV.

1. The charge ratio: Comparison of F_2 structure functions in reactions of muons and neutrinos

Currently, the strongest upper limit on parton CSV distributions is obtained by comparing the F_2 structure functions measured in CC reactions induced by ν and $\bar{\nu}$, and the F_2 structure function for charged lepton DIS, both measured on isoscalar targets. Using the relation derived in Eq. (29), at sufficiently high energies we can construct the ratio

$$R_c(x) \equiv \frac{F_2^{\gamma N_0}(x) + x[s^+(x) + c^+(x)]/6}{5\bar{F}_2^{WN_0}(x)/18},$$
$$R_c(x) \approx 1 + \frac{3[\delta u^+(x) - \delta d^+(x)]}{10\sum_j q_j^+(x)}. \tag{52}$$

In Eq. (52) the function $\overline{F_2}^{WN_0}(x)$ is the average of the CC F_2 structure functions induced by ν and $\bar{\nu}$ and defined in Eq. (30). In the denominator of the second line of Eq. (52) the sum is taken over all quark flavors. Equation (52) shows that in the limit of exact charge symmetry the ratio of the muon and neutrino F_2 structure functions, when corrected for heavy quark contributions and the factor 5/18, should be one independent of x and Q^2, in the naive parton model. The factor 5/18 in Eq. (29) and in Eq. (52) reflects the fact that the virtual photon couples to the squared charge of the quarks while the weak interactions couple to the weak isospin. The quantity R_c is sometimes called the "charge ratio," and the relation between the F_2 structure functions is often termed the "5/18 rule." In Eq. (52) the final line is expanded to lowest order in the (presumably small) CSV terms.

The quantity $R_c(x)$ requires knowledge of the heavy quark PDFs. For example, the observables most sensitive to strange quark distributions are cross sections for opposite sign dimuon events produced from neutrino DIS on nuclei (Bazarko *et al.*, 1995; Goncharov *et al.*, 2001). Once the strange quark distributions have been extracted from the dimuon production process, they can be inserted into Eq. (52). The intrinsic charm PDFs are generally quite small; however, a significant amount of data is collected near charm quark threshold, where it is important to take proper account of the charm mass. Comparing the F_2 structure functions for lepton-induced processes with the F_2 structure functions from weak processes mediated by W exchange, one can in principle measure both the magnitude and x dependence of parton CSV. Clearly, since extraction of parton CSV distributions depends on precise knowledge of strange and charm PDFs, our knowledge of these quantities will be strongly correlated. Certainly this is the case at low x, where the sea quark distributions (including strange quarks) are large.

The charge ratio provides the strongest direct limits to date on parton CSV. There should be no additional QCD corrections to this relation so it should be independent of Q^2, *provided* that the structure functions are calculated in the so-called DIS scheme, where the F_2 structure functions are defined to have the form $F_2(x) = x\Sigma_i e_i^2 q_i^+(x)$ to all orders, where e_i is the quark charge appropriate for either the electromagnetic or weak inter-

actions. For example, the CTEQ4D parton distributions (Lai *et al.*, 1997) were determined in the DIS scheme.

Ever since one has been able to extract the F_2 structure functions and hence the parton distribution functions from both muon and neutrino DIS, one has had the possibility of constructing the charge ratio using Eq. (52). Within error bars, the results have always been consistent with the assumption of parton charge symmetry. However, until a few years ago the charge ratio gave only qualitative upper limits on CSV because of the great difficulty in obtaining precise absolute neutrino cross sections and because of the number of corrections that must be taken into account. These corrections include relative normalization between lepton and neutrino cross sections, contributions from strange and charm quarks, higher twist effects on PDFs, and heavy quark threshold effects. In addition, one must be able to separate F_2 and F_3 structure functions in ν CC reactions. Another potentially important effect is heavy target corrections in neutrino reactions. The most precise lepton structure functions are obtained from deuteron targets, while the most accurate neutrino cross sections are extracted from experiments on heavy targets such as iron, so it is necessary to correct the neutrino F_2 structure functions for heavy target effects and also for effects arising from the fact that iron is not an isoscalar target. These effects include shadowing and antishadowing at small $x \leqslant 0.1$, EMC effects for $0.2 \leqslant x \leqslant 0.6$ (Ashman *et al.*, 1988, 1989), and Fermi motion at large x.

Earlier analyses compared the muon F_2 structure functions of Meyers *et al.* on iron (Meyers *et al.*, 1986) to F_2 obtained from Caltech-Columbia-Fermilab-Rochester-Rockefeller (CCFRR) neutrino measurements (Macfarlane *et al.*, 1984). The extracted ratio R_c of Eq. (52) was consistent with unity, except possibly at the largest value $x=0.65$. The experimental data were consistent with zero charge-symmetry violation and ruled out very large violation of parton charge symmetry. However, the extracted charge ratio had errors of several percent. Because of the factor of 3/10 in the last line of Eq. (52), an error of 5% in the charge ratio would lead to upper limits on parton CSV at roughly the 15% level. From our discussion of the phenomenological and theoretical estimates of parton CSV summarized earlier, we expect that the CSV contribution to the charge ratio will not exceed a few percent at any value of x. Consequently, a measurable deviation of the charge ratio from unity, at any value of x, would be interesting but experimentally quite challenging.

In recent years we have obtained significantly more precise DIS data for both muons and neutrinos. This should allow us to make more stringent tests of parton charge symmetry. The New Muon Collaboration (NMC) group (Amaudruz *et al.*, 1991, 1992; Arneodo *et al.*, 1997) measured the F_2 structure function for muon interactions on deuterium at energy $E_\mu=90$ and 280 GeV. The NMC measurements are more precise than the earlier Bologna-CERN-Dubna-Munich-Saclay (BCDMS) muon scattering results on deuterium (Benvenuti *et al.*, 1990)

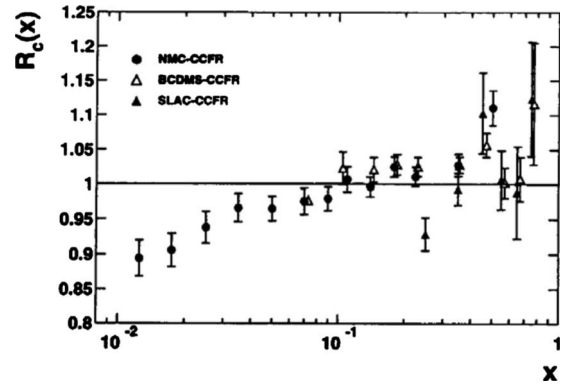

FIG. 11. Charge ratio $R_c^\nu(x)$ of Eq. (52) vs x. Solid circles, CCFR ν-Fe data (Seligman *et al.*, 1997) and $\mu+D$ measurements from NMC (Amaudruz *et al.*, 1991, 1992; Arneodo *et al.*, 1997). Open triangles, CCFR ν data and $\mu+D$ measurements from BCDMS (Benvenuti *et al.*, 1990). Solid triangles, CCFR and SLAC electron scattering data (Whitlow *et al.*, 1990; 1992).

and carbon (Benvenuti *et al.*, 1987), or the SLAC electron scattering results (Whitlow *et al.*, 1990, 1992). The CCFR group (Seligman *et al.*, 1997) extracted the F_2 structure function for ν and $\bar{\nu}$ interactions on iron using the quadrupole triplet beam at Fermilab. They also performed a comprehensive comparison of their neutrino data with the NMC muon results (Seligman, 1997; Seligman *et al.*, 1997). In Fig. 11 we plot the charge ratio R_c of Eq. (52) vs x. The solid circles give the charge ratio comparing the NMC and CCFR measurements. The open triangles give the charge ratio comparing CCFR with BCDMS data, and the solid triangles compare CCFR neutrino data with the SLAC electron scattering measurements.

Analysis of the charge ratio as a function of x should in principle provide a test of parton charge symmetry in both the valence and sea regimes. In the region $0.1 \leqslant x \leqslant 0.4$, where valence quarks should dominate, the charge ratio is consistent with unity, with errors on the charge ratio at about the 3% level. From Eq. (52), this would provide upper limits on valence quark CSV of about 10%. For larger values of x the upper limit on errors in the charge ratio is in the 5–10 % level, due primarily to the poorer statistics and the large Fermi motion corrections that become important at very large x. Particularly after including heavy target corrections for the ν-iron measurements, the charge ratio appeared to deviate significantly from one at the smallest values $x<0.1$ (Boros *et al.*, 1998b). The deviation appeared to grow with decreasing x and reached values as large as 15–20 %. This is apparent from Fig. 11 which shows that R_c^ν is definitely less than 1 for small $x<0.1$. Boros *et al.* (1998a) and Boros, Londergan, and Thomas (1999) studied the origin of this discrepancy. They suggested that, assuming that the identification of the neutrino F_2 CC structure functions was reliable, the most likely explanation for this anomaly was a substantial violation of charge symmetry in the nucleon sea.

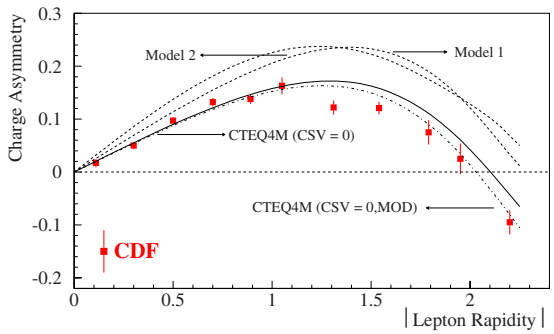

FIG. 12. (Color online) The W charge asymmetry from $p\bar{p}$ reactions at the Fermilab Tevatron. The experimental points are those of the CDF group (Abe *et al.*, 1998). The solid and dash-dotted curves represent two fits using the CTEQ4M PDFs (Lai *et al.*, 1997) with no CSV terms. The dashed and dotted curves represent two different assumptions by Bodek *et al.* (1999) using sea quark CSV distributions calculated by Boros *et al.* (1998a) and Boros, Londergan, and Thomas (1999).

Boros *et al.* showed that one needed sea quark CSV of at least 25% in order to explain this discrepancy in the charge ratio. This apparent violation of charge symmetry was extremely surprising, as it was at least an order of magnitude larger than theoretical estimates. Bodek *et al.* (1999) questioned whether such a large CSV effect was consistent with other experiments. They analyzed the W boson charge asymmetry obtained in $p\bar{p}$ experiments from the CDF group at the Fermilab Tevatron (Abe *et al.*, 1998). Since this experiment involves proton-antiproton scattering, CSV effects do not enter directly. However, Bodek and collaborators argued that the most precise PDFs arise from charged lepton DIS on isoscalar targets. Because the F_2 structure functions are weighted by the squared charge of the quarks, they are most sensitive to up quarks in the proton and neutron. Thus to a significant degree our identification of d^p is obtained from u^n plus the assumption of parton charge symmetry. Bodek examined two different methods for extracting CSV distributions from the data, and calculated the effect on the W charge asymmetry which would arise from CSV effects of the magnitude assumed by Boros *et al.* The results are shown in Fig. 12.

In Fig. 12, the solid and dashed-dotted curves are fits to the CDF data (Abe *et al.*, 1998) using the CTEQ4M parton distributions (Lai *et al.*, 1997) with no parton CSV terms. The dashed and dotted curves resulted from two different assumptions by Bodek *et al.* for the large sea quark CSV terms of Boros *et al.* (1998a) and Boros, Londergan, and Thomas (1999). The CDF measurements are very sensitive to the sea quark distributions, and Bodek argued that the large sea quark CSV was incompatible with those experimental results. Although Bodek and collaborators examined only two potential ways of defining parton CSV distributions, it is hard to imagine that sea quark CSV of this magnitude could be made consistent with the W charge asymmetry data.

This issue was eventually resolved when the CCFR Collaboration reanalyzed its neutrino data (Yang *et al.*, 2001) and the low-x discrepancy disappeared. There were two primary reasons for this change. The first was an improved treatment of charm mass corrections. This was particularly important for the low-x data, which were taken in a region close to charm threshold. In analyzing these data it is necessary to take into account accurately the charm quark mass. The initial analysis used a "slow rescaling" hypothesis due to Georgi and Politzer (Barnett, 1976; Georgi and Politzer, 1976) to account for charm mass corrections. The reanalysis involved NLO calculations, which account for massive charm production using variable-flavor techniques (Aivazis, Collins, *et al.*, 1994; Thorne and Roberts, 1998; Boros, Steffens, *et al.*, 1999).

The second significant effect involved the separation of structure functions in charged-current ν DIS. The sum of ν and $\bar{\nu}$ charged-current DIS cross sections gives a linear combination of F_2 and F_3 structure functions,

$$\frac{d^2\sigma^{\nu}_{\rm CC}}{dx\,dy}+\frac{d^2\sigma^{\bar{\nu}}_{\rm CC}}{dx\,dy}\sim 2(1-y-y^2/2)\bar{F}_2^{WN_0}(x,Q^2) + (y-y^2/2)\Delta xF_3(x,Q^2). \tag{53}$$

In Eq. (53), $\Delta xF_3(x)$ is the difference in the F_3 charged-current structure functions for neutrino and antineutrino beams,

$$\begin{aligned}\Delta xF_3(x)&=xF_3^{W^+}(x)-xF_3^{W^-}(x),\\ \Delta xF_3^{N_0}(x)&\to x\{2[s^+(x)-c^+(x)]+\delta d^+(x)-\delta u^+(x)\}.\end{aligned} \tag{54}$$

The second line in Eq. (54) is valid to leading order in QCD for an isoscalar target and for sufficiently high Q^2. In these limits, assuming the validity of charge symmetry, ΔxF_3 is sensitive only to heavy quark distributions.

For simplicity in Eq. (53) we have dropped terms of order M^2/s and have set the longitudinal to transverse ratio R to zero (these approximations were not made in reanalyzing the data). In the initial analysis (Seligman *et al.*, 1997), the data for a given x bin were averaged over all y, and the ΔxF_3 structure function was estimated using phenomenological PDFs. In the reanalysis the data was binned in x and y so that both $\bar{F}_2$ and ΔxF_3 could be extracted (Yang *et al.*, 2001). The experimental values for ΔxF_3 differed substantially from the phenomenological predictions. From Eq. (53), a change in ΔxF_3 will affect the values extracted for the charged-current F_2 neutrino structure functions. The combined effect of the NLO treatment of charm production and the model-independent extraction of ΔxF_3 removed the small-x discrepancy. The charge ratio R_c of Eq. (52) is now unity to within experimental error even at small x.

The results are shown in Fig. 13. These graphs plot the ratio $5F_2^{\nu}/18F_2^{\mu}$ from the CCFR reanalysis versus Q^2 for various values of x. The different data points involve muon DIS experiments from NMC, BCDMS, and SLAC (Benvenuti *et al.*, 1987, 1990; Whitlow *et al.*, 1992; Arneodo *et al.*, 1997). The curves are NLO analyses using various methods for including charm mass effects

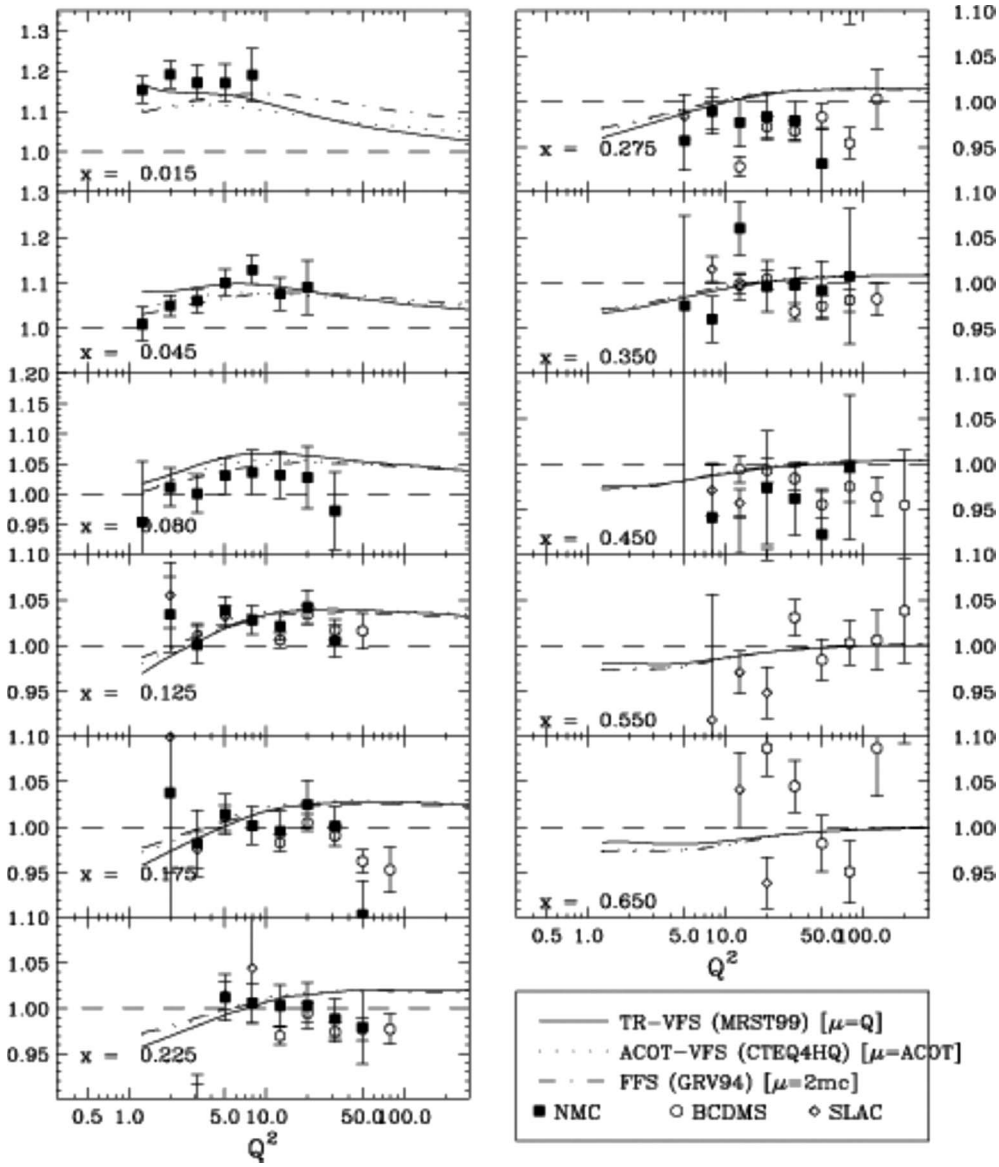

FIG. 13. The ratio $5F_2^{\nu}/18F_2^{\mu}$ calculated by the CCFR Collaboration (Yang *et al.*, 2001). Curves are for various NLO parton calculations. Solid curve, Thorne and Roberts (1998); dotted curve, Aivazis, Collins, *et al.* (1994); and dash-dotted curve, Glück *et al.* (1995). Neutrino structure functions from the CCFR group (Yang *et al.*, 2001). Solid points, NMC muon data (Arneodo *et al.*, 1997); open circles, BCDMS data (Benvenuti *et al.*, 1987); and diamonds, SLAC data (Whitlow *et al.*, 1992).

(Aivazis, Collins, *et al.*, 1994; Glück *et al.*, 1995; Thorne and Roberts, 1998; Boros, Steffens, *et al.*, 1999). The previous low-x discrepancy between theory and experiment has largely disappeared. This allows one to place qualitative limits of $<10\%$ on the magnitude of CSV effects in the sea for values $x \geqslant 0.015$. To obtain more quantitative limits on CSV, it will be necessary to obtain reliable estimates for the few remaining uncertainties in this comparison. Perhaps the largest undetermined correction remains the shadowing of parton distributions for ν-Fe interactions. Experimental analyses have assumed that the nuclear shadowing corrections are the same for neutrinos (virtual W's) as for charged leptons (virtual photons). Boros *et al.* (1998b) showed that one could expect substantially different shadowing for W's than for photons, primarily because the W's couple to axial currents as well as to vector currents. This was further expanded by Kovalenko *et al.* (2002) and Brodsky *et al.* (2004) who calculated both shadowing and antishadowing effects for neutrino DIS.

2. Charge symmetry and determination of the weak mixing angle

The NuTeV group (Zeller *et al.*, 2002a, 2002b) have measured total charged-current and neutral-current cross sections for ν and $\bar{\nu}$ on an iron target. From these measurements they made an independent determination of the weak mixing angle, motivated by a procedure initially suggested by Paschos and Wolfenstein (1973). Paschos and Wolfenstein showed that a ratio of total cross sections for NC and CC interactions for ν and $\bar{\nu}$ on an

isoscalar target N_0 gave the simple Paschos-Wolfenstein (PW) relation

$$R^- \equiv \frac{\langle\sigma_{\rm NC}^{\nu N_0}\rangle - \langle\sigma_{\rm NC}^{\bar\nu N_0}\rangle}{\rho_0^2[\langle\sigma_{\rm CC}^{\nu N_0}\rangle - \langle\sigma_{\rm CC}^{\bar\nu N_0}\rangle]} = \frac{1}{2} - \sin^2\theta_W. \tag{55}$$

In Eq. (55), the quantities are the total NC and CC cross sections for ν and $\bar\nu$ on an isoscalar target, and $\rho_0 \equiv M_W/M_Z\cos\theta_W$ is one in the standard model. The brackets denote integration of the cross sections over all Bjorken x. Although the individual cross sections depend on details of parton distributions, the ratio of these combinations contains no dependence upon PDFs, and in addition a number of experimental effects cancel.

The NuTeV Collaboration used the sign selected quadrupole train beamline at Fermilab to separate ν and $\bar\nu$ arising from pion and kaon decays following the interaction of 800 GeV protons. The resulting interaction events were observed in the NuTeV detector, where they were required to deposit between 20 and 180 GeV in the calorimeter. CC and NC events were distinguished by the event length in the counters, as CC events contained a final muon that penetrated substantially farther than the hadron shower. The NuTeV Collaboration measured the individual ratios R^ν and $R^{\bar\nu}$ defined by

$$R^\nu = \frac{\langle\sigma_{\rm NC}^{\nu N_0}\rangle}{\rho_0^2\langle\sigma_{\rm CC}^{\nu N_0}\rangle}, \quad R^{\bar\nu} = \frac{\langle\sigma_{\rm NC}^{\bar\nu N_0}\rangle}{\rho_0^2\langle\sigma_{\rm CC}^{\bar\nu N_0}\rangle},$$
$$r = \frac{\langle\sigma_{\rm CC}^{\bar\nu N_0}\rangle}{\langle\sigma_{\rm CC}^{\nu N_0}\rangle}. \tag{56}$$

In terms of the ratios defined in Eq. (56), the PW ratio has the form

$$R^- = \frac{R^\nu - rR^{\bar\nu}}{1-r}. \tag{57}$$

The NuTeV group measured $R^\nu = 0.3916 \pm 0.0007$ and $R^{\bar\nu} = 0.4050 \pm 0.0016$. The quantity $r = 0.499 \pm 0.005$ was taken from the world average of ν-Fe charged-current DIS reactions (Blair *et al.*, 1983; Berge *et al.*, 1987) and from measurements by the CCFR Collaboration (Seligman *et al.*, 1997). Since acceptances and cuts differ for ν and $\bar\nu$ reactions, they did not directly construct the Paschos-Wolfenstein ratio via Eq. (55); instead the measured NC/CC ratios were compared with a Monte Carlo simulation of the experiment, from which they extracted the on-shell value for the weak mixing angle $\sin^2\theta_W = 0.2277 \pm 0.0013(\text{stat}) \pm 0.0009(\text{syst})$. This value is three standard deviations above the measured fit to other electroweak processes, $\sin^2\theta_W = 0.2227 \pm 0.00037$ (Abbaneo *et al.*, 2001).

In a given renormalization scheme, the effective weak mixing angle $\sin^2\theta_W$ will acquire a Q^2 dependence from radiative and loop corrections (Czarnecki and Marciano, 1996, 2000; Erler and Ramsey-Musolf, 2005). Figure 14 is due to Erler and Langacker and appeared in the 2008 Particle Review (Amsler *et al.*, 2008), and plots the effective value for $\sin^2\theta_W$ vs Q with the results of several

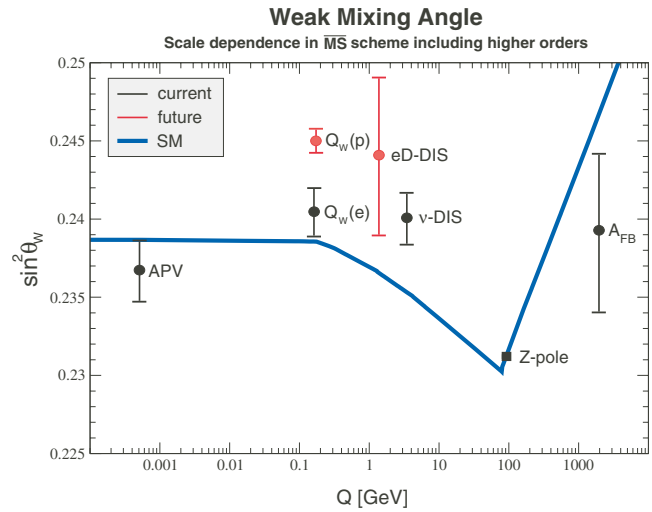

FIG. 14. (Color online) Effective value for $\sin^2\theta_W$ vs Q as calculated by Erler and Langacker in Amsler *et al.* (2008). The solid curve is a standard model calculation in $\overline{\rm MS}$ scheme. Experimental points represent atomic parity violation (APV), Møller scattering $[Q_w(e)]$, measurements at the Z pole, NuTeV (ν-DIS), and forward-backward asymmetry from CDF (A_{FB}). Points represent Q values and error estimates for two proposed experiments, e-D parity violating scattering (eD-DIS), and the Q-weak experiment $[Q_w(p)]$.

experiments. The solid curve is a standard model result (Erler and Ramsey-Musolf, 2005) calculated in minimal subtraction ($\overline{\rm MS}$) scheme. The experimental points represent a recent atomic parity violation (APV) in cesium (Bennett and Wieman, 1999) [this point has now shifted due to a reevaluation of this process (Porsev *et al.*, 2009)], a Møller scattering measurement from experiment E158 at SLAC $[Q_w(e)]$ (Anthony *et al.*, 2005), a series of measurements at the Z pole at LEP and SLAC (Z pole) (Schael *et al.*, 2006), the forward-backward asymmetry of e^+e^- pairs produced from $\bar p p$ collisions at the Fermilab Tevatron by the CDF group (A_{FB}) (Abazov *et al.*, 2008a), and the NuTeV result (ν-DIS) (Zeller *et al.*, 2002a). Additional points give error estimates for two proposed experiments, e-D parity-violation in DIS (eD-DIS) (Souder, 2008), and the Q-weak experiment involving polarized electrons on protons at Jefferson Laboratory $[Q_w(p)]$ (Opper, 2008). Although the error bars on some of the experiments are fairly large, the APV and E158 experiments establish the Q dependence of the effective weak mixing angle at the 6σ level, and the NuTeV experiment appears to differ from the standard model curve by 3σ.

The NuTeV result, which implies an effective left-handed coupling of light quarks to the neutral current that is about 1.2% smaller than obtained from other electroweak data, is rather surprising. The status of what has been termed the NuTeV anomaly has recently been summarized (Londergan, 2005). Davidson *et al.* (2002) considered a number of corrections from physics outside the standard model. A comprehensive review of electroweak physics and constraints on new physics was

given by Erler and Langacker and appeared in Amsler *et al.* (2008). It is quite difficult for new physics to explain the NuTeV finding since such effects have to agree with both the NuTeV result and also with the precise measurements of EW effects at LEP, which constrain some parameters to a few parts per thousand. As a result, most recent efforts have focused on effects within the standard model. At present the three most likely QCD effects are the following: effects due to radiative corrections or nuclear effects in the neutrino reactions, contributions from strange quark momentum asymmetry, charge-symmetry violation in parton distributions, or nuclear corrections to parton distributions. We estimate the probable size of each of these effects on the NuTeV result.

To lowest order in the strong coupling α_s, one can calculate various analytic corrections to the Paschos-Wolfenstein relation. These can be written in the form

$$\delta R^- = \frac{(-1+\frac{7}{3}\sin^2\theta_W)}{U_v+D_v}\left[\frac{(N-Z)}{A}(U_v-D_v)+S^- + \frac{\delta D_v-\delta U_v}{2}\right]. \tag{58}$$

Equation (58) gives estimates of the corrections to the NuTeV result. Terms of the form Q_v denote the second moment (integral over all x) of a given flavor valence distribution, e.g., $U_v=\langle x[u(x)-\bar{u}(x)]\rangle$ represents the total fraction of the proton momentum carried by up valence quarks. The first term is an isoscalar correction due to excess neutrons in the iron target. The NuTeV Collaboration has taken this correction into account. The correction is large (of order −0.008) but should be known to within a couple percent. The second and third terms represent contributions from a possible strange quark momentum asymmetry and from parton charge-symmetry violation, respectively.

Because the NuTeV group did not directly construct the Paschos-Wolfenstein ratio, Eq. (58) gives only an estimate of the effects of these contributions to the NuTeV experiment. The NuTeV group has provided functionals that give the sensitivity of their experiment (in Bjorken x) to various quantities (Zeller *et al.*, 2002b), e.g., charge-symmetry violation or a strange quark momentum asymmetry. To obtain a quantitative result for a particular effect, one multiplies the effect in question by the appropriate functional and integrates over x. For example, corrections to the Paschos-Wolfenstein relation depend only on valence quark properties; sea quarks give no contribution to that relation. Sea quark corrections to the NuTeV experiment are much smaller than the corresponding valence quark contributions, but they are not zero.

Radiative corrections, which involve coupling of soft photons to the final muon line, are important for CC events and constitute a substantial correction. Recently, Diener *et al.* recalculated the radiative corrections, including all corrections of order $\mathcal{O}(\alpha)$ and a number of additional higher-order corrections (Diener *et al.*, 2004, 2005). They found some differences from the older radiative correction program of Bardin and Dokuchaeva (1984). Diener *et al.* also included new terms that result from electromagnetic coupling in the QCD evolution equations. Such terms have recently been included by the MRST group (Martin *et al.*, 2005), and by Glück *et al.* (2005); these contributions were reviewed in Sec. III.B.1. Diener *et al.* estimated that radiative correction effects would remove about one-fourth of the NuTeV anomaly (Diener *et al.*, 2005). Note that these corrections are renormalization scheme dependent. The NuTeV group is currently reanalyzing their data, using a radiative corrections code provided by Diener *et al.* (Bernstein, 2009).

The NuTeV measurements require nuclear corrections for the structure functions. Kumano (2002) calculated a modified PW relation for nuclei, and Hirai *et al.* (2005) estimated that nuclear effects could remove up to one-third of the NuTeV anomaly. They assumed that nuclear shadowing for neutrinos is identical to that for charged leptons (Hirai *et al.*, 2004). Kulagin and Petti (2006, 2007a) also considered nuclear effects, particularly in neutrino deep inelastic-scattering reactions. Miller and Thomas (2005) pointed out that ν shadowing effects could differ significantly from shadowing of muons (Boros *et al.*, 1998b). They also emphasized that shadowing produces different effects for CC and NC events. Kovalenko *et al.* (2002) and Brodsky *et al.* (2004) made a detailed calculation of shadowing and antishadowing arising from multigluon exchange. They concluded that nuclear shadowing effects could account for roughly 20% of the NuTeV anomaly.

Another effect that might contribute to the NuTeV result arises from a strange quark momentum asymmetry; this is the second term in Eq. (58). As discussed in Sec. II.B, it is possible that $s(x)\neq\bar{s}(x)$. Although the first moment of $s-\bar{s}$ must be zero (there is zero net strangeness in the proton), the second moment

$$S^- \equiv \langle x[s(x)-\bar{s}(x)]\rangle = \langle xs^-(x)\rangle \tag{59}$$

[see Eqs. (14)–(16)] need not vanish. A nonzero value for S^- would mean that the net momentum carried by strange quarks and antiquarks was unequal. From Eq. (58) we see that if the strange quark momentum asymmetry S^- is positive (in this case, strange quarks would carry more of the nucleon's momentum than strange antiquarks), this would decrease the extracted value of $\sin^2\theta_W$ and decrease the discrepancy with the expected value of the weak mixing angle; conversely, a negative value of S^- would increase the discrepancy.

The most direct knowledge of strange quark distributions comes from measurements of opposite sign dimuons produced in neutrino-induced nuclear reactions. In such reactions, dimuon production from ν ($\bar{\nu}$) beams is sensitive to the s ($\bar{s}$) distribution so that in principle comparison of these cross sections could enable one to determine differences between s and $\bar{s}$ PDFs. These cross sections have been extracted by the CCFR (Bazarko *et al.*, 1995) and NuTeV (Goncharov *et al.*,

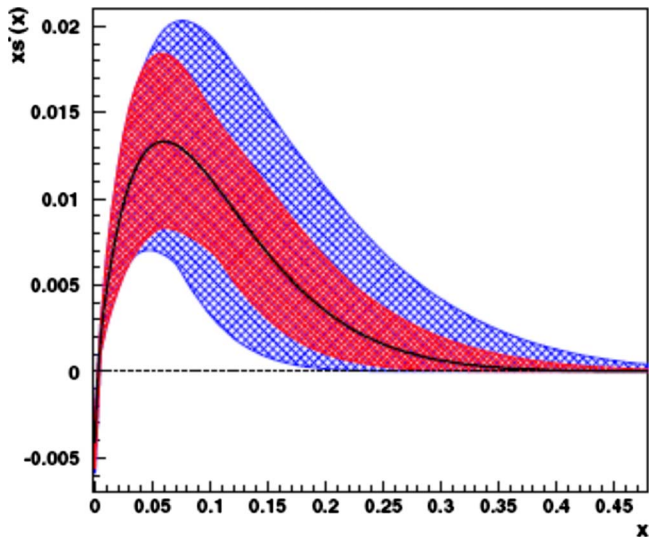

FIG. 15. (Color online) The quantity $xs^-(x)=x[s(x)-\bar{s}(x)]$ vs x, as extracted by the NuTeV Collaboration. Values are obtained for $Q^2=16$ GeV^2. The outer error band is the combined error, while the inner band is without the uncertainty in the semileptonic branching ratio B_c. From Mason *et al.*, 2007.

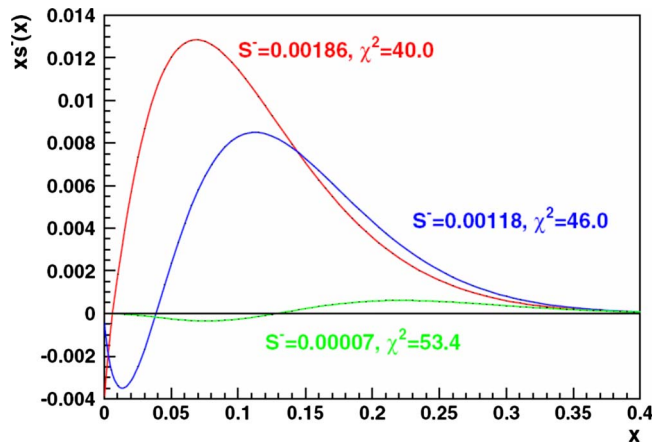

FIG. 16. (Color online) The quantity $xs^-(x)=x[s(x)-\bar{s}(x)]$ vs x, as extracted by the NuTeV Collaboration. Three different results are shown, corresponding to different values of the zero-crossing point. The χ^2 value is listed for each curve. From Mason *et al.*, 2007.

2001) Collaborations. In the CCFR experiment the ν and $\bar{\nu}$ beams are not separated and the type of reaction is inferred from the charge of the faster muon, while the NuTeV experiment uses separated ν and $\bar{\nu}$ beams.

For some time there was disagreement as to the interpretation of the dimuon experiments and extraction of the strange quark PDFs. The NuTeV group analyzed the dimuon cross sections and extracted strange distributions (Zeller *et al.*, 2002b). Their results were consistent with a small value for $s^-(x)$, with a second moment that was zero or slightly negative (Zeller *et al.*, 2002b); the value that they extracted would increase the discrepancy in the weak mixing angle to about 3.7σ. On the other hand, the CTEQ group (Kretzer *et al.*, 2004) estimated that S^- was most likely positive, and they suggested that this could remove roughly one-third of the NuTeV anomaly. The CTEQ global analysis of $s^-(x)$ was dominated by the CCFR and NuTeV data (Bazarko *et al.*, 1995; Goncharov *et al.*, 2001) for opposite-sign dimuon production in neutrino DIS, so it was unclear why the two groups obtained differing results. Since then the CTEQ and NuTeV groups have collaborated on the data analysis, recently obtaining consistent results.

The latest NuTeV result obtained by Mason *et al.* (2007) yields a best value for S^- that is positive. Figure 15 plots the quantity $xs^-(x)$ vs x from the latest NuTeV analysis. This results in a quantity

$$S^- = 0.00196 \pm 0.00046(\text{stat}) \pm 0.00045(\text{syst})^{+0.00148}_{-0.00107}(\text{external}). \tag{60}$$

In Eq. (60), the quantity external refers to the contribution due to uncertainties on external measurements. The strange quark asymmetry of Eq. (60) would remove roughly one-third of the NuTeV anomaly. The NuTeV group provided a detailed error analysis of the quantity S^-. It is quite sensitive to two quantities. First is the semileptonic branching ratio B_c; the outer band in Fig. 15 shows the result for S^- with the B_c uncertainty, and the inner band is the result without the B_c uncertainty. The second is the point at which the quantity $xs^-(x)$ crosses zero (it must cross zero at least once so the first moment of $s-\bar{s}$ is zero). The current best fit crosses zero at a very small value $x\sim 0.004$. This means that $s^-(x)$ would have a very large negative spike at very low x. It is difficult to imagine a physical mechanism that would cause $s^-(x)$ to change sign at such a small value of x.

If one allows the zero-crossing point to increase, then the resulting value of S^- decreases, but the χ^2 value also increases somewhat. The best value obtained by Mason *et al.* $S^-=0.001\,96$ occurs for a zero crossing of $x=0.004$ and $\chi^2=38.2$ for 37.8 effective degrees of freedom. Figure 16 provides examples of the relation between the zero-crossing point, the resulting curve of $s^-(x)$ vs x, and the resulting χ^2. For example, when the zero crossing moves to $x=0.15$, then one obtains $S^-=0.000\,07$ but χ^2 increases to 53.4. Figure 16 shows the strong correlation between strange quark momentum asymmetry $s^-(x)$ and the zero-crossing point.

The contribution from charge-symmetry violating parton distributions to the NuTeV anomaly [the last term in Eq. (58)] can be estimated by folding quark CSV distributions with the functionals provided by the NuTeV group. This contribution is dominated by valence CSV distributions. Using the phenomenological CSV PDFs obtained by the MRST global fit (Martin *et al.*, 2004), valence CSV with $\kappa=-0.6$ would completely remove the NuTeV anomaly, whereas the value $\kappa=+0.6$ would make it twice as large. Both of these values are within the 90% confidence level in the MRST global fit. Thus the uncertainty in parton charge-symmetry violation as calculated by MRST is capable of removing completely the NuTeV anomaly in the weak mixing angle.

We can also investigate parton CSV contributions to the NuTeV result from theoretical calculations. From Eq. (58), the contribution from CSV to the PW ratio is given by

$$\delta R^{-}_{\mathrm{CSV}} \propto \frac{\delta D_v - \delta U_v}{U_v + D_v}. \tag{61}$$

Thus the contribution from CSV to the PW ratio is related to the second moment of the CSV valence PDFs, divided by the total momentum carried by up and down valence quarks. In Sec. III.B we showed that Sather's analytic approximation for valence charge-symmetry violation gave an analytic expression for the second moment of these distributions [see Eq. (44)]. Since these quantities depend only on total momentum carried by valence up and down quarks, quantities which are reasonably well determined, it was argued that the second moments of valence parton CSV were essentially model-independent quantities (Londergan and Thomas, 2003a). This partonic CSV correction would decrease the anomaly in the PW ratio by roughly 40%.

However, as we have stated the NuTeV group did not measure the Paschos-Wolfenstein ratio. If instead one uses the theoretical CSV distributions from Rodionov *et al.* (1994) with the functionals provided by NuTeV, then one finds that valence parton CSV removes about one-third of the anomaly in $\sin^2\theta_W$ (Londergan and Thomas, 2003a, 2003b). Charge-symmetry violation arising from the QED splitting mechanism described in Sec. III.B.1 would remove another one-third of the anomaly.

Davidson and Burkardt (1997) estimated the effect on the Paschos-Wolfenstein relation arising from nuclear charge-symmetry violation, i.e., the fact that protons are more weakly bound than neutrons due to Coulomb effects. Their results suggest that these nuclear Coulomb effects would increase the magnitude of the NuTeV anomaly by roughly 20%.

We have shown that it is necessary to consider a number of QCD effects within the standard model, in order to obtain precise results for the NuTeV experiment. Small but non-negligible contributions are likely from nuclear effects on parton distributions and strange quark effects. Within current experimental limits, charge-symmetry violation appears to be the only mechanism capable of single handedly removing the entire NuTeV anomaly. However, a new nuclear mechanism has recently been suggested by Cloët *et al.* (2009). This nuclear isospin-dependent effect produces results that mimic those arising from charge-symmetry violation, and is capable of making a substantial contribution to the NuTeV measurement. We discuss this effect and the implications for the NuTeV experiment in the following section.

Another possibility would be that a new treatment of radiative corrections might produce significant corrections to the extracted value for the weak mixing angle. However, a reanalysis of the NuTeV data using the newer radiative corrections (Diener *et al.*, 2004, 2005) has not been published at this time (Bernstein, 2009).

D. Isospin-dependent nuclear effects

Many of the tests of partonic charge-symmetry violation, and some applications that rely on CSV, have been carried out with neutrino beams and often with an Fe target—simply to increase the event rate. The NuTeV anomaly, as an example, was carried out with an Fe target, even though the Paschos-Wolfenstein relation is only valid for an isoscalar target. Of course, the cross sections for ν and $\bar{\nu}$ scattering were corrected for the small number of excess neutrons. However, as pointed out by Cloët *et al.* (2009), this will in general not be sufficient. It has been understood for some time (Geesaman *et al.*, 1995) that the famous "EMC effect" (Ashman *et al.*, 1988, 1989), the nuclear modification of the F_2 structure function in electromagnetic DIS reactions, cannot be understood simply in terms of the Fermi motion and binding of free nucleons, but the actual quark structure of the bound nucleon must also be modified in a significant way. A number of relatively successful models have been constructed (Saito *et al.*, 1992; Cloët *et al.*, 2005, 2006), based on the self-consistent modification of the bound nucleon structure in the relativistic mean scalar and vector potentials generated in a nuclear medium. The new realization in the case of Fe, and indeed any other nucleus with $N \neq Z$, is that there will be an isovector piece of the EMC modification of the bound nucleon structure associated with the extra neutrons. Most important, this effect will modify the structure of all of the neutrons and protons in the nucleus, not just the excess neutrons.

As the dominant piece of the isovector interaction in a relativistic mean field theory is usually associated with the ρ meson, it will have a Lorentz vector character, with the d quarks feeling more repulsion and the u quarks more attraction. For this reason the sign of the effect is exactly the same as that found in the calculations of CSV which we have described earlier. If one ignores this medium modification, it will *appear* as though the CSV is enhanced in a nucleus with $N > Z$. We stress that there is no violation of charge symmetry—the isovector interaction is completely consistent with isospin invariance—but to an observer unaware of the isovector EMC effect it will appear like CSV. An estimate of the impact of this additional EMC effect on the NuTeV analysis (Cloët *et al.*, 2009) based on a nuclear matter calculation reduces the NuTeV result for $\sin^2\theta_W$ from 0.2277 to 0.2245, within 1σ of the standard model value.

We have shown that the effects of both true CSV (Londergan and Thomas, 2003a, 2003b) discussed in the previous section and the nuclear isospin-dependent effect just discussed should reduce the discrepancy between the NuTeV result and other determinations of the weak mixing angle. Indeed, a recent theoretical analysis of the contributions of strange quarks, true CSV and the nuclear isospin dependence (Bentz *et al.*, 2009) shows that the combined result of these three effects completely removes the NuTeV discrepancy in the weak mixing angle.

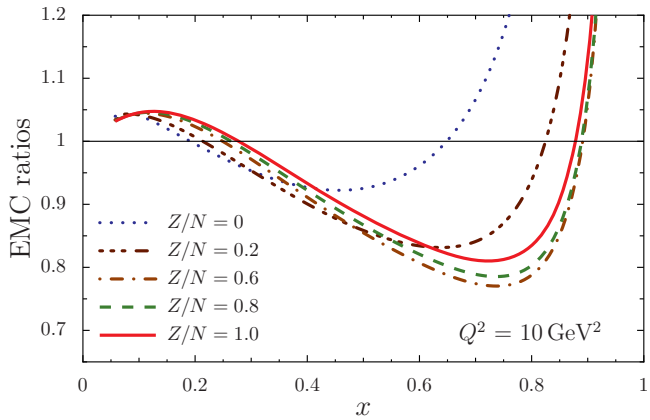

FIG. 17. (Color online) The EMC ratio $F_2^A(x)/F_2^D(x)$ vs x, at a value Q^2=10 GeV^2, predicted by the model of Cloët, Bentz, and Thomas (2009) as a function of the proton/neutron ratio $Z/N \leqslant 1$. Solid curve, Z/N=1; dashed curve, Z/N=0.8; dash-dotted curve, Z/N=0.6; triple dot-dashed curve, Z/N=0.2; and dotted curve, neutron matter (Z/N=0).

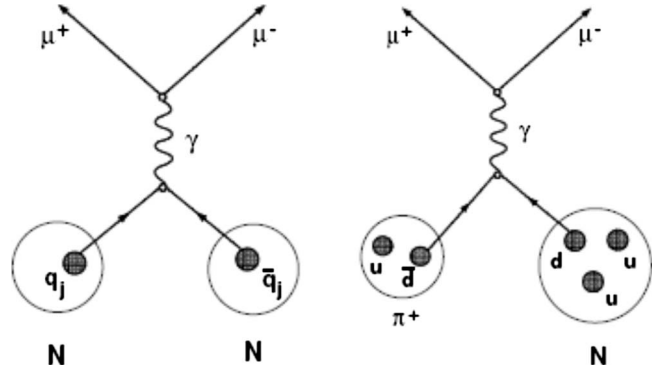

FIG. 18. Schematic of the Drell-Yan (DY) process, production of a μ^+-μ^- pair with high invariant mass through a virtual photon. Left, NN DY process; a quark in one nucleon annihilates with an antiquark of the same flavor in the second nucleon. Right, π^+p DY process in the valence-dominated region of x for both π^+ and p.

It will clearly be important to look for specific processes which could confirm this theoretical analysis of the isovector EMC effect. This model predicts a significant and characteristic A dependence of the ratio of the nuclear F_2 electromagnetic structure function with that for the deuteron. Figure 17 shows the EMC ratio $F_2^A(x)/F_2^D(x)$ vs x at Q^2=10 GeV^2, for various values of $N \geqslant Z$. For a neutron excess, the medium modification of the u quarks should be enhanced by coupling to the ρ^0 field, while the d quark distribution should be less modified. For small neutron excess the EMC effect, which is initially dominated by the u quarks, increases. However, eventually the d quark distribution dominates and the EMC ratio is predicted to decrease in the valence quark region. For example, in Au where $N \sim 1.5Z$, a large difference is predicted between the ratio of $u(x)$ in Au to that in the deuteron, compared with the same ratio for d quarks. This could be investigated in experiments at Jefferson Laboratory following the 12 GeV upgrade.

If the nuclear isospin-dependent effect outlined here is confirmed experimentally, then it would seem that rather than presenting evidence for new physics beyond the standard model the NuTeV result rather confirms in a fairly dramatic fashion the concept that the partonic structure of a bound nucleon is modified in a profound way.

E. Dedicated experiments sensitive to valence quark charge symmetry

In the preceding section we reviewed existing experiments and showed the limits they placed on charge symmetry and flavor symmetry violation in parton distributions. In this section we propose a series of dedicated experiments that might tighten the limits on parton charge symmetry, and we review the conditions that would be necessary in order that these experiments could detect parton CSV at levels that are allowed from current phenomenological limits.

As explained, the experiments described are looking for quite small effects, of the order of 1 or a few percent. In addition, one generally has additional terms arising from other effects such as heavy quark contributions. These must be under control before one can isolate parton CSV effects. Finally, several of these require subtracting cross sections from two separate measurements. These experiments are then very sensitive to relative normalizations. Although these are not easy experiments, it is also true that even tighter upper limits on CSV contributions to parton distribution functions could improve dramatically our understanding of these effects.

1. Drell-Yan processes initiated by charged pions

A suitable probe for charge-symmetry effects should differentiate between up quarks in the proton and down quarks in the neutron. This can be accomplished by comparing Drell-Yan (DY) processes induced by charged pions on isoscalar targets. Drell-Yan processes (Drell and Yan, 1970, 1971) proceed via a quark (antiquark) from the projectile annihilating an antiquark (quark) of the same flavor from the target, producing a virtual photon that eventually decays into a pair of oppositely charged muons with large Q^2. The process is shown schematically in Fig. 18. The left figure shows the mechanism for the NN Drell-Yan process. The right figure shows a schematic diagram for π^+-p Drell-Yan processes, in the kinematic regime where valence quarks dominate for both the pion and nucleon.

We review here the calculation of Londergan *et al.* (1994, 1995), who suggested using Drell-Yan processes initiated by pions to study partonic CSV. At large momentum fraction x, the nucleon distribution is dominated by its three valence quarks, while at large x_π the pion is predominantly a valence q-$\bar{q}$ pair. For DY processes induced by charged pion beams on nucleon targets, in the kinematic region of reasonably large Bjorken

x for both projectile and target quarks the annihilating quarks will come predominantly from the nucleon and the antiquarks from the pion. The π^+ contains a valence $\bar{d}$ (and will annihilate a d quark in the nucleon) and π^- a valence $\bar{u}$ (and will annihilate a nucleon u quark).

Therefore, comparison of π^+ and π^- induced DY processes on an isoscalar target such as the deuteron should provide a sensitive method for comparing d and u valence distributions in the nucleon. As the x and x_π values of interest for the proposed measurements are large, a beam of 50 GeV pions will produce sufficiently massive dilepton pairs that the Drell-Yan mechanism is applicable. A flux of more than 10^9 pions/s is desirable. These experiments might be feasible for fixed target experiments using the Fermilab Main Injector (Reimer, 2007). Alternatively, such experiments would be possible in the COMPASS experiment at CERN (Bradamante, 2008) provided that one used charged pion rather than muon beams. There exist some data for π^+ Drell-Yan scattering from nuclear targets dating from about 30 years ago, Fermilab experiment E444 (Anderson *et al.*, 1979) and CERN experiment WA39 (Corden *et al.*, 1980). As a general rule Drell-Yan experiments with π^+ beams are more difficult than π^- since the pions are generally secondary beams arising from proton bombardment and one must be able to separate the π^+ from protons. In addition, the DY cross sections for π^- will generally be larger than the corresponding DY cross section induced by π^+, as seen from Eq. (62).

Consider the DY process for a charged pion on a deuteron target. Neglecting for the moment sea quark effects, at sufficiently large x and x_π the $\pi^\pm$-D DY cross sections are given by

$$\sigma^{\rm DY}_{\pi^+D}(x,x_\pi) \sim \tfrac{1}{9}[d^p(x)+d^n(x)]\bar{d}^{\pi^+}(x_\pi),$$
$$\sigma^{\rm DY}_{\pi^-D}(x,x_\pi) \sim \tfrac{4}{9}[u^p(x)+u^n(x)]\bar{u}^{\pi^-}(x_\pi). \tag{62}$$

Consider the ratio $R^{\rm DY}_{\pi D}(x,x_\pi)$, defined by

$$R^{\rm DY}_{\pi D}(x,x_\pi) = \frac{4\sigma^{\rm DY}_{\pi^+D}(x,x_\pi) - \sigma^{\rm DY}_{\pi^-D}(x,x_\pi)}{\sigma^{\rm DY}_{\pi^-D}(x,x_\pi) - \sigma^{\rm DY}_{\pi^+D}(x,x_\pi)}. \tag{63}$$

This ratio will be sensitive to charge-symmetry violating (CSV) terms in the nucleon valence parton distributions. Since theoretical CSV effects are no greater than a few percent, sea quark contributions for both nucleon and pion must be included. To first order in small quantities the DY ratio for pions can be written as (Londergan *et al.*, 1994, 2005)

$$R^{\rm DY}_{\pi D}(x,x_\pi) \approx \left(1+\frac{2\pi_S(x_\pi)}{\pi_v(x_\pi)}\right)[R_{CS}(x)+R_{SV}(x,x_\pi)] + R^{\pi}_{CS}(x_\pi), \tag{64}$$

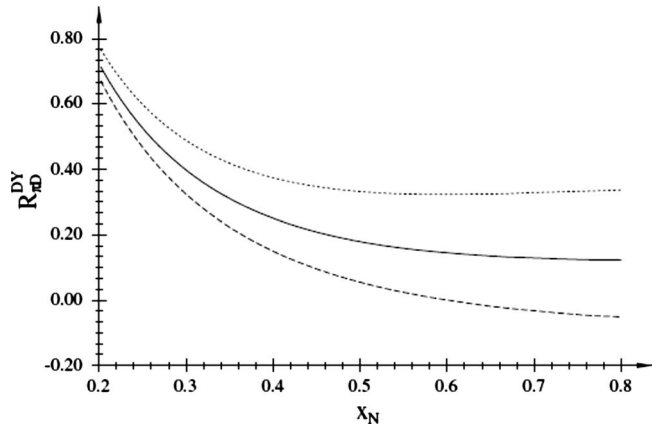

FIG. 19. Theoretical estimate of nucleon CSV term R_{CS} of Eq. (64) vs x for x_π=0.4 and Q^2=25 GeV^2. Solid curve, no CSV terms, κ=0; dashed curve, κ=+0.65; and dotted curve, κ=−0.8. From Londergan *et al.*, 2005.

$$R_{CS}(x) = \frac{4[\delta d_v(x) - \delta u_v(x)]}{3[u_v(x)+d_v(x)]}.$$

The term $R_{SV}(x,x_\pi)$ in Eq. (64) contains sea-valence interference terms which are given by Londergan *et al.* (1994). In Eq. (64) the term $R^{\pi}_{CS}(x_\pi)$ represents a pion CSV contribution; theoretical models predict a very small effect from this term (Londergan *et al.*, 1994).

If we assume charge conjugation invariance and charge symmetry for the pion PDFs, then terms in Eq. (64) have the form

$$\pi_v(x) = u_v^{\pi^+}(x) = \bar{d}_v^{\pi^+}(x) = d_v^{\pi^-}(x) = \bar{u}_v^{\pi^-}(x),$$
$$\pi_S(x) = q_S^{\pi^+}(x) = \bar{q}_S^{\pi^+}(x) = q_S^{\pi^-}(x) = \bar{q}_S^{\pi^-}(x) \tag{65}$$
$$[q=u,d].$$

Equation (64) is valid at sufficiently large x and x_π. It is expanded to lowest order in both sea quark and CSV terms.

The relative DY fluxes for charged pions can be obtained by measuring the yield of J/ψ's from π^+-D and π^--D, which should be identical to within 1% or 2%. The nucleon CSV term $R_{CS}(x)$ in Eq. (64) is a function only of x. A number of systematic errors should cancel in taking the ratio of cross sections. In particular, Eq. (64) is not sensitive to differences between parton distributions in the free nucleon and in the deuteron (Bodek and Ritchie, 1981; Bickerstaff and Thomas, 1982; Frankfurt and Strikman, 1988; Melnitchouk *et al.*, 1994a) provided that both neutron and proton parton distributions are modified in the same way.

In Fig. 19 we show the ratio $R^{\rm DY}_{\pi D}(x,x_\pi)$ vs x for x_π =0.4. For the nucleon PDFs, we used the MRST global fit distributions including a valence CSV contribution of the form of Eq. (35). The pion PDFs were taken from those of Sutton *et al.* (1992). These were fit to older pion DY NA10 and E615 experiments (Betev *et al.*, 1985; Conway *et al.*, 1989); these pion distributions can be

evolved to higher Q^2 using interpolating matrices supplied by the MRST group. Sutton *et al.* (1992) provided several different pion PDFs; for Fig. 19 the authors used pion PDFs for which 10% of the pion momentum was carried by the sea. The pion and nucleon PDFs were evolved to a typical value $Q^2=25$ GeV^2. In Fig. 19, the solid curve corresponds to zero CSV contribution, the dashed curve to $\kappa=+0.65$, and the dotted curve to $\kappa=-0.8$. These curves represent the 90% confidence limit on the CSV distributions for the MRST global fit to valence quark CSV (Martin *et al.*, 2004), given in Eq. (35). The CSV contribution is surprisingly large. At $x=0.5$ the limit of the two CSV terms represents about a 50% correction to the ratio, while at $x=0.8$ the contribution is nearly 100%.

This large contribution from charge-symmetry violation is almost certainly an artifact of the fact that the MRST CSV PDFs are independent of Q^2, while the parton distributions in the denominator depend upon Q^2. This was discussed in Sec. III.A. At large values of Q^2, DGLAP evolution causes valence parton distributions to move to progressively smaller x values. For values $x \geqslant 0.3$, the numerator (Q^2 independent) will remain large while the denominator will become progressively smaller. We expect that the ratios shown in Fig. 19 would decrease substantially if the CSV parton distributions were evolved in Q^2.

In a Drell-Yan π-D experiment, one would first measure DY cross sections over a wide kinematic region, and extract the pion valence and sea distributions. One would then construct the DY ratio of Eq. (64). The ratio could be predicted from the known nucleon PDFs and the pion PDFs that have been extracted from this experiment (assuming no nucleon CSV). The nucleon CSV distributions can then be extracted by comparing the predicted DY ratio with the observed value. Since the DY ratio of Eq. (64) results from subtracting two large and approximately equal terms, it is necessary to determine the relative DY cross sections to a few percent in order for this ratio to be statistically meaningful. Note that one can also exploit the fact that the CSV contribution to the DY ratio depends only on x while the sea-valence term depends upon both x and x_π. If the CSV term is sufficiently large, the process of extracting the CSV distributions may have to be carried out in an iterative fashion.

2. Parity-violating asymmetry in electron scattering

The observation of parity violation in the scattering of polarized electrons from the deuteron, carried out in 1978 by Prescott *et al.* (1978), played a major role in validating the standard model. Recent advances in the technology of parity-violating experiments provide the possibility of repeating such experiments with an increase in precision of better than an order of magnitude (Young *et al.*, 2007; Arrington *et al.*, 2009). These new experiments would allow a new precision measurement of the weak mixing angle, they could probe physics beyond the standard model at the multi-TeV scale, and could provide tight constraints on nucleon parton distribution functions at large Bjorken x. In particular, the ratio $d(x)/u(x)$ at very large x is not well determined (Botje, 2000). As we will show, parity-violating electron scattering also has the possibility of observing parton charge-symmetry violation at large Bjorken x.

The parity-violating (PV) asymmetry $A_{\rm PV}$ for electron scattering on a nucleon can be written to lowest order in the γ-Z interference in terms of the structure functions

$$A_{\rm PV}(x,y) = \frac{-G_F Q^2}{4\sqrt{2}\pi\alpha}[g_A^e r_1(x) + f(y) g_V^e r_2(x)],$$

$$f(y) = \frac{1-(1-y)^2}{[1+(1-y)^2]}, \quad y \equiv 1 - \frac{E'}{E},$$

$$r_1(x) \equiv \frac{F_1^{\gamma Z}(x)}{F_1^{\gamma}(x)} = \frac{2\sum_q e_q g_V^q q^+(x)}{\sum_q e_q^2 q^+(x)}, \tag{66}$$

$$r_2(x) \equiv \frac{F_3^{\gamma Z}(x)}{2F_1^{\gamma}(x)} = \frac{2\sum_q e_q g_A^q q^-(x)}{\sum_q e_q^2 q^+(x)},$$

$$g_V^e = -1 + 4\sin^2\theta_W, \quad g_A^e = -1.$$

In Eq. (66), we dropped some small corrections to the quantity $f(y)$ and assumed the Bjorken limit where the longitudinal cross section is negligible relative to the transverse cross section. The additional terms are included in work by Hobbs and Melnitchouk (2008). In the proposed Jefferson Laboratory PV experiment, the incident electron energy E will be in the range 10–11 GeV and the outgoing E' will run from 2 to 4 GeV. The parton model expressions for the ratios of structure functions are given by r_1 and r_2 in Eq. (66).

If we confine our attention to the region of x above 0.3 then the contribution to Eq. (66) from sea quarks should be quite small. Assuming that electron-deuteron scattering is given by the impulse approximation (the sum of scattering from proton plus neutron), and also assuming parton charge symmetry the expression for PV e-D scattering can be written as

$$A_{\rm PV}^{eD}(x,y) = \frac{-G_F Q^2}{4\sqrt{2}\pi\alpha}[a_1^d + f(y) a_3^d]. \tag{67}$$

In Eq. (67), for couplings at the tree level we have

$$a_1^d = \frac{6g_A^e}{5}(2g_V^u - g_V^d),$$

$$a_3^d = \frac{6g_V^e}{5}(2g_A^u - g_A^d). \tag{68}$$

In Eq. (68), the quark vector couplings are given in Eq. (27), and the quark axial couplings are

$$g_A^u = \tfrac{1}{2}, \quad g_A^d = -\tfrac{1}{2}. \tag{69}$$

In this region and with these assumptions, the PV asymmetry for e-D scattering depends weakly on y [the second term in Eq. (67) is significantly smaller than the first term] and is independent of x and of quark PDFs.

We can now include the lowest-order CSV contribution to the parity-violating e-D asymmetry. In Eq. (67), the terms a_1^d and a_3^d are modified to

$$\begin{aligned} a_1^d &\to a_1^{d(0)} + \delta^{(\mathrm{CSV})} a_1^d, \\ a_3^d &\to a_3^{d(0)} + \delta^{(\mathrm{CSV})} a_3^d, \\ \frac{\delta^{(\mathrm{CSV})} a_1^d}{a_1^{d(0)}} &= \left[-\frac{3}{10} + \frac{2g_V^u + g_V^d}{2(2g_V^u - g_V^d)} \right] \frac{\delta u(x) - \delta d(x)}{u(x) + d(x)}, \\ \frac{\delta^{(\mathrm{CSV})} a_3^d}{a_3^{d(0)}} &= \left[-\frac{3}{10} + \frac{2g_A^u + g_A^d}{2(2g_A^u - g_A^d)} \right] \frac{\delta u(x) - \delta d(x)}{u(x) + d(x)}. \end{aligned} \tag{70}$$

We note that in Eq. (70) the largest contribution to the CSV effect in the parity-violating electron scattering asymmetry comes from the CSV contribution to the denominator, i.e., from the structure function $F_1^{\gamma D}(x)$ (this is the origin of the 3/10 term). The CSV terms will produce a correction to the PV asymmetry which has a characteristic dependence on Bjorken x.

Figure 20 shows the change in the e-D PV asymmetry $\delta A_{\mathrm{PV}}^{eD}/A_{\mathrm{PV}}^{eD}$ arising from CSV effects, calculated by Hobbs and Melnitchouk (2008). This is obtained from Eq. (70) vs Bjorken x, for electron incident energy 10 GeV. The first graph plots the ratio for $Q^2=5$ GeV^2 and the second graph is for $Q^2=10$ GeV^2. The CSV PDFs are obtained from the phenomenological global fit to high-energy data from the MRST group (Martin *et al.*, 2004). The valence CSV distributions were parametrized using Eq. (35). The three dashed curves represent different values for the overall parameter κ. One curve shows the best-fit value $\kappa=-0.2$. The outer curves represent the values $\kappa=-0.8$ and $+0.65$; these two values denote the 90% confidence limit for the valence CSV allowed in the MRST global fit.

Within the 90% confidence limit, the predicted CSV contribution to the PV asymmetry tends to increase with increasing Bjorken x. The magnitude of the CSV contribution increases with increasing Q^2; for $Q^2=10$ GeV^2, the CSV contributions allowed within the MRST 90% confidence level range between roughly -0.025 and $+0.03$ at a value $x=0.7$. Thus if experiments could achieve a precision of about 1% in the asymmetry, it should be possible either to observe effects of partonic CSV in this experiment or alternatively to put strong constraints on upper limits for partonic charge-symmetry violating effects. Note that our results are model dependent, as the MRST group chose the particular functional form given in Eq. (35) for their partonic CSV PDFs. In addition, for simplicity MRST neglected the Q^2 dependence of the CSV parton distribution functions in their global fits to high-energy data.

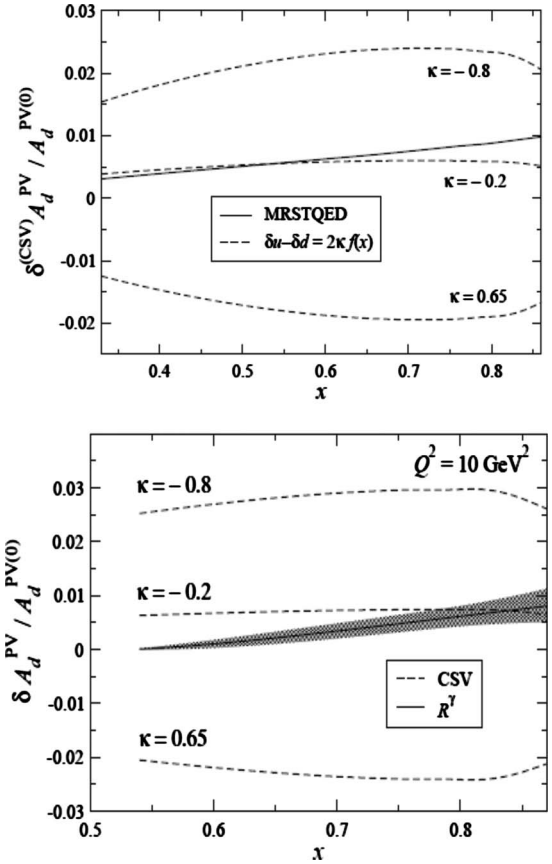

FIG. 20. The contribution from partonic CSV effects to the PV asymmetry for e-D scattering with incident electron energy 10 GeV (Hobbs and Melnitchouk, 2008). The CSV contribution is given by Eq. (70). Curves are labeled by the value of κ from the phenomenological fit of valence CSV distributions determined from the MRST group (Martin *et al.*, 2004) and Eq. (35). The best fit $\kappa=-0.2$ and the 90% confidence limits are represented by $\kappa=+0.65$ and $\kappa=-0.8$. Upper figure, $Q^2=5$ GeV^2. Lower figure, $Q^2=10$ GeV^2.

There is an additional uncertainty in the parity-violating asymmetries. Since our predicted PV asymmetry becomes significant only at large x, we need to account for the fact that the d/u ratio in the proton is rather poorly known in this region. This uncertainty was studied by Botje (2000) who extracted quark PDFs from a QCD analysis of combined HERA and fixed-target data. A precise determination of d/u at large x comes from the NMC measurements of muon DIS on proton and deuteron targets (Amaudruz *et al.*, 1991, 1992; Arneodo *et al.*, 1997). However, in both cases the limit on accuracy is not the data but the theoretical understanding of the EMC effect in deuterium. For example, the covariant treatment of Fermi motion and binding by Melnitchouk and Thomas (1996) showed that, contrary to the conclusions in the original paper, the SLAC data were consistent with the perturbative QCD predictions for the u/d ratio as $x\to 1$. For $x>0.4$ the errors on the QCD predictions grow fairly rapidly. This occurs because the electromagnetic coupling is weighted by the squared charge of the quark flavor.

An independent measurement of d/u in the proton can be obtained by measuring W production in p-$\bar{p}$ collisions. In these reactions a W^+ tends to be produced by annihilation of a u quark from the proton and a $\bar{d}$ from the antiproton, while a W^- is produced from a d quark in the proton and a $\bar{u}$ from the antiproton. Because the u quark carries a larger momentum fraction than the d quark, W^+ production will tend to be boosted in the proton direction while W^- will be boosted in the antiproton direction. One measures a forward-backward asymmetry $A(y_l)$, where

$$A(y_l) = \frac{d\sigma(\ell^+)/dy_l - d\sigma(\ell^-)/dy_l}{d\sigma(\ell^+)/dy_l + d\sigma(\ell^-)/dy_l}. \tag{71}$$

In Eq. (71), y_l is the rapidity of the lepton arising from decay of the W, and $d\sigma(\ell^\pm)/dy_l$ is the differential cross section for charged lepton production. This is a convolution of the cross section for W production, with the relevant $W \to \ell\nu$ decay distribution (Martin *et al.*, 1990; Melnitchouk and Peng, 1997).

The forward-backward asymmetries have been measured by the CDF (Acosta *et al.*, 2005) and D0 (Abazov *et al.*, 2008a, 2008b) groups at the Fermilab Tevatron for p-$\bar{p}$ collisions at $\sqrt{s}=1.96$ TeV. The asymmetries tend to be particularly sensitive to the slope of the d/u ratio. The higher the rapidity, the larger the x range for which d/u can be studied (Abazov *et al.*, 2008a).

The d/u ratio could also be determined from large-x parity-violating electron scattering on hydrogen since the PV amplitude preferentially couples to the down quark. This information could in principle fix the d/u ratio in the proton and eliminate some of the uncertainty in PV DIS reactions on deuterium.

3. Charged pion leptoproduction from isoscalar targets

In the preceding section it was pointed out that DY processes for charged pions on nucleons can test CSV because the $\pi^\pm$ contain different valence antiquarks. For this reason, semi-inclusive pion production, from lepton DIS on nuclear targets, could be a sensitive probe of CSV effects in nucleon valence parton distributions (Londergan *et al.*, 1996, 2005). The cross section for this process is given by (Levelt *et al.*, 1991)

$$\frac{1}{\sigma_N(x)}\frac{d\sigma_N^h(x,z)}{dz} = \frac{N^{Nh}(x,z)}{\sum_i e_i^2 q_i^N(x)},$$
$$N^{Nh} \equiv \sum_i e_i^2 q_i^N(x) D_i^h(z). \tag{72}$$

The quantity N^{Nh} in Eq. (72) is the yield of hadron h per scattering from nucleon N, and $D_i^h(z)$ is the fragmentation function for a quark of flavor i into hadron h. $D_i^h(z)$ depends on the quark longitudinal momentum fraction $z=E_h/\nu$, where E_h and ν are the energy of the hadron and the virtual photon, respectively.

For pion electroproduction on an isoscalar target, charge symmetry relates the "favored" production of charged pions from valence quarks by

$$N_{\rm fav}^{D\pi^+}(x,z) = 4N_{\rm fav}^{D\pi^-}(x,z). \tag{73}$$

In Eq. (73), $N_{\rm fav}^{D\pi^+}(x,z)$ represents the yield of π^+ per scattering from the deuteron, via the favored mode of production [for π^+ (π^-) production, the favored mode of charged pion production is from the target up (down) quarks]. The HERMES Collaboration at HERA (van der Steenhoven, 1996a, 1996b) has measured semi-inclusive pion production from hydrogen and deuterium.

Londergan *et al.* (1996, 2005) showed that the ratio $R^\Delta(x,z)$ is sensitive to parton CSV effects, where the ratio is defined by

$$R^\Delta(x,z) \equiv \frac{8\{N^{D\pi^-}(x,z)/[1+4\Delta(z)] - N^{D\pi^+}(x,z)/[4+\Delta(z)]\}}{N^{D\pi^+}(x,z) - N^{D\pi^-}(x,z)},$$
$$R^\Delta(x,z) = C^\Delta(z)[R_{CS}(x) + R_{SV}(x,z)], \quad \Delta(z) \equiv \frac{D_u^{\pi^-}(z)}{D_u^{\pi^+}(z)}, \quad C^\Delta(z) = \frac{8[1+\Delta(z)]}{[1+4\Delta(z)][4+\Delta(z)]}. \tag{74}$$

Equation (74) is evaluated at moderately large x, where the sea/valence ratio is small. It has been expanded to first order in the CSV nucleon terms and the sea quark distributions. The term $R_{CS}(x)$ is given by Eq. (64), and $R_{SV}(x,z)$ is a sea-valence interference term given by Londergan *et al.* (1996). A CSV part of the fragmentation function has been dropped as theoretical estimates suggest that this term should be very small (Londergan *et al.*, 1996).

The ratio R^Δ of Eq. (74) has an overall factor that depends only on z; the normalization of the ratio is chosen to make this term close to one for moderate values of z. The remainder of this ratio contains two terms. The first term depends only on x, and is proportional to the nucleon valence CSV fraction; it is identical to the term $R_{CS}(x)$ defined in Eq. (64), which could be measured in pion Drell-Yan reactions. The final term in Eq. (74) depends on both x and z; it is proportional to the sea quark

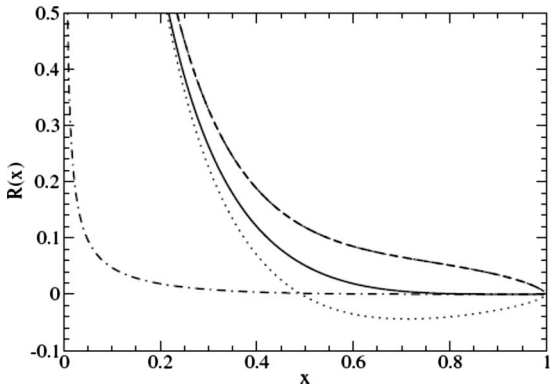

FIG. 21. Contributions of various terms to the ratio $R^{\Delta}(x,z)$ defined in Eq. (74) vs x at fixed $z=0.4$. Solid (dot-dashed) curves, nonstrange and strange sea quark contributions. Long dash-dotted (dotted) curves, CSV contributions from Eq. (74) for $\kappa=-0.8$ and +0.65, respectively. Curves are calculated for $Q^2=2.5$ GeV^2.

contributions and becomes progressively less important at large x.

Figure 21 shows the x-dependent contributions to the ratio $R^{\Delta}(x,z)$ of Eq. (74) vs x at fixed $z=0.4$ (Londergan *et al.*, 2005). The solid (dot-dashed) curves show the nonstrange (strange) sea contributions to the ratio. The strange quark contribution is negligible except at extremely low x. The long dashed-dotted and dotted curves show the contributions from quark CSV contributions from the MRST global fit with $\kappa=-0.8$ and +0.65, respectively; these represent the 90% confidence limits for the MRST CSV PDFs. At this value of z, the coefficient $C^{\Delta}(z)$ from Eq. (74) has a value very close to 1. The CSV terms are substantial only for large $x\geqslant 0.4$. The ratio requires precise experimental measurements of the x dependence of $R^{\Delta}(x,z)$ for fixed z. Note that this depends critically on the validity of the factorization hypothesis for the semi-inclusive yields, as given by Eq. (72).

For $x\geqslant 0.4$, the contributions from charge-symmetry violating PDFs are substantial, and they rapidly become the dominant contribution at larger x. Thus, at the levels determined by the MRST global fit, it would appear that precise measurements of charged pion production in semi-inclusive DIS electroproduction reactions on deuterium have the possibility of observing these isospin-violating effects, or they would be able to lower the current allowed limits on partonic CSV effects. Theoretically it would be possible to observe such effects in measurements of $e+D\to\pi^{\pm}+X$ at Jefferson Laboratory. However, the validity of Eq. (74) requires that factorization (the fragmentation function for quarks into pions) be valid to within a few percent. It would be necessary to demonstrate that factorization is obeyed to a very high degree, at energies available at Jefferson Laboratory.

The validity of factorization has been checked for semi-inclusive deep inelastic reactions at Jefferson Laboratory energies. Navasardyan *et al.* (2007) measured charged pion electroproduction from p and D with 5.5 GeV electrons. They were compared with a factorization hypothesis

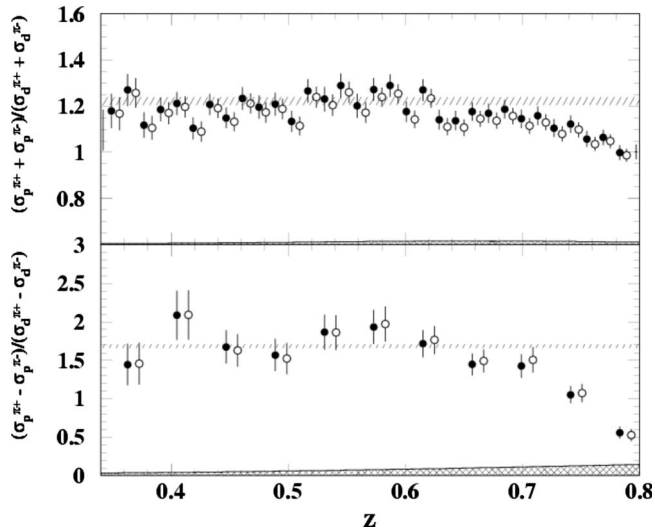

FIG. 22. Ratios of proton to deuteron semi-inclusive charged pion electroproduction cross sections on proton and deuteron at fixed $x=0.32$ as a function of z (Navasardyan *et al.*, 2007). Solid (open) symbols reflect data after (before) subtraction of coherent ρ production events. Symbols are offset slightly in z for clarity. Top curve, sum of π^+ and π^- cross sections [first equation in Eq. (76)]; bottom curve, difference of cross sections [second equation in Eq. (76)]. The hatched area in the bottom curve indicates systematic uncertainties. The shaded bands represent a variety of calculations in both leading and next-to-leading order QCDs from CTEQ (Lai *et al.*, 2000) and GRV (Glück *et al.*, 1998).

$$d\sigma \sim \sum_q e_q^2 q(x,Q^2) D_{q\to\pi}(z,Q^2) \times e^{-bp_T^2}\left[\frac{1+A\cos\phi+b\cos(2\phi)}{2\pi}\right]. \tag{75}$$

With factorization, the semi-inclusive cross section appears as the product of a parton distribution function depending on x but not z, times a fragmentation function for a quark to a pion that depends on z but not x. Assuming factorization, one can derive expressions for ratios of the pion electroproduction cross sections on protons and deuterium,

$$\frac{\sigma_p(\pi^+)+\sigma_p(\pi^-)}{\sigma_D(\pi^+)+\sigma_D(\pi^-)} = \frac{4u^+(x)+d^+(x)}{5[u^+(x)+d^+(x)]},$$
$$\frac{\sigma_p(\pi^+)-\sigma_p(\pi^-)}{\sigma_D(\pi^+)-\sigma_D(\pi^-)} = \frac{4u_v(x)-d_v(x)}{3[u_v(x)+d_v(x)]}. \tag{76}$$

Figure 22 shows ratios of pion electroproduction cross sections on p and D at fixed $x=0.32$ vs z. From Eq. (76), these linear combinations should be independent of z. Now, a number of assumptions have gone into Eq. (76); in addition to factorization, this relation assumes parton charge symmetry, neglects contributions from heavy

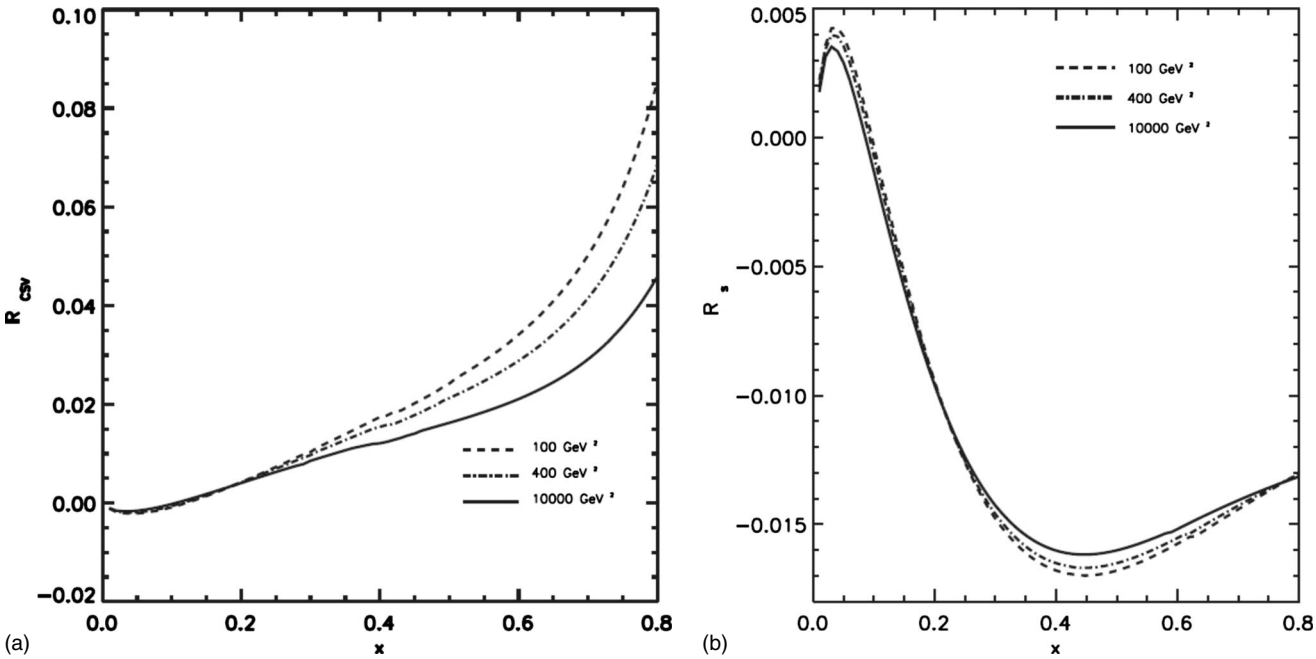

FIG. 23. Contributions to the ratio of F_2 structure functions in charged-current electroweak interactions [the quantity $R_W(x)$ in Eq. (78)]. Left, theoretical estimates of CSV contribution to $R_W(x)$. Right, strange quark contribution to $R_W(x)$ (Londergan *et al.*, 1998).

quarks and also contributions from any p_T dependence of parton distributions. Nevertheless, to within about 10% the ratios show little dependence on z for $z<0.7$. The deviation from these curves for $z>0.7$ results from the $N\to\Delta$ transition region. Furthermore, the shaded bands show the ratio that is expected from phenomenological parton distributions from the CTEQ Collaboration (Lai *et al.*, 2000) and from GRV (Glück *et al.*, 1998). A strong test of factorization requires data over a wide range of Q^2; however, within the available Q^2 range the Jefferson Laboratory experimental results are consistent with the factorization hypothesis.

Despite the perhaps surprisingly good agreement with the factorization hypothesis in this energy region, nevertheless factorization is not sufficiently accurate to carry out tests of charge-symmetry violation in pion electroproduction reactions, at current Jefferson Laboratory energies. The relations given in Eq. (74) would be more reliable at a possible future electron-ion collider, where factorization should be assured to a high degree. As Eq. (74) was derived in lowest-order QCD, it is necessary to check whether the results remain essentially unchanged in NLO.

4. Test of weak current relation $F_2^{W^+N_0}(x)=F_2^{W^-N_0}(x)$

From Eq. (28), at high energies the F_2 structure functions for charge-changing neutrino and antineutrino interactions on an isoscalar target are equal except for contributions from valence quark CSV, plus strange and charm quark terms, i.e.,

$$F_2^{W^+N_0}(x,Q^2)-F_2^{W^-N_0}(x,Q^2) = x\{\delta d_v(x)-\delta u_v(x)+2[s^-(x)-c^-(x)]\}. \tag{77}$$

These cross sections might be measured at various experimental facilities. At a high-energy electron collider, weak interaction processes such as $e^-p\to\nu_e X$ are no longer completely negligible with respect to the electromagnetic process $e^-p\to e^-X$. Charged-current cross sections in $e^\pm$-p reactions were measured at HERA (Adloff *et al.*, 2003), where precise structure functions and parton distributions were determined for momentum transfers $Q^2>100$ GeV^2. Tests of parton charge symmetry would require collisions of electrons with an isospin-zero nucleus such as the deuteron. Then by comparing charge-changing weak interactions induced by electrons and positrons Eq. (77) could be measured. This might be feasible at a future electron-ion collider.

Alternatively with very high-energy neutrinos, the ratio of Eq. (77) could be measured by comparing W boson production on an isoscalar target induced by neutrinos and antineutrinos. Theoretical estimates of this process were made by Londergan *et al.* (1998). One constructs the ratio

$$\begin{aligned} R_W(x) &\equiv \frac{2[F_2^{W^+D}(x)-F_2^{W^-D}(x)]}{F_2^{W^+D}(x)+F_2^{W^-D}(x)} \\ &\approx \frac{\delta d_v(x)-\delta u_v(x)+2[s^-(x)-c^-(x)]}{\sum_j q_j^+(x)} \\ &\equiv R_{\mathrm{CSV}}(x)+R_S(x). \end{aligned} \tag{78}$$

At sufficiently high energies, the only quantities contrib-

uting to the ratio R_W are "valence" strange and charm distributions or valence quark CSV terms. The ratio could also be checked for any isoscalar nuclear target, replacing the nucleon parton distributions by their nuclear counterparts.

Figure 23 (left) shows the theoretical CSV contribution, $R_{CSV}(x)$ from Eq. (78). The dashed curve is calculated for $Q^2=100$ GeV^2, the dot-dashed curve is calculated for $Q^2=400$ GeV^2, and the dashed-triple dotted curve is calculated for $Q^2=10\,000$ GeV^2. The quantity $R_{\mathrm{CSV}}(x)$ is predicted to be greater than 0.02 provided $x>0.4$, using CSV estimates of Rodionov *et al.* (1994). All theoretical calculations predict that in the valence region, $\delta d_v(x)$ is positive and $\delta u_v(x)$ negative, so their effects should add, producing several percent effects at the largest values of x. The term R_s of Eq. (78), proportional to the difference between strange quark and antiquark distributions (we neglect possible contributions from charm quarks), is shown in Fig. 23 (right).

As mentioned in Sec. II.B and expanded upon in Sec. III.C.2, there are now experimental measurements from which one can extract the strange quark asymmetry $s^-(x)=s(x)-\bar{s}(x)$. These come from production of opposite-sign dimuon pairs in reactions initiated by ν or $\bar{\nu}$ beams, from the CCFR and NuTeV groups (Bazarko *et al.*, 1995; Goncharov *et al.*, 2001). The first moment $\langle s^-(x)\rangle$ must be zero since there is no net strangeness in the nucleon. This means that if there is a nonzero strange quark asymmetry, it must have at least one node in x. The latest analysis of these results by Mason *et al.* (2007) gives a positive value for the second moment $S^-=\langle xs^-(x)\rangle$; this is in agreement with analyses of these experiments by the CTEQ group (Kretzer *et al.*, 2004).

Note that these results have the opposite sign for the strange quark asymmetry from the calculations of Braendler *et al.* shown in Fig. 23. Those results were calculated in the framework of "meson-cloud" models (Signal and Thomas, 1987; Ji and Tang, 1995; Brodsky and Ma, 1996; Holtmann *et al.*, 1996; Melnitchouk and Malheiro, 1997; Speth and Thomas, 1997) extended to include strange quarks. In these models the nucleon fluctuates to a configuration $N\to K+Y$, where Y represents a Λ or Σ baryon. The $\bar{s}$ quark is associated with the virtual kaon production, while the s quark resides with the residual strange baryon (Signal and Thomas, 1987). Figure 24 shows the quantity $s(x)-\bar{s}(x)$ calculated using the model of Melnitchouk and Malheiro (1997). The curves show values of $s-\bar{s}$ calculated using various values for the $N\to KY$ form factor, and the shading represents the uncertainty in the calculations. In the Melnitchouk-Malheiro calculation the $s(x)-\bar{s}(x)$ difference also has the opposite sign from the experimental determination although it should be noted that to within one standard deviation the experimental result is consistent with zero. For both the meson-cloud and experimental values for $s(x)-\bar{s}(x)$, the magnitude of the strange quark contribution to R_W in Eq. (78) is comparable to the contribution arising from CSV although the x dependence of the two contributions is quite different.

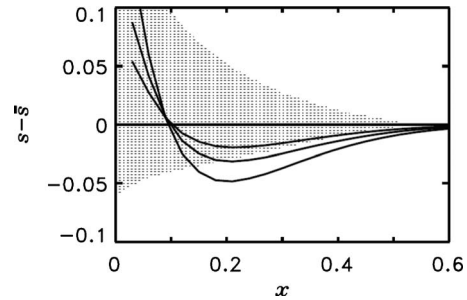

FIG. 24. The strange quark asymmetry $s(x)-\bar{s}(x)$ calculated in a meson-cloud model. The curves correspond to different values for the *NKY* form factor. The shaded region is an estimate of the uncertainty in the calculations. From Melnitchouk and Malheiro, 1997.

IV. CHARGE-SYMMETRY VIOLATION FOR SEA QUARKS

For valence quark charge symmetry, several theoretical models give quantitatively similar predictions for charge-symmetry violating PDFs. Estimates of valence quark CSV by Sather (1992) and Rodionov *et al.* (1994) are in rather good agreement, and both the magnitude and shape of those valence CSV PDFs agree quite well with the best phenomenological global fit from the MRST group (Martin *et al.*, 2004). The situation is much different for charge symmetry in the sea quark sector. It is considerably more difficult to construct reliable theoretical models to estimate sea quark CSV effects, and until recently the phenomenological situation was less certain. As we have seen, one problem is that the tests of charge symmetry generally combine effects from heavy quarks in addition to CSV terms. At sufficiently large x the contributions from heavy quarks should become extremely small relative to valence quark CSV effects. However, at small x strange quark contributions are significant. Unless these contributions are known quite precisely, it is difficult to determine the upper limits on parton CSV in the sea.

A. Estimates of sea quark CSV

The MRST group also searched for the presence of charge-symmetry violation in the sea quark sector (Martin *et al.*, 2004). They chose a specific functional form for sea quark CSV, dependent on a single parameter $\tilde{\delta}$,

$$\bar{u}^n(x)=\bar{d}^p(x)[1+\tilde{\delta}],$$
$$\bar{d}^n(x)=\bar{u}^p(x)[1-\tilde{\delta}]. \tag{79}$$

With the form chosen by MRST, the net momentum carried by antiquarks in the neutron and proton are approximately equal; although this quantity is not conserved in QCD evolution, the change in momentum carried by antiquarks in the neutron was found to be very small in the kinematic region of interest. Using Eq. (79) to represent sea quark CSV effects, the MRST

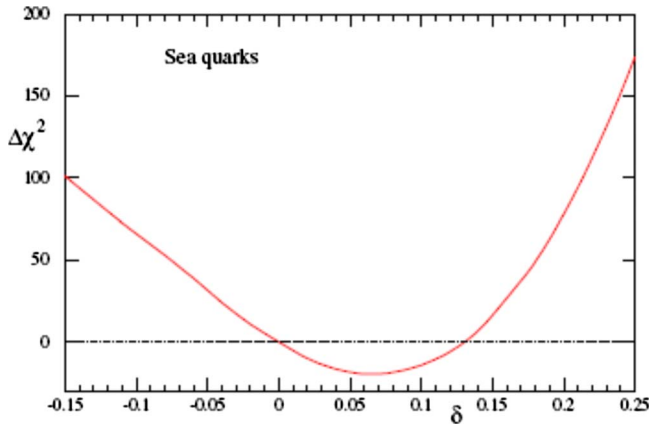

FIG. 25. (Color online) The χ^2 obtained by MRST for a global fit to high-energy data of parton distribution functions including sea quark CSV with the functional form defined in Eq. (79). χ^2 is plotted vs the free parameter $\tilde{\delta}$ (which MRST label δ). From Martin *et al.*, 2004.

group performed a global fit to a wide array of high-energy data, where the coefficient $\tilde{\delta}$ was varied to obtain the best fit. (The MRST group refer to the sea quark CSV parameter as δ; however, we use the notation $\tilde{\delta}$ to avoid confusion with our definitions of partonic charge symmetry.)

Somewhat surprisingly, evidence for sea quark CSV in the MRST global fit was substantially stronger than for valence quark CSV. The χ^2 they obtain is plotted versus the parameter $\tilde{\delta}$ in Fig. 25. The best fit was obtained for $\tilde{\delta}=0.08$, i.e., an 8% violation of charge symmetry in the nucleon sea. The χ^2 corresponding to this value is substantially better than with no charge-symmetry violation, primarily because of the improvement in the fit to the NMC μ-D DIS data (Amaudruz *et al.*, 1991, 1992; Arneodo *et al.*, 1997) when $\bar{u}^n$ is increased. The fit to the E605 Drell-Yan data (Moreno *et al.*, 1991) was also substantially improved by the sea quark CSV term.

Note that the MRST parametrization does not satisfy the "weak form" of charge symmetry as described in Eq. (20). The weak form of charge symmetry would require that the first moments of sea quark CSV should vanish, i.e.,

$$\langle \delta\bar{u}\rangle = \langle \delta\bar{d}\rangle = 0. \tag{80}$$

In fact, using the MRST parametrization of Eq. (79) for sea quark CSV and either the MRST or CTEQ phenomenological sea quark parton distribution functions, then both of the first moments in Eq. (80) would be infinite.

Benesh and Londergan used quark models to estimate the magnitude of sea quark CSV (Benesh and Londergan, 1998). They included sea quarks in quark model wave functions and attempted to calculate the sign and magnitude of sea quark CSV in such models. Reasonably model-independent estimates have been made for valence quark CSV, but calculations of sea quark CSV require additional assumptions, and such calculations are likely to have substantial model dependence. Benesh and Londergan predicted very small CSV effects for antiquarks. They estimated that the fractional amount of CSV in the sea, $\delta\bar{q}/\bar{q}$, should be at least an order of magnitude smaller than the corresponding fractional CSV effects for valence quarks. In quark model calculations, qualitative arguments would suggest that sea quark CSV effects should be small. The relative magnitude of CSV effects is given by

$$\frac{\delta\bar{q}}{\bar{q}} \sim \frac{\delta M}{\langle M\rangle}, \tag{81}$$

where $\langle M\rangle$ is the energy of the lowest contributing intermediate states and δM is the mass difference for intermediate states related by charge symmetry. For antiquarks, the lowest energy states are four-quark states, whose energy is roughly twice the energy of the lowest diquark states that contribute for valence quarks. The mass difference between charge symmetric four-quark states is given by $\delta M \approx M_n - M_p = 1.3$ MeV or three times smaller than the mass difference for minority valence quarks. This naive estimate suggests that sea quark CSV effects should be roughly an order of magnitude smaller than for valence quarks. Cao and Signal carried out meson-cloud calculations of sea quark CSV (Cao and Signal, 2000); they suggested that the bag model calculations of Benesh and Londergan neglected higher-order contributions that might be substantial.

In their quark model estimates of sea quark CSV, Benesh and Londergan found that the sea quark CSV contributions $\delta\bar{u}(x)$ and $\delta\bar{d}(x)$ tended to be roughly the same magnitude and to have opposite sign; this is similar to the situation with the valence quark CSV. However, from Eq. (79) the phenomenological sea quark CSV form assumed by the MRST group obeys

$$\delta\bar{u}(x) + \delta\bar{d}(x) = -\tilde{\delta}[\bar{d}(x) - \bar{u}(x)]. \tag{82}$$

The quantity $\bar{d}(x) - \bar{u}(x)$ has been measured by the E866 group (Hawker *et al.*, 1998; Towell *et al.*, 2001), who compared Drell-Yan pD and pp experiments. Their measurements are in agreement with measurements of the same quantity at HERMES (Ackerstaff *et al.*, 1998). At HERMES this quantity was extracted from semi-inclusive DIS experiments of charged pion production from e-p and e-D reactions. We discuss the measurements of this quantity in Sec. IV.C.1.

B. Limits on sea quark CSV

There are relatively few experimental limits on charge-symmetry violation for sea quark parton distributions. As mentioned in Sec. III.C.1, one can obtain rather strong experimental constraints on sea quark PDFs from experimental measurements of the W charge asymmetry in $p\bar{p}$ reactions (Abe *et al.*, 1998). Such measurements place some limits on the magnitude of charge-symmetry violating sea quark PDFs (Sterman *et al.*, 1999), but they primarily rule out very large CSV

for sea quarks. As mentioned, most tests of parton charge symmetry have contributions from heavy quark PDFs. Strong tests of parton CSV will require rather precise knowledge particularly of strange quark parton distributions. Since sea quark parton distributions increase quite rapidly at small x, it is difficult to separate contributions from partonic CSV in this region from effects due to strange quarks. The results obtained from the global fits of the MRST group to high-energy data (Martin *et al.*, 2004), discussed in the preceding section, appeared to show a several percent CSV effect.

Perhaps the most promising area to search for sea quark CSV is to look for contributions to DIS sum rules (Sterman *et al.*, 1995; Hinchliffe and Kwiatkowski, 1996). The lowest-order sum rules often involve integrals of parton distributions over all x. As discussed in Sec. II.B, valence quark normalization requires that the first moment of the valence quark CSV terms vanish. Consequently, when one integrates parton distributions over all x, the only remaining charge-symmetry violating contribution will arise from sea quarks. As discussed in the following section, sea quark CSV terms will contribute to various sum rules, particularly the Gottfried sum rule (Gottfried, 1967), and possibly also the Adler sum rule (Adler, 1966).

1. *W* production asymmetry at a hadron collider

Production of W bosons resulting from the scattering of protons on an isospin-zero target represents an area where, in principle, one could test parton charge symmetry. On an isospin-zero target, e.g., the deuteron, we are interested in semi-inclusive reactions of the type $p+D \to W^+ + X$ and $p+D \to W^- + X$. We can then define the sum of W^+ and W^- cross sections and the forward-backward asymmetry

$$\sigma_S(x_F) \equiv \left(\frac{d\sigma(x_F)}{dx_F}\right)^{W^+} + \left(\frac{d\sigma(x_F)}{dx_F}\right)^{W^-},$$
$$A(x_F) = \frac{\sigma_S(x_F) - \sigma_S(-x_F)}{\sigma_S(x_F) + \sigma_S(-x_F)}. \tag{83}$$

In Eq. (83) the Cabibbo-favored terms in σ_S are invariant under the transformation $x_F \to -x_F$ for Feynman $x_F = x_1 - x_2$. In the forward-backward asymmetry $A(x_F)$, the only terms that survive are charge-symmetry violating terms plus heavy quark terms in the Cabibbo-unfavored sector.

As discussed in Sec. III.C.1, when the CCFR group performed its initial analysis (Seligman, 1997; Seligman *et al.*, 1997) of the "charge ratio" R_c defined in Eq. (52), at small x the charge ratio appeared to deviate from 1, with the deviation growing with decreasing x. It was pointed out by Boros *et al.* (1998a) and Boros, Londergan, and Thomas (1999) that, if the analysis of these data was accurate, a likely explanation of this discrepancy was a surprisingly large violation of charge symmetry in the nucleon sea quark PDFs. This CSV term in the sea quark distributions was sufficiently large that one would expect the forward-backward asymmetry $A(x_F)$ of Eq. (83) to be as large as several percent (Boros, Londergan, and Thomas, 1999).

However, as discussed in Sec. III.C.1, the low-x discrepancy disappeared upon reanalysis of the CCFR experiment (Yang *et al.*, 2001). Londergan *et al.* then analyzed the prospects for W forward-backward asymmetry (Londergan *et al.*, 2006) using the (much smaller) sea quark CSV obtained in the MRST global fit to high-energy data (Martin *et al.*, 2005). The asymmetries obtained were extremely small, generally less than 1%. The sea quark CSV terms were substantially smaller than suggested by the original CCFR analysis. In addition, the strange quark contributions, which were originally much smaller than the CSV terms, were now no longer negligible, and they tended to cancel the CSV contribution. As a result of these newer results, it was concluded that these W production asymmetries no longer represent a promising prospect to determine charge-symmetry violation in quark PDFs.

2. Limits on charge-symmetry violation for gluon distributions

It is possible that gluon distributions are different for proton and neutron. In fact, if sea quark distributions are charge asymmetric, then this would lead to a small charge-symmetry violation in gluon distributions since sea quark and gluon distributions are coupled through the DGLAP evolution equations (Gribov and Lipatov, 1972; Altarelli and Parisi, 1977; Dokshitzer, 1977). It is also conceivable that some other mechanism might give rise to charge-symmetry violation in gluon distributions.

Piller and Thomas (1996) pointed out that CSV in gluon distributions might be probed through measurements of heavy quarkonium production. For example, if one considers J/ψ production arising from nucleon-nucleon collisions, then the differential cross section can be written as the sum of two terms

$$\frac{d^2\sigma(c\bar{c})}{dx_F dM^2} = \sum_{i,j} \frac{1}{s\sqrt{x_F^2 + 4M^2/s}} \{\hat{\sigma}_{gg} g_i(x_b) g_j(x_t) + \hat{\sigma}_{qq}[q_i(x_b)\bar{q}_j(x_t) + \bar{q}_i(x_b) q_j(x_t)]\}. \tag{84}$$

In Eq. (84), the first term represents the contribution from gluon-gluon fusion and the second term is from quark-antiquark annihilation leading to heavy quarkonium. The corresponding quantities $\hat{\sigma}_{gg}$ and $\hat{\sigma}_{qq}$ represent the subprocess cross sections for gluon-gluon fusion and quark-antiquark annihilation, respectively.

If one focuses on J/ψ production in proton-neutron collisions then charge-symmetry violation in either the quark or gluon distributions will produce a forward-backward asymmetry in the resulting cross sections. Hence such a forward-backward asymmetry in J/ψ production would be sensitive to partonic CSV. If we define the forward-backward asymmetry in terms of Feynman $x_F = x_b - x_t$, we obtain

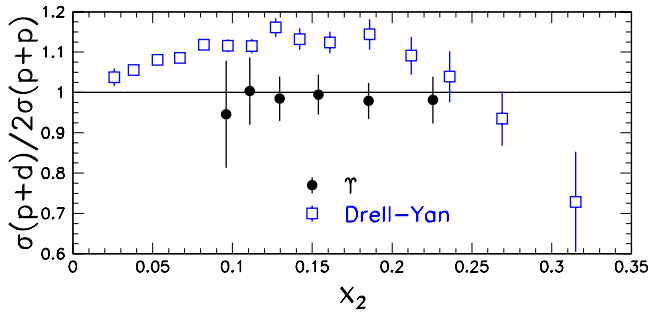

FIG. 26. (Color online) The ratio $\sigma(p+D)/2\sigma(p+p)$ as a function of target x for Υ resonance production cross sections for $p+D$ and $p+p$ reactions from the E866/NuSea Collaboration (Zhu *et al.*, 2008). Solid circles are the Υ production cross sections. For comparison the open squares are the corresponding ratios for the E866 Drell-Yan cross sections (Towell *et al.*, 2001).

$$\Delta\sigma_{pn}(x_F) \equiv \left.\frac{d\sigma(J/\psi)}{dx_F}\right|_{x_F} - \left.\frac{d\sigma(J/\psi)}{dx_F}\right|_{-x_F}, \tag{85}$$

then it is straightforward to show that

$$\begin{aligned}\Delta\sigma_{pn}(x_F) \sim\ & \hat{\sigma}_{gg} g(x_t)\,\delta g(x_b) + \hat{\sigma}_{qq}[u(x_t)\,\delta\bar{d}(x_b) \\ & + \bar{u}(x_t)\,\delta d(x_b) + d(x_t)\,\delta\bar{u}(x_b) + \bar{d}(x_t)\,\delta u(x_b)] \\ & - [x_b \leftrightarrow x_t].\end{aligned} \tag{86}$$

In Eq. (86), $\delta g(x) = g^p(x) - g^n(x)$. Piller and Thomas showed that CSV contributions in the gluon distribution and in sea quark PDFs would be most important at small x_F while contributions from valence quark CSV should dominate at large values of x_F.

The E866/NuSea group has recently measured Υ production in reactions arising from 800 GeV protons on hydrogen and deuterium targets (Zhu *et al.*, 2008). At these energies, the dominant contribution to Υ production comes from gluon-gluon fusion. In this case one expects the resonance cross-section ratio

$$\frac{\sigma(p+D\to\Upsilon)}{2\sigma(p+p\to\Upsilon)} \to \left[1 - \frac{\delta g(x_t)}{2g(x_t)}\right]. \tag{87}$$

Thus CSV in gluon distributions would be manifested by a deviation of the Υ production ratio in Eq. (87) from 1. Figure 26 shows the E866/NuSea Collaboration plot of the cross section ratio for Υ production in pp and pD reactions versus target x. These are plotted as the solid circles in Fig. 26. Within statistics they found no measurable deviation from 1. This is in contrast to significant deviations which were seen for the ratio of pD and pp Drell-Yan processes (these are shown as the open squares in Fig. 26). The asymmetry in DY processes arose from differences between $\bar{u}$ and $\bar{d}$ distributions in the proton, as will be discussed in Sec. IV.C.1. From the Υ measurement we can put upper limits of roughly 10% on possible CSV effects in gluon distributions.

C. Charge-symmetry contributions to DIS sum rules

Sum rules can provide extremely useful information on a single moment of parton distributions. If we choose the first moment of quark PDFs over x, we can invoke the quark normalization conditions both on the valence quark distributions and on valence quark CSV, as expressed in Eqs. (17) and (18), respectively. Consequently, terms which contribute to lowest-order sum rules will depend on integers that represent valence quark normalizations, plus the first moments of antiquark distributions and sea quark CSV. Sum rules that measure the first moments of various structure functions are extremely useful in that if one chooses appropriate linear combinations of structure functions, contributions from heavy quark CSVs will cancel out. This removes a major source of uncertainty since for sea quarks the contributions from sea quark CSV and from heavy quark distributions are generally difficult to separate.

Two sum rules, the Adler sum rule (Adler, 1966) and Gross–Llewellyn Smith sum rule (Gross and Llewellyn Smith, 1969), can be directly related to linear combinations of quark normalization integrals. We discuss the Gottfried sum rule (GSR) (Gottfried, 1967) in the following section. Unlike the Adler or Gross–Llewellyn Smith sum rules, the "naive" Gottfried sum rule expectation $S_G = 1/3$ is obtained only if one assumes both charge symmetry for parton distributions and equality of light sea quark distributions in the proton sea, $\bar{u}^p(x) = \bar{d}^p(x)$, or more precisely the equality of the first moment of these light sea quark PDFs. The expectation that the light quark sea distributions should be equal is often referred to as SU(2) flavor symmetry. This is an unfortunate connotation since the $\bar{u}^p(x)$ and $\bar{d}^p(x)$ distributions are not related by any underlying dynamical symmetry. However, if all of the light sea quarks were generated through gluon radiation, then one would expect the sea quark distributions to be identical except for effects due to light quark mass differences and small electromagnetic effects.

As discussed in Sec. III, theoretical expectations for CSV effects in parton distributions are expected to be no larger than a few percent. In Sec. III.C we showed that current experimental upper limits on CSV are of the order of several percent for $x \leqslant 0.4$ and larger than 10% for $x > 0.4$. It would therefore be useful to construct sum rules which could in principle distinguish between CSV effects and effects arising from sea quark flavor asymmetry. In this section, we review the current status of the Adler, Gross–Llewellyn Smith, and Gottfried sum rules, with particular attention to the contributions from partonic CSV effects. Good reviews of DIS sum rules up to about 1996 can be found in Sterman *et al.* (1995) and Hinchliffe and Kwiatkowski (1996). We reviewed sum rules and parton CSV in detail in our previous review article (Londergan and Thomas, 1998). There has been little change in the status of the experimental Adler and Gross–Llewellyn Smith sum rules since the publication of that review article.

1. Gottfried sum rule: Sea quark flavor and charge symmetry

In the past 15 years we have obtained much quantitative information on sea quark flavor asymmetry $[\bar{d}^p(x) \neq \bar{u}^p(x)]$ in the nucleon. Information on the first moment of these distributions can be extracted from measurements of the GSR (Gottfried, 1967), obtained from the difference of F_2 structure functions from charged lepton DIS on neutrons and protons. The Gottfried sum rule is also known as the *valence isospin sum rule* (Hinchliffe and Kwiatkowski, 1996). Using Eq. (34), we obtain

$$S_G \equiv \int_0^1 dx \frac{[F_2^{\ell p}(x) - F_2^{\ell n}(x)]}{x} = \frac{1}{3} - \frac{2}{3}\int_0^1 dx[\bar{d}^p(x) - \bar{u}^p(x)] + \frac{2}{9}\int_0^1 dx[4\delta\bar{d}(x) + \delta\bar{u}(x)]. \tag{88}$$

If the nucleon sea is charge symmetric, and the first moment of the proton antiquark distributions are equal, then we obtain the "naive" expectation $S_G = 1/3$. Earlier measurements of the GSR (Benvenuti *et al.*, 1987; Ashman *et al.*, 1988, 1989; Dasu *et al.*, 1988; Whitlow *et al.*, 1992) obtained results that appeared to be less than the naive expectation of 1/3, but with significant error bars. The first really precise GSR value was obtained by the New Muon Collaboration (NMC) (Amaudruz *et al.*, 1991, 1992). The NMC result (Amaudruz *et al.*, 1991, 1992; Arneodo *et al.*, 1994) $S_G = 0.235 \pm 0.026$ was more than four standard deviations below 1/3. Assuming charge symmetry, this implies a substantial excess $\bar{d}^p > \bar{u}^p$. This effect is much larger than can be accommodated by perturbative QCD. Next-to-leading order (NLO) and next-to-next-to-leading order (NNLO) QCD calculations predict very small effects (Ross and Sachrajda, 1979). However, the NMC result could be due to a combination of charge symmetry and flavor symmetry violating effects.

Note that all three of the sum rules which we discuss here—the Gottfried, Adler, and Gross–Llewellyn Smith sum rules—involve dividing the F_2 or xF_3 structure functions by x. This emphasizes the contributions from small x. In all of these sum rules we invoke quark normalization conditions as given by Eqs. (17) and (18). These normalization conditions hold only after integration over all x. In reality one measures the sum rule down to some smallest value $x_{\min}$. In that case one must estimate the contributions from the unmeasured region $0 < x \leq x_{\min}$.

The GSR provides information only on the first moment of proton sea quark differences. It was proposed to make a "direct" measurement of sea quark flavor asymmetry by comparing Drell-Yan processes initiated by protons, on proton and deuteron targets. This was suggested first by Ericson and Thomas (1984) in the context of the pionic explanation of the EMC effect and later by Ellis and Stirling (1991). In the Drell-Yan (DY) process (Drell and Yan, 1970) hadronic collisions produce opposite sign lepton pairs with large invariant mass. The charged leptons are formed from the decay of a virtual photon arising from annihilation of a quark (antiquark) in the projectile with an antiquark (quark) of the same flavor from the target.

The experiments measure the ratios of DY cross sections for incident protons on deuteron and proton targets. Assuming the validity of the impulse approximation, the ratio is given by

$$R^{\mathrm{DY}}(x_1,x_2) \equiv \frac{\sigma_{\mathrm{DY}}^{pD}}{2\sigma_{\mathrm{DY}}^{pp}} \to \frac{1}{2}\left(1 + \frac{\bar{d}(x_2) - \delta\bar{d}(x_2)}{\bar{u}(x_2)}\right). \tag{89}$$

The last line of Eq. (89) follows in the limit of large Feynman $x_F = x_1 - x_2$ assuming that

$$\frac{d(x)}{u(x)} \to 0, \quad x \to 1, \tag{90}$$

where x_1 and x_2 are the longitudinal momentum fractions carried by the projectile (target) quarks or antiquarks, respectively. If charge symmetry holds then from Eq. (89), in the limit of large x_F, the ratio of pD to pp Drell-Yan cross sections would directly measure the ratio of the down antiquark to up antiquark distributions in the proton, at a given value of x_2.

Experiment NA51 at CERN (Baldit *et al.*, 1994) measured Drell-Yan processes for 450 GeV protons on proton and deuteron targets, obtaining a ratio $\bar{u}^p/\bar{d}^p = 0.51 \pm 0.04(\mathrm{stat}) \pm 0.05(\mathrm{syst})$ for a single averaged point $\langle x \rangle = 0.18$. The E866 group at Fermilab (Hawker *et al.*, 1998; Peng *et al.*, 1998; Towell *et al.*, 2001) compared Drell-Yan processes for 800 GeV protons on liquid hydrogen and deuterium targets. Figure 27 shows results from E866. For values $x_2 < 0.2$ the ratio is greater than 1, and appears to decrease at higher values of x_2, perhaps becoming less than 1 at $x_2 \sim 0.3$. Both the NA51 and E866 experiments show a substantial excess $\bar{d}^p > \bar{u}^p$ at small x. This measurement was confirmed by subsequent semi-inclusive DIS (SIDIS) measurements, comparing yields of positive and negative pions from scattering of energetic positrons on proton and deuteron targets at HERMES (Ackerstaff *et al.*, 1998). The E866 group obtained the first moment of the light sea quark difference

$$\langle \bar{d} - \bar{u} \rangle = 0.118 \pm 0.012. \tag{91}$$

Comprehensive review articles on light sea quark asymmetries have been given by Kumano (1998) and by Garvey and Peng (2001).

In order to obtain the result of Eq. (91), however, the E866 group assumed parton charge symmetry. Equation (89) shows that the Drell-Yan ratios could also have contributions from sea quark CSV effects. One cannot extract the magnitude of flavor symmetry violating effects without assuming sea quark charge symmetry, as emphasized by Ma (1992) and Ma *et al.* (1993). Ma claimed that

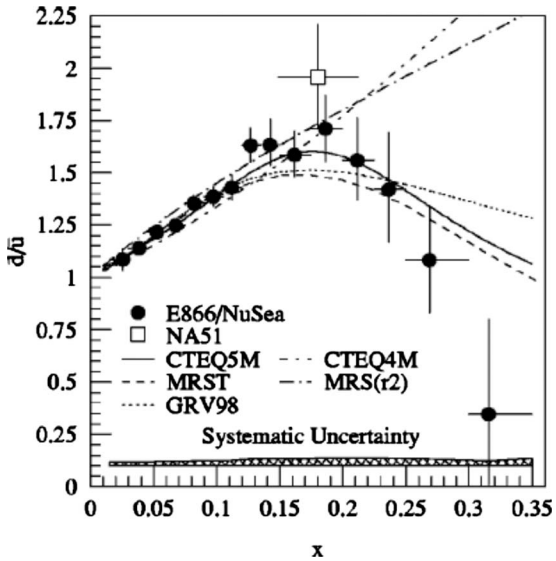

FIG. 27. The ratio $\bar{d}^p(x)/\bar{u}^p(x)$ as a function of target x, obtained from Drell-Yan cross sections for pp and pD reactions. Solid circles are data from the E866 Collaboration (Hawker *et al.*, 1998; Towell *et al.*, 2001); the open square is the NA51 point (Baldit *et al.*, 1994). Curves are results of calculations using various phenomenological PDFs.

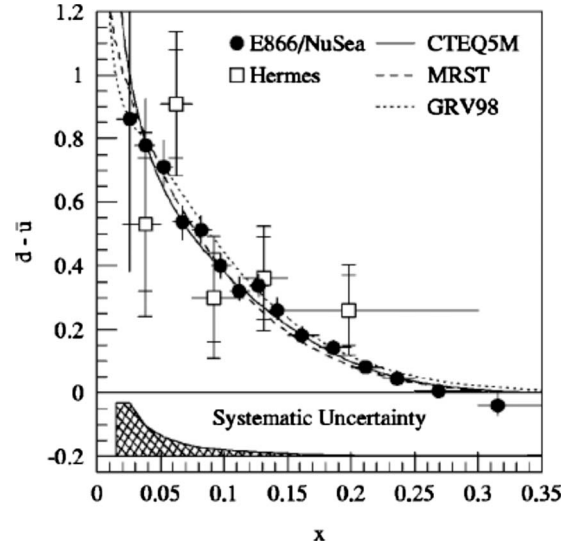

FIG. 28. The quantity $\bar{d}^p(x)-\bar{u}^p(x)$ as a function of target x. Solid circles, data from the E866 DY cross sections scaled to fixed $Q^2=54$ GeV^2 (Hawker *et al.*, 1998; Towell *et al.*, 2001). Open squares, results from SIDIS measurements at HERMES (Ackerstaff *et al.*, 1998), corresponding to $\langle Q^2\rangle=2.3$ GeV^2. Curves are calculations using various phenomenological PDFs.

in principle one could explain the entire effect on the Gottfried sum rule from parton charge symmetry violation even if parton flavor symmetry was exact. However, this would require sea quark CSV effects an order of magnitude larger than those obtained in the MRST phenomenological fit to high-energy data (Martin *et al.*, 2004). A more natural source of the $\bar{d}$-$\bar{u}$ difference was predicted by Thomas (1983). This incorporates effects of the pion cloud of the nucleon; the proton predominantly emits a π^+, which contains a valence $\bar{d}$ quark, leading to an excess $\bar{d}>\bar{u}$.

In Fig. 28 we plot the quantity $\bar{d}^p(x)-\bar{u}^p(x)$. The solid circles are the E866 DY points from Hawker *et al.* (1998) and Towell *et al.* (2001) scaled to fixed $Q^2=54$ GeV^2. The open squares are the results from the SIDIS measurements at HERMES (Ackerstaff *et al.*, 1998), which correspond to an averaged value $\langle Q^2\rangle=2.3$ GeV^2. The curves are calculations using various phenomenological PDFs from GRV98 (Glück *et al.*, 1998) (dotted curve), MRST (Martin *et al.*, 1998) (dashed curve), and CTEQ5M (Lai *et al.*, 2000) (solid curve).

We first review results obtained for the Gottfried sum rule with the MRST2001 (Martin *et al.*, 2002) global fit PDFs with no isospin violation. In this parametrization, the sea quark distributions are obtained at a starting scale $Q_0^2=1$ GeV^2 and values at higher Q^2 can be obtained through DGLAP evolution. The MRST2001 fit obtains

$$S_G=\tfrac{1}{3}-\tfrac{2}{3}\langle\bar{d}-\bar{u}\rangle=0.266. \tag{92}$$

The MRST result for the Gottfried sum rule is just over 1σ above the NMC value. The E866 pp and pD DY data essentially determine the MRST value for the $\bar{d}$-$\bar{u}$ asymmetry in the proton. These results are basically consistent with the NA51 DY point (Baldit *et al.*, 1994) and with the HERMES semi-inclusive DIS measurements of positive and negative pion production in ep and eD scattering (Ackerstaff *et al.*, 1998).

If one includes the phenomenological sea quark CSV effects obtained by MRST (Martin *et al.*, 2004), then the contribution to the Drell-Yan ratio in the limit of large x_F will be

$$R^{\mathrm{DY}}(x_1,x_2)\to\frac{1}{2}\left(1+\frac{1.08\bar{d}(x_2)}{\bar{u}(x_2)}\right). \tag{93}$$

Thus, including the MRST sea quark CSV term would decrease the extracted sea quark flavor asymmetry by roughly 8% [one needs to take care since Eq. (93) is true only in the limit of large Feynman x]. In principle, one could insert the sea quark distributions from the 2003 MRST global fit including CSV and calculate the contribution from sea quark CSV to the Gottfried sum rule. However, using the MRST functional form from Eq. (79) gives an infinite result for S_G. This is due to the fact that MRST choose the sea quark CSV proportional to the sea quark PDFs, which have infinite first moment. The MRST group plans to carry out future global fits assuming a modified functional form for sea quark CSV (Thorne, 2008); this would produce finite CSV contributions to the Gottfried sum rule.

From Eq. (89) it is apparent that in comparing pp and pD Drell-Yan cross sections one has contributions from both sea quark flavor asymmetry, i.e., $\bar{d}(x)\neq\bar{u}(x)$, but also from parton charge-symmetry violation. Peng and Jansen (1995) pointed out that one can obtain informa-

tion on $\bar{d}/\bar{u}$ from measurements of W or Z production in pp collisions, which have no CSV contributions. For example, if one measures the ratio of W^+ and W^- production then one obtains

$$R(x_F) \equiv \frac{d\sigma/dx_F(p+p\to W^+)}{d\sigma/dx_F(p+p\to W^-)},$$

$$R(x_F)_{(x_F=0)} \approx \frac{u(x)}{d(x)}\frac{\bar{d}(x)}{\bar{u}(x)}, \tag{94}$$

$$R(x_F)_{(x_F\gg 0)} \approx \frac{u(x_1)}{d(x_1)}\frac{\bar{d}(x_2)}{\bar{u}(x_2)}.$$

In Eq. (94), the final two equations are true in the limit where one neglects strange quark contributions. Peng and Jansen showed that these W-production ratios were quite sensitive to different phenomenological predictions for light sea quark distributions.

2. Adler sum rule

The Adler sum rule (Adler, 1966) is given by the integral of the F_2 structure functions for charged current ν and $\bar{\nu}$ DIS on the proton. The Adler sum rule S_A is defined (in the limit $Q^2\to\infty$) as

$$S_A \to \int_0^1 dx\left[\frac{F_2^{W^-p}(x,Q^2)-F_2^{W^+p}(x,Q^2)}{2x}\right]$$
$$= \int_0^1 dx[u_v^p(x)-d_v^p(x)(1-|V_{td}|^2)-s^-(x)] \approx 1. \tag{95}$$

We obtain the result $S_A=1$ if we neglect the term $|V_{td}|^2 \approx 1\times 10^{-4}$. The Adler sum rule thus requires subtracting the F_2 structure function for antineutrinos and neutrinos on protons and dividing by x (this emphasizes the contribution from very small x). The Adler sum rule then follows from the normalization of the valence quark distributions. As a consequence of the algebra of SU(2) charges, the Adler sum rule has no QCD corrections. Since the Adler sum rule involves measurements only on the proton, it has no CSV corrections.

Another name for the Adler sum rule is the *isospin sum rule* (Hinchliffe and Kwiatkowski, 1996). Note that different overall normalizations for the Adler sum rule appear in the literature. An alternative normalization is a factor of 2 larger than ours (Hinchliffe and Kwiatkowski, 1996; Leader and Predazzi, 1996). Our normalization agrees with that used by the WA25 experimental group (Allasia *et al.*, 1984, 1985).

The best experimental data to date are from the WA25 experiment (Allasia *et al.*, 1984, 1985), who used the CERN-SPS wideband neutrino beams in the BEBC H and D bubble chambers. Note that the WA25 measurements involve neutrino CC measurements on neutrons (e.g., deuterons) and protons, and not $\bar{\nu}$ and ν on protons, as given in the definition of the Adler sum rule [Eq. (95)]. This was done because ν beams generally have much higher fluxes than $\bar{\nu}$. The WA25 experiment substituted neutrinos on neutron targets using

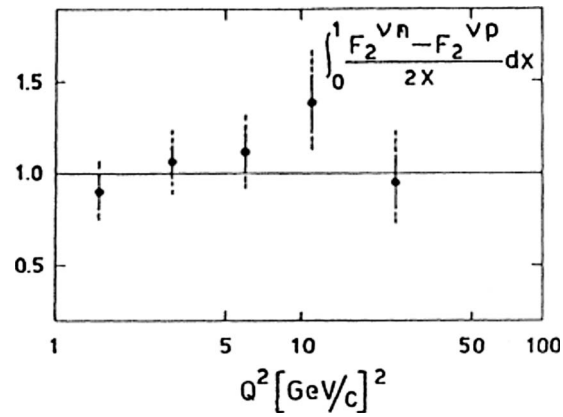

FIG. 29. Experimental results for the "Adler sum rule" from the WA25 group (Allasia *et al.*, 1984, 1985). Note that what is measured is given by Eq. (97) and not the Adler sum rule of Eq. (95).

$$F_2^{W^+n}(x,Q^2) = F_2^{W^-p}(x,Q^2) + 2x[s^-(x)-\delta u(x)-\delta\bar{d}(x)], \tag{96}$$

as discussed in Sec. I. Thus, the WA25 group does not measure the integral S_A of Eq. (95) but instead measures a different quantity

$$\tilde{S}_A \equiv \int_0^1 dx\left[\frac{F_2^{W^+n}(x,Q^2)-F_2^{W^+p}(x,Q^2)}{2x}\right]$$
$$= \int_0^1 dx[u_v^p(x)-d_v^p(x)-\delta u(x)-\delta\bar{d}(x)]$$
$$= S_A - \int_0^1 dx[\delta\bar{u}(x)+\delta\bar{d}(x)]. \tag{97}$$

From Eq. (97) we see that the difference between the Adler sum rule and the measurements from WA25 involves the first moment of contributions from sea quark CSV. If charge symmetry is exact, or if the "weak form" of charge symmetry holds [see Eq. (20)], then the Adler sum rule would be identical to what was measured by WA25, i.e., $S_A=\tilde{S}_A$.

Figure 29 shows the experimental results using the Adler sum rule. The experimental points are from the WA25 experiment (Allasia *et al.*, 1984, 1985). The experimental data are shown for several values of Q^2. The average value is $\tilde{S}_A=1.01\pm0.08(\text{stat})\pm0.18(\text{syst})$. However, the total νN cross section used by the WA25 group is smaller than the presently accepted value (Blair *et al.*, 1983; Berge *et al.*, 1987). If the WA25 value is readjusted to fit this total cross section, their result becomes $\tilde{S}_A=1.08\pm0.08(\text{stat})\pm0.18(\text{syst})$.

The results show no significant Q^2 dependence. The large errors arise from the factor $1/x$ in the integral [Eq. (95)], which gives a heavy weighting to the data at small x. The paucity of data in this region and the relatively

large error bars there give a large uncertainty in the sum rule value. There are currently efforts underway to develop new generation neutrino experiments, with substantially higher fluxes than were available in the past. If these efforts come to fruition, it might be possible to test the Adler sum rule with ν and $\bar{\nu}$ beams on a proton target.

We can use the phenomenological sea quark CSV amplitudes determined by MRST (Martin *et al.*, 2004) to estimate the CSV contribution to the WA25 measurement. Assuming that the quark normalization integral is indeed 1, then inserting the MRST sea quark function of Eq. (82) into the Adler sum rule one obtains

$$\tilde{S}_A = S_A - \int_0^1 dx[\delta\bar{u}(x) + \delta\bar{d}(x)]$$
$$= 1 + \tilde{\delta}\langle\bar{d}^p - \bar{u}^p\rangle = 1.008. \tag{98}$$

The MRST result for sea quark CSV implies a difference of less than 1% between the Adler sum rule and the quantity measured in the WA25 experiment. Note that this result could be strongly model dependent because of the functional form assumed by MRST.

One could also in principle measure a sum rule using antineutrino beams on protons and deuterium and obtain

$$\bar{S}_A \equiv \int_0^1 dx\left[\frac{F_2^{W^-p}(x,Q^2) - F_2^{W^-n}(x,Q^2)}{2x}\right]$$
$$= S_A + \int_0^1 dx[\delta\bar{u}(x) + \delta\bar{d}(x)]$$
$$= 1 - \tilde{\delta}\langle\bar{d}^p - \bar{u}^p\rangle = 0.992. \tag{99}$$

The last line of Eq. (99) holds if we assume the MRST result for sea quark CSV. Note that if the weak form of charge symmetry holds [see Eq. (20)], then $S_A = \tilde{S}_A$ and $S_A = \bar{S}_A$. We discuss this in more detail in Sec. IV.C.4 in connection with a charge-symmetry sum rule.

One could also imagine measuring a similar quantity on a nucleus, rather than the proton. If one compares the integral of the F_2 structure function for a nucleus with Z protons and $N = A - Z$ neutrons, then one would expect

$$S_A^A = \int_0^{M_A/M} dx\left[\frac{F_2^{W^-A}(x,Q^2)}{2x} - \frac{F_2^{W^+A}(x,Q^2)}{2x}\right]$$
$$= \frac{Z-N}{A}. \tag{100}$$

In Eq. (100) M_A is the nuclear mass and M is the nucleon mass, the structure functions F_2 are normalized per nucleon, and we have assumed the impulse approximation. Nuclear effects in neutrino DIS have been evaluated by Kulagin and Petti (2006, 2007a, 2007b). They calculated nuclear modifications to structure functions arising from three general sources. The first category of effects, incoherent scattering from bound nucleons, tends to affect structure functions mainly at large Bjorken x. These are evaluated by Kulagin and collaborators through Fermi motion and nuclear binding effects. It can be shown that Fermi motion and binding effects give zero contribution to the nuclear Adler sum rule. The second types of corrections tend to affect the structure functions in the region $x \sim 0.1$. These can arise from off-shell effects or from nuclear modifications of the meson cloud. The third type of corrections arises from coherent nuclear shadowing or antishadowing effects. These predominantly affect the structure functions in the region of low $x < 0.1$.

Because of the isovector nature of the Adler sum rule, nuclear pion corrections give zero contribution. Kulagin and Petti (2007a, 2007b) required cancellation of the isovector off-shell and nuclear shadowing corrections to the Adler sum rule. This provided constraints on these corrections. Kumano and collaborators (Kumano, 2002; Hirai *et al.*, 2004, 2005) also made systematic considerations of nuclear corrections to structure functions and nuclear parton distributions.

3. Gross–Llewellyn Smith sum rule

The Gross–Llewellyn Smith (GLS) sum rule (Gross and Llewellyn Smith, 1969) is derived from the F_3 structure functions for neutrinos and antineutrinos. This is also called the *baryon sum rule* (Hinchliffe and Kwiatkowski, 1996). If we sum the F_3 structure functions for neutrinos and antineutrinos on an isoscalar target, then from Eq. (33) we obtain

$$S_{\rm GLS} \equiv \int_0^1 \frac{dx}{2x}[xF_3^{W^+N_0}(x) + xF_3^{W^-N_0}(x)]$$
$$= \int_0^1 \left[u_v(x) + d_v(x) + s^-(x) - \frac{\delta u_v(x) + \delta d_v(x)}{2}\right]dx$$
$$= 3\left[1 - \frac{\alpha_s(Q^2)}{\pi} - a(n_f)\left(\frac{\alpha_s(Q^2)}{\pi}\right)^2 - b(n_f)\left(\frac{\alpha_s(Q^2)}{\pi}\right)^3\right] + \Delta HT. \tag{101}$$

The result $S_{\rm GLS} = 3$ follows from the normalization of the quark valence distributions. An identical prediction would be obtained using either a proton or neutron target in the sum rule. The Gross–Llewellyn Smith sum rule holds only in leading twist approximation, and only to lowest order in the strong coupling constant α_s. Our expression for the GLS sum rule thus includes a QCD correction [the term in square brackets in the last line of Eq. (101)], which was derived by Larin and Vermaseren (1991), and the quantity ΔHT represents a higher twist contribution (Braun and Kolesnichenko, 1987).

As is the case for the Adler and Gottfried sum rules, the Gross–Llewellyn Smith sum rule requires that the structure function be divided by x in performing the in-

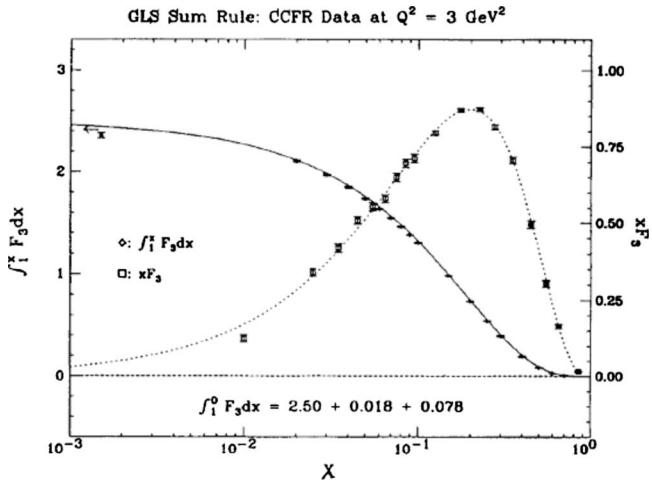

FIG. 30. Experimental results for Gross–Llewellyn Smith sum rule [Eq. (101)] from CCFR (Leung *et al.*, 1993). Squares, $x\bar{F}_3(x)$, sum of neutrinos plus antineutrinos, at $Q^2=3$ GeV^2. Dashed curve, analytic fit to $x\bar{F}_3$. Diamonds, approximation to the integral $S_{\rm GLS}(x)$ of Eq. (102). Solid line, fit to the integral $S_{\rm GLS}(x)$.

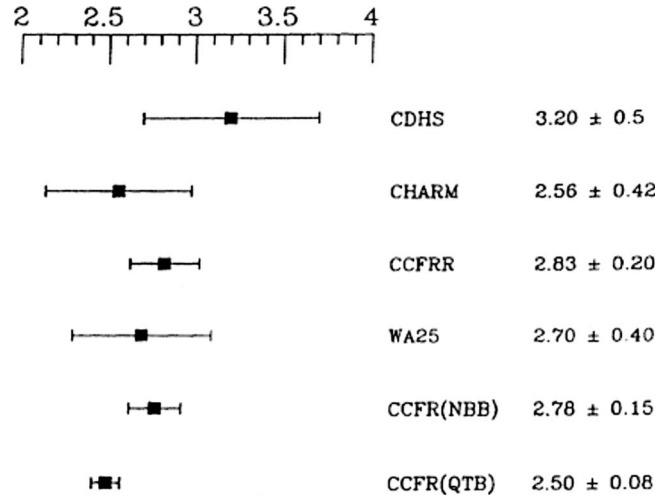

FIG. 31. Experimental results for Gross–Llewellyn Smith sum rule, and their errors, for a series of experiments in chronological order from top to bottom.

tegral. This gives a strong weighting to the small-x region, such that as much as 90% of the sum rule comes from the region $x\leqslant 0.1$. Of the three sum rules discussed in this review, the GLS sum rule is experimentally the best determined. The most precise value has been obtained by the CCFR Collaboration (Leung *et al.*, 1993), which measured neutrino and antineutrino cross sections on iron targets, using the quadrupole triplet beam (QTB) at Fermilab. A summary of experimental details for precision measurements using high-energy neutrino beams is given by Conrad *et al.* (1998).

In Fig. 30 we show the CCFR measurements and the experimental values of $x\bar{F}_3(x)$ (the sum of xF_3 for neutrinos plus that for antineutrinos) vs x. They obtained cross sections at several values of x and Q^2. The squares give the value of $x\bar{F}_3(x)$ interpolated to an average momentum transfer $Q^2=3$ GeV^2 (this is the mean Q^2 for the lowest x bin in the CCFR experiment since the lowest x values contribute the greatest amount to the GLS sum rule). The dashed curve is the best fit to $x\bar{F}_3$ of the form $Ax^b(1-x)^c$. The CCFR reported value for the sum rule at this Q^2 value is $S_{\rm GLS}=2.50\pm0.018({\rm stat})\pm0.078({\rm syst})$. The GLS sum rule is therefore known to 3%. Because of the large contribution to the GLS sum rule from small x, one measures xF_3 at various values of x and evaluates the integral

$$S_{\rm GLS}(x)=\int_x^1 \frac{dy}{2y}[yF_3^{W^+N_0}(y)+yF_3^{W^-N_0}(y)]. \tag{102}$$

The Gross–Llewellyn Smith sum rule is then obtained by estimating the limit

$$S_{\rm GLS}=\lim_{x\to 0} S_{\rm GLS}(x). \tag{103}$$

The solid curve in Fig. 30 is $S_{\rm GLS}(x)$.

A theoretical value for the Gross–Llewellyn Smith sum rule requires evaluating the QCD corrections. Calculations of the GLS sum rule include next-to-leading order QCD corrections, using a QCD scale parameter $\Lambda_{\rm QCD}=213\pm50$ MeV. With this scale parameter and NLO QCD corrections, one obtains a theoretical prediction $S_{\rm GLS}=2.63\pm0.04$ (Mishra, 1990). The theoretical prediction is two standard deviations above the experimental value. In Fig. 31 we show the evolution over time of the GLS sum rule value. The measurements shown are from the CDHS (de Groot *et al.*, 1979), CHARM (Bergsma *et al.*, 1983), CCFRR (Macfarlane *et al.*, 1984), and WA25 (Allasia *et al.*, 1984) Collaborations. There are also two points from the CCFR measurements, the first using the narrow-band beam (NBB) neutrino data (Mishra and Sciulli, 1989; Oltman *et al.*, 1992) and the second using the QTB data (Leung *et al.*, 1993) from the Fermilab Tevatron.

The errors on the GLS sum rule are now at a level where the value of the strong coupling constant α_s is a major source of error. The CCFR group now have data on xF_3 over a wide enough range of Q^2 that, together with renormalized data from several other experiments, they may be able to evaluate the GLS sum rule without extrapolation for a large range of Q^2 values. This raises the hope that one can calculate the Gross–Llewellyn Smith sum rule as a function of Q^2 and use the resulting Q^2 dependence of the sum rule to determine $\alpha_s(Q^2)$. The CCFR group has recalculated both the GLS sum rule and the strong coupling constant α_s (Harris *et al.*, 1995). With data of this quality over a large Q^2 range, it may be possible to use the Q^2 dependence to put constraints on the strong coupling constant. Additional information regarding this procedure can be found in Seligman (1997).

The structure functions $xF_3^{W^+N_0}(x)+xF_3^{W^-N_0}(x)$, which form the integrand for the GLS sum rule, are obtained by taking the difference between cross sections for neutrinos and antineutrino charged-current processes on isoscalar targets (Conrad *et al.*, 1998). In the limit of exact charge symmetry, the F_2 structure functions exactly cancel in this subtraction, and only the F_3 structure functions survive. However, CSV effects make additional contributions to this integrand, i.e., using Eq. (28),

$$\begin{aligned}\frac{3\pi}{2G^2M_NE}&(d\sigma^{\nu N_0}/dx - d\sigma^{\bar{\nu}N_0}/dx)\\ &= \frac{1}{2}[xF_3^{W^+N_0}(x,Q^2)+xF_3^{W^-N_0}(x,Q^2)]\\ &\quad + F_2^{W^+N_0}(x,Q^2) - F_2^{W^-N_0}(x,Q^2)\\ &= x\Bigg[u_v^p(x)+d_v^p(x)+3s^-(x)-c^-(x)\\ &\quad -\frac{3}{2}\delta u_v(x)+\frac{1}{2}\delta d_v(x)\Bigg].\end{aligned} \tag{104}$$

In addition to the light valence quark distributions, Eq. (104) contains additional contributions from strange and CSV "valence" quark distributions. However, the CSV amplitudes have no effect on the GLS sum rule value. Since quark valence distributions obey the normalization conditions of Eqs. (17) and (18), the contributions from valence strange and CSV terms must integrate to zero. Note, however, that the valence quark CSV effects contribute to the integral $S_{\rm GLS}(x)$ at any finite value of x and that the CSV effects vanish only upon integration over all x.

Since the GLS sum rule is evaluated on nuclear targets (for the CCFR measurement, on iron), we need to consider nuclear modifications of structure functions and their potential effect on the GLS sum rule. Such an investigation has been carried out by Kulagin and Petti (2007a), using methods that were summarized in discussing the Adler sum rule (see Sec. IV.C.2). As for the Adler sum rule, the Fermi motion and nuclear binding corrections have zero effect on the GLS sum rule. In the limit $Q^2\to\infty$, the off-shell and nuclear shadowing corrections also tend to cancel. In Fig. 32 we show the GLS sum rule as a function of Q^2. The experimental points are the CCFR measurements on iron versus Q^2. The curves are nuclear calculations of Kulagin and Petti (2007a) for various nuclei. The dotted curve is for the nucleon and the solid curve for iron. This gives an idea of the magnitude of nuclear corrections to the GLS sum rule and their Q^2 dependence. In addition there may be additional corrections from the pseudo-CSV effects suggested by Cloët *et al.* (2009) and discussed in Sec. III.D.

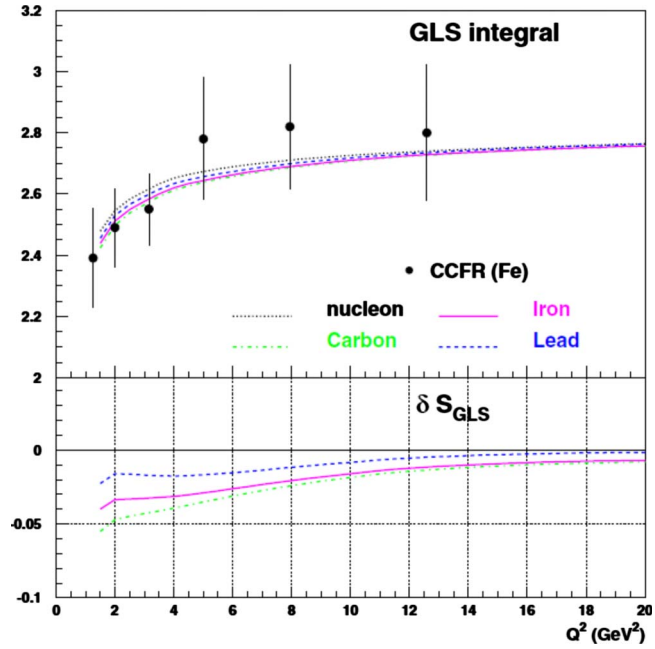

FIG. 32. (Color online) Nuclear corrections to the Gross–Llewellyn Smith sum rule, as a function of Q^2 (Kulagin and Petti, 2007a). Data points are CCFR measurements on iron (Leung *et al.*, 1993). Dotted curve, nucleon results; dot-dashed curve, results for carbon; solid curve, results for iron; and dashed curve, results for lead.

4. A charge-symmetry sum rule

In Sec. IV.C.1 we showed that the Gottfried sum rule contains contributions both from charge-symmetry violation and from sea quark flavor asymmetry. If sufficiently accurate experimental data can be obtained, one could define sum rules which could differentiate between effects due to parton charge-symmetry violation and those arising from differences in light sea PDFs, i.e., $\bar{d}^p(x)\neq\bar{u}^p(x)$. Ma (1992) defined a "charge-symmetry" sum rule in terms of the F_2 structure functions for charged-current neutrino and antineutrino interactions on the neutron and proton,

$$\begin{aligned}S_{CS} &\equiv \int_0^1 \frac{dx}{x}[F_2^{W^+p}(x)+F_2^{W^-p}(x)-F_2^{W^+D}(x)\\ &\quad -F_2^{W^-D}(x)]\\ &= 2\int_0^1 dx[\delta\bar{u}(x)+\delta\bar{d}(x)].\end{aligned} \tag{105}$$

In Eq. (105), $F_2^{W^+D}(x)$ is the F_2 structure function per nucleon for neutrino charged-current DIS on the deuteron. From Eq. (105) we see that if either the strong or weak form of charge symmetry holds for the nucleon sea quark distributions, then S_{CS} will be zero. A deviation of this sum rule from zero would signal either a violation of parton charge symmetry or a contribution from higher twist terms. The higher twist terms would be expected to become progressively smaller with increasing Q^2. Just as for the Adler sum rule, there are no QCD corrections to the charge-symmetry sum rule.

The charge-symmetry sum rule of Eq. (105) is closely related to what has been measured as the Adler sum

rule (see the discussion in Sec. IV.C.2). We can easily see that

$$\tilde{S}_A = \int_0^1 dx \left[\frac{F_2^{W^+n}(x,Q^2) - F_2^{W^+p}(x,Q^2)}{2x} \right] = S_A - \frac{S_{CS}}{2}. \tag{106}$$

The WA25 group (Allasia *et al.*, 1984) measured cross sections from neutrinos on protons and deuterium, so their integral should give the Adler sum rule minus one-half the charge-symmetry sum rule. However, as shown in Fig. 29, errors in the WA25 measurement are of the order of 20%, so the charge-symmetry sum rule at present is consistent with zero at the 40% level, if we assume that the Adler sum rule is 1. We can obtain an estimate of the charge-symmetry sum rule from the MRST global fit including sea quark CSV discussed in Sec. IV.B. Using the MRST form for sea quark CSV, Eq. (98) with best value $\tilde{\delta}=0.08$ predicts $S_{CS}\sim -0.016$. The predicted quantity is extremely small; however, we stress that this result is based on the (strongly model-dependent) functional form for sea quark CSV chosen by MRST [see Eq. (79)].

V. SUMMARY AND OUTLOOK

We have reviewed the features of charge symmetry, an approximate symmetry in particle and nuclear systems, as it relates to parton distributions. First, we reviewed the relation between high-energy cross sections and parton distributions, in terms of structure functions. Then we wrote the structure functions in terms of parton distribution functions. Until recently, phenomenological parton distribution functions assumed the validity of charge symmetry. This meant that PDFs for the neutron could be given in terms of those for the proton. If we relax this assumption, we must differentiate between neutron and proton PDFs. This requires the introduction of charge-symmetry violating PDFs.

In Sec. II.C we expanded the structure functions in terms of parton distributions without making the assumption of charge symmetry. We then derived relations between these structure functions. Some relations that exist in the limit of exact parton charge symmetry must be modified if we relax that assumption.

In Secs. III.A and III.B we reviewed the phenomenological and theoretical situation regarding parton charge symmetry. One theoretical method for predicting partonic CSV contributions is to examine the dependence of quark models for parton distributions on variations in quark and nucleon mass. For valence quarks, we showed that this leads to predictions for the magnitude and sign of the CSV terms. The quantities $\delta u_v(x)=u_v^p(x)-d_v^n(x)$ and $\delta d_v(x)=d_v^p(x)-u_v^n(x)$ are found to be opposite in sign and roughly equal in magnitude. Since at large Bjorken x one has $d_v(x)\ll u_v(x)$, the fact that the valence CSV distributions are predicted to be roughly equal implies that the percent charge-symmetry violation for the "minority" valence quark distribution should be substantially greater than for the "majority" valence quark distribution.

There now exist phenomenological valence CSV PDFs from the MRST group (Martin *et al.*, 2004). They assumed a particular functional form with one overall free parameter. That parameter was varied in a global fit of high-energy experimental data. MRST obtained a very shallow minimum in fitting the high-energy data. At the 90% confidence level the free parameter κ multiplying this phenomenological form could range between −0.8 and +0.65, with a best-fit value $\kappa=-0.2$. MRST chose a functional form such that δu_v and δd_v were required to be equal and opposite. This ensured that the total momentum carried by valence quarks in the neutron and proton were equal (this quantity is reasonably well fixed by experiment). This choice by MRST agrees reasonably well with theoretical valence quark CSV PDFs obtained from quark models. In fact the best fit of MRST is in surprisingly good agreement with theoretical valence CSV parton distributions from Sather (1992) and Rodionov *et al.* (1994).

In Sec. III.B.1 we discussed an additional mechanism for charge-symmetry violation. This occurs when a quark radiates a photon, in analogy with the well-known case where a quark radiates a gluon. If one incorporates these photon radiation terms into the QCD evolution equations, these give rise to a new type of charge-symmetry violation. These "QED splitting" terms have been analyzed by two groups (Glück *et al.*, 2005; Martin *et al.*, 2005) with qualitatively similar results.

In Sec. III.C we reviewed experimental limits on parton charge symmetry. Parton charge-symmetry violation has never been directly observed. The strongest upper limits on parton CSV come from comparison of the F_2 structure functions obtained from charged lepton DIS with those extracted from charged-current DIS arising from neutrinos and antineutrinos, with both taken on isoscalar targets. We reviewed the upper limits that can be extracted by comparison of the NMC μ-D reactions (Amaudruz *et al.*, 1991, 1992; Arneodo *et al.*, 1997) with charged-current DIS for ν and $\bar{\nu}$ on Fe, from the CCFR (Seligman *et al.*, 1997) and NuTeV (Yang *et al.*, 2001) experiments. Comparison of these experiments requires a number of corrections, from absolute cross section normalizations to nuclear effects and shadowing corrections. However, the most thorough studies to date place upper limits of parton CSV at about the 6–10% level in the region $0.03\leqslant x\leqslant 0.4$.

The NuTeV group obtained an independent measurement of the weak mixing angle by measuring charged-current and neutral-current DIS for ν and $\bar{\nu}$ on an iron target (Zeller *et al.*, 2002a, 2002b). They obtained a value for $\sin^2\theta_W$ that differs by three standard deviations from the value obtained at the Z pole. In Sec. III.C.2 we reviewed this situation in detail. We reviewed possible contributions from a number of QCD effects on the NuTeV measurement. In particular, we showed that valence parton CSV effects had the possibility to make

substantial contributions to the NuTeV weak mixing angle measurement. At the 90% confidence level obtained in the MRST phenomenological fit, partonic CSV could completely remove the NuTeV anomaly or alternatively could make it twice as large. We showed that theoretical CSV effects predicted by quark models and obtained from QED splitting are likely to remove approximately one-half of the NuTeV anomaly in the weak mixing angle.

In Sec. III.D we discussed a new nuclear reaction mechanism. This concerns the differential effect of ρ exchange on protons and neutrons. Cloët *et al.* (2009) pointed out that this will produce effects that mimic those of CSV in a nucleus with $N>Z$. This *nuclear isospin-dependent* effect should produce a characteristic A dependence of the EMC effect; experiments have been proposed to look for evidence of this effect. It is estimated that this effect would account for roughly half of the NuTeV discrepancy in the weak mixing angle. If this effect is verified experimentally then the NuTeV result could be viewed as providing a dramatic confirmation of the modification of the partonic structure for bound nucleons.

From our discussion it appears that the combined effects of strange quarks, partonic charge-symmetry violation, and the nucleon isospin dependence of Cloët *et al.* (2009) should remove essentially all of the NuTeV anomaly in the weak mixing angle. Indeed, a recent theoretical reanalysis of the NuTeV result (Bentz *et al.*, 2009) showed that the assumption of reasonable values for these three quantities moves the NuTeV result onto the curve predicting the running of the effective weak mixing angle with Q^2 (i.e., the curve appearing in Fig. 14).

The current upper limits on partonic CSV for valence quarks are still reasonably large. Both the 90% confidence level of the MRST phenomenological fit and the best direct measurement from comparison of the F_2 structure functions for charged-lepton and charged-current DIS give upper limits on valence quark CSV of the order of a few percent. Medium- and high-energy facilities have now reached a precision where one could envision dedicated experiments that would either measure parton charge-symmetry violation or significantly reduce the upper limits on partonic CSV.

In Sec. III.E we discussed four such experiments. Since tests of parton charge symmetry require comparison of PDFs in the neutron and proton, all of these experiments require isoscalar targets. The first of these is a comparison of Drell-Yan cross sections for π^+ and π^- projectiles on a target such as deuterium. Studies in the valence region for both pion and nucleon have the possibility of revealing valence quark CSV effects. A second experiment would be parity-violating DIS in e-D reactions. Such an experiment is currently being planned at Jefferson Laboratory following the 12 GeV upgrade; it would have the potential to measure CSV effects if the PV asymmetry could be measured to roughly 1%.

A third experiment that might test parton charge symmetry is a comparison of π^+ and π^- electroproduction from deuterium. Sufficiently precise experiments also have the possibility of revealing CSV effects. Identification of CSV effects requires that factorization be valid to a few percent, so such experiments might be most reliably carried out at a future electron-ion collider. One final experiment would be a comparison of W^+ and W^- production from neutrino and antineutrino charged-current DIS on an isoscalar target. In all of these cases we have shown estimates of the magnitude of CSV effects expected in these reactions.

In Sec. IV we reviewed the situation regarding sea quark CSV effects. Theoretically, the situation for sea quark charge symmetry is not nearly as well founded as for valence quarks. In the valence region, sea quark contributions are quite small, whereas they are substantial at small x. It is difficult to disentangle heavy quark and CSV effects at small x. On rather general grounds one can argue that the magnitude of partonic CSV effects should be given by

$$\frac{\delta q}{q} \sim \frac{\delta m}{\langle M \rangle}. \tag{107}$$

In Eq. (107), the quantity δm would represent quark mass differences, in the range 1 to 5 MeV, and $\langle M \rangle$ denotes an effective mass of the system after removal of a quark. For valence quark CSV one would estimate $\langle M \rangle \sim 500$ MeV, or a typical diquark mass, while for sea quark CSV one would expect $\langle M \rangle \sim 1.3$ GeV, a typical mass for a three quark–one antiquark state. From this rather general argument one would expect that sea quark CSV effects should be significantly smaller than those for valence quark CSV.

In Sec. IV.A we discussed the phenomenological sea quark CSV studies by the MRST group (Martin *et al.*, 2004). They assumed a functional form for sea quark CSV with an overall free parameter which was varied in a global fit to high-energy data. Their best fit was obtained with a surprisingly large value, about 8%, for sea quark CSV. As mentioned, at small values of x sea quarks, gluons, and heavy quarks all contribute, making it difficult to isolate sea quark CSV effects.

Since sea quark and gluon distributions are connected through QCD evolution equations, sea quark CSV should in principle lead to charge-symmetry violation in gluon distributions. In Sec. IV.B.2 we reviewed possibilities for testing CSV in gluon distributions. A recent experiment measuring Υ production in pp and pD scattering could place upper limits on gluonic charge-symmetry violation (Zhu *et al.*, 2008).

In Sec. IV.C we reviewed one possibility to search for sea quark CSV, which is to look for contributions to DIS sum rules. Several of these sum rules involve the first moments of parton distributions. The valence CSV distributions and heavy quark "valence" distributions must give zero first moment in order to respect valence quark normalization. In some of these sum rules the only terms whose first moment survives are sea quark CSV contributions.

We showed that CSV contributions to the nucleon sea

have no effect on the Gross–Llewellyn Smith or Adler sum rules, but in principle they affect the Gottfried sum rule. The Gottfried sum rule has contributions both from asymmetries in the light quark sea [the fact that $\bar{d}(x) \neq \bar{u}(x)$] and from sea quark CSV. We also pointed out that the best experimental "test" of the Adler sum rule actually measures a somewhat different quantity, one that contains a nonzero contribution from sea quark CSV. The Adler sum rule measurement can thus be used to place an upper limit on parton sea quark CSV. Finally, we introduced a new sum rule, a charge-symmetry sum rule which would be zero if either the "strong form" or the "weak form" of charge symmetry holds. A test of this charge-symmetry sum rule would require measuring the structure functions for neutrino and antineutrino charged-current reactions on protons and deuterium, with particular attention to the small-x region. If one assumes the validity of the Adler sum rule then similar information could be obtained from measurements of either neutrinos or antineutrinos on an isoscalar target.

In conclusion, in recent years much progress has been made in precision measurements of structure functions. From these one can extract parton distribution functions which are now known to considerable accuracy. Recent experiments are now able to focus on specific questions such as the gluon distributions (both spin-independent and spin-dependent) and the flavor content of spin structure functions. We know that parton distributions should have small charge-symmetry-violating components. Recently, global fits of parton distributions have been carried out where one drops the assumption of charge symmetry. This gives indirect indications of the magnitude and shape of parton CSV. We also discussed a series of experiments that could in principle reveal charge-symmetry violation in parton distributions. Such experiments require great precision, coupled with an accurate knowledge of heavy quark distributions. However, we are optimistic that such experiments either can lower the upper limits on parton CSV or can find direct experimental evidence for parton charge-symmetry violation.

ACKNOWLEDGMENTS

Research by one of the authors (J.T.L.) was supported in part by the U.S. National Science Foundation under research Contracts No. NSF-PHY0555232 and No. PHY0854805. Research by one of the authors (A.W.T.) was supported by the Australian Research Council through an Australian Laureate Fellowship as well as by the U.S. Department of Energy under Contract No. DE-AC05-06OR23177, under which Jefferson Science Associates, LLC operates Jefferson Laboratory. Research by one of the authors (J.C.P.) was supported in part by the U.S. National Science Foundation under research Contract No. NSF-PHY0601067. The authors would like to acknowledge discussions with and contributions by C. Boros, W. Melnitchouk, G. A. Miller, and D. J. Murdock. One of the authors (J.T.L.) acknowledges several discussions with S. E. Vigdor regarding this review and also discussions with C. Benesh, S. Gottlieb, S. Kulagin, K. Kumar, E. J. Stephenson, and R. S. Thorne. One of the authors (A.W.T.) wishes to acknowledge discussions with W. Bentz and I. Cloët. One of the authors (J.C.P.) acknowledges discussions with G. T. Garvey and J. M. Moss.

REFERENCES

Abazov, V. M., *et al.* (D0), 2008a, Phys. Rev. Lett. **101**, 211801.
Abazov, V. M., *et al.* (D0), 2008b, Phys. Rev. D **77**, 011106.
Abbaneo, D., *et al.* (ALEPH), 2001, e-print arXiv:hep-ex/0112021.
Abe, F., *et al.* (CDF), 1998, Phys. Rev. Lett. **81**, 5742.
Ackerstaff, K., *et al.* (HERMES), 1998, Phys. Rev. Lett. **81**, 5519.
Acosta, D. E., *et al.* (CDF), 2005, Phys. Rev. D **71**, 051104.
Adler, S. L., 1966, Phys. Rev. **143**, 1144.
Adloff, C., *et al.* (H1), 2003, Eur. Phys. J. C **30**, 1.
Aivazis, M. A. G., J. C. Collins, F. I. Olness, and W.-K. Tung, 1994, Phys. Rev. D **50**, 3102.
Aivazis, M. A. G., F. I. Olness, and W.-K. Tung, 1994, Phys. Rev. D **50**, 3085.
Allasia, D., *et al.* (WA25), 1984, Phys. Lett. **135B**, 231.
Allasia, D., *et al.*, 1985, Z. Phys. C **28**, 321.
Altarelli, G., and G. Parisi, 1977, Nucl. Phys. B **126**, 298.
Amaudruz, P., *et al.* (New Muon), 1991, Phys. Rev. Lett. **66**, 2712.
Amaudruz, P., *et al.* (New Muon), 1992, Phys. Lett. B **295**, 159.
Amsler, C., *et al.* (Particle Data Group), 2008, Phys. Lett. B **667**, 1.
Anderson, K. J., *et al.*, 1979, Phys. Rev. Lett. **42**, 944.
Anthony, P. L., *et al.* (SLAC E158), 2005, Phys. Rev. Lett. **95**, 081601.
Arneodo, M., *et al.* (New Muon), 1994, Phys. Rev. D **50**, R1.
Arneodo, M., *et al.* (New Muon), 1997, Nucl. Phys. B **483**, 3.
Arrington, J., *et al.*, 2009, letter of intent to Jefferson Laboratory for e-D parity-violating DIS experiment, Hall C at 11 GeV, unpublished.
Ashman, J., *et al.* (European Muon), 1988, Phys. Lett. B **206**, 364.
Ashman, J., *et al.* (European Muon), 1989, Nucl. Phys. B **328**, 1.
Baldit, A., *et al.* (NA51), 1994, Phys. Lett. B **332**, 244.
Bardin, D. Y., and V. A. Dokuchaeva, 1984, Nucl. Phys. B **246**, 221.
Barnett, R. M., 1976, Phys. Rev. D **14**, 70.
Bazarko, A. O., *et al.* (CCFR), 1995, Z. Phys. C **65**, 189.
Benesh, C. J., and J. T. Goldman, 1997, Phys. Rev. C **55**, 441.
Benesh, C. J., and J. T. Londergan, 1998, Phys. Rev. C **58**, 1218.
Bennett, S. C., and C. E. Wieman, 1999, Phys. Rev. Lett. **82**, 2484.
Bentz, W., I. C. Cloët, J. T. Londergan, and A. W. Thomas, 2009, e-print arXiv:0908.3198.
Benvenuti, A. C., *et al.* (BCDMS), 1987, Phys. Lett. B **195**, 91.
Benvenuti, A. C., *et al.* (BCDMS), 1990, Phys. Lett. B **237**, 592.
Berge, J. P., *et al.*, 1987, Z. Phys. C **35**, 443.
Bergsma, F., *et al.* (CHARM), 1983, Phys. Lett. **123B**, 269.
Bernstein, R., 2009, private communication.
Betev, B., *et al.* (NA10), 1985, Z. Phys. C **28**, 9.
Bethe, H., and E. E. Salpeter, 1957, *Quantum Mechanics of One- and Two-Electron Atoms* (Academic, New York).
Bickerstaff, R. P., and A. W. Thomas, 1982, Phys. Rev. D **25**, 1869.

Bickerstaff, R. P., and A. W. Thomas, 1989, J. Phys. G **15**, 1523.
Blair, R., *et al.*, 1983, Phys. Rev. Lett. **51**, 343.
Blum, T., T. Doi, M. Hayakawa, T. Izubuchi, and N. Yamada, 2007, Phys. Rev. D **76**, 114508.
Bodek, A., Q. Fan, M. Lancaster, K. S. McFarland, and U.-K. Yang, 1999, Phys. Rev. Lett. **83**, 2892.
Bodek, A., and J. L. Ritchie, 1981, Phys. Rev. D **23**, 1070.
Boros, C., J. T. Londergan, and A. W. Thomas, 1998a, Phys. Rev. Lett. **81**, 4075.
Boros, C., J. T. Londergan, and A. W. Thomas, 1998b, Phys. Rev. D **58**, 114030.
Boros, C., J. T. Londergan, and A. W. Thomas, 1999, Phys. Rev. D **59**, 074021.
Boros, C., F. M. Steffens, J. T. Londergan, and A. W. Thomas, 1999, Phys. Lett. B **468**, 161.
Botje, M., 2000, Eur. Phys. J. C **14**, 285.
Bradamante, F. (COMPASS), 2008, AIP Conf. Proc. **1056**, 436.
Braun, V. M., and A. V. Kolesnichenko, 1987, Nucl. Phys. B **283**, 723.
Brodsky, S. J., and B.-Q. Ma, 1996, Phys. Lett. B **381**, 317.
Brodsky, S. J., I. Schmidt, and J.-J. Yang, 2004, Phys. Rev. D **70**, 116003.
Cabibbo, N., 1963, Phys. Rev. Lett. **10**, 531.
Cao, F.-G., and A. I. Signal, 2000, Phys. Rev. C **62**, 015203.
Cloët, I. C., W. Bentz, and A. W. Thomas, 2005, Phys. Rev. Lett. **95**, 052302.
Cloët, I. C., W. Bentz, and A. W. Thomas, 2006, Phys. Lett. B **642**, 210.
Cloët, I. C., W. Bentz, and A. W. Thomas, 2009, Phys. Rev. Lett. **102**, 252301.
Close, F. E., and A. W. Thomas, 1988, Phys. Lett. B **212**, 227.
Conrad, J. M., M. H. Shaevitz, and T. Bolton, 1998, Rev. Mod. Phys. **70**, 1341.
Conway, J. S., *et al.*, 1989, Phys. Rev. D **39**, 92.
Corden, M., *et al.*, 1980, Phys. Lett. **96B**, 417.
Czarnecki, A., and W. J. Marciano, 1996, Phys. Rev. D **53**, 1066.
Czarnecki, A., and W. J. Marciano, 2000, Int. J. Mod. Phys. A **15**, 2365.
Dasu, S., *et al.*, 1988, Phys. Rev. Lett. **61**, 1061.
Davidson, R. M., and M. Burkardt, 1997, Phys. Lett. B **403**, 134.
Davidson, S., S. Forte, P. Gambino, N. Rius, and A. Strumia, 2002, J. High Energy Phys. **02**, 037.
de Groot, J. G. H., *et al.*, 1979, Phys. Lett. **82B**, 292.
Diener, K. P. O., S. Dittmaier, and W. Hollik, 2004, Phys. Rev. D **69**, 073005.
Diener, K. P. O., S. Dittmaier, and W. Hollik, 2005, Phys. Rev. D **72**, 093002.
Dokshitzer, Y. L., 1977, Sov. Phys. JETP **46**, 641.
Drell, S. D., and T.-M. Yan, 1970, Phys. Rev. Lett. **25**, 316.
Drell, S. D., and T.-M. Yan, 1971, Ann. Phys. (Paris) **66**, 578.
Ellis, S. D., and W. J. Stirling, 1991, Phys. Lett. B **256**, 258.
Ericson, M., and A. W. Thomas, 1984, Phys. Lett. **148B**, 191.
Erler, J., and M. J. Ramsey-Musolf, 2005, Phys. Rev. D **72**, 073003.
Foudas, C., *et al.*, 1990, Phys. Rev. Lett. **64**, 1207.
Frankfurt, L. L., and M. I. Strikman, 1978, Phys. Lett. **76B**, 333.
Frankfurt, L. L., and M. I. Strikman, 1981, Phys. Rep. **76**, 215.
Frankfurt, L. L., and M. I. Strikman, 1988, Phys. Rep. **160**, 235.
Frankfurt, L. L., *et al.*, 1989, Phys. Lett. B **230**, 141.
Garvey, G. T., and J.-C. Peng, 2001, Prog. Part. Nucl. Phys. **47**, 203.
Geesaman, D. F., K. Saito, and A. W. Thomas, 1995, Annu. Rev. Nucl. Part. Sci. **45**, 337.
Georgi, H., and H. D. Politzer, 1976, Phys. Rev. D **14**, 1829.
Glück, M., P. Jimenez-Delgado, and E. Reya, 2005, Phys. Rev. Lett. **95**, 022002.
Glück, M., S. Kretzer, and E. Reya, 1996, Phys. Lett. B **380**, 171.
Glück, M., E. Reya, and A. Vogt, 1995, Z. Phys. C **67**, 433.
Glück, M., E. Reya, and A. Vogt, 1998, Eur. Phys. J. C **5**, 461.
Goncharov, M., *et al.* (NuTeV), 2001, Phys. Rev. D **64**, 112006.
Gottfried, K., 1967, Phys. Rev. Lett. **18**, 1174.
Gribov, V. N., and L. N. Lipatov, 1972, Sov. J. Nucl. Phys. **15**, 438.
Gross, D. J., and C. H. Llewellyn Smith, 1969, Nucl. Phys. B **14**, 337.
Harris, D. A., *et al.* (CCFR-NUTEV), 1995, e-print arXiv:hep-ex/9506010.
Hawker, E. A., *et al.* (FNAL E866/NuSea), 1998, Phys. Rev. Lett. **80**, 3715.
Henley, E., and G. A. Miller, 1979, in *Mesons in Nuclei*, edited by M. Rho and D. Wilkinson (North-Holland, Amsterdam), p. 116.
Henley, E. M., and G. A. Miller, 1990, Phys. Lett. B **251**, 453.
Hinchliffe, I., and A. Kwiatkowski, 1996, Annu. Rev. Nucl. Part. Sci. **46**, 609.
Hirai, M., S. Kumano, and T. H. Nagai, 2004, Phys. Rev. C **70**, 044905.
Hirai, M., S. Kumano, and T. H. Nagai, 2005, Phys. Rev. D **71**, 113007.
Hobbs, T., and W. Melnitchouk, 2008, Phys. Rev. D **77**, 114023.
Holtmann, H., A. Szczurek, and J. Speth, 1996, Nucl. Phys. A **596**, 631.
Jaffe, R. L., 1983, Nucl. Phys. B **229**, 205.
Ji, X.-D., and J. Tang, 1995, Phys. Lett. B **362**, 182.
Kobayashi, M., and T. Maskawa, 1973, Prog. Theor. Phys. **49**, 652.
Kovalenko, S., I. Schmidt, and J.-J. Yang, 2002, Phys. Lett. B **546**, 68.
Kretzer, S., *et al.*, 2004, Phys. Rev. Lett. **93**, 041802.
Kulagin, S. A., and R. Petti, 2006, Nucl. Phys. A **765**, 126.
Kulagin, S. A., and R. Petti, 2007a, Phys. Rev. D **76**, 094023.
Kulagin, S. A., and R. Petti, 2007b, AIP Conf. Proc. **967**, 94.
Kumano, S., 1998, Phys. Rep. **303**, 183.
Kumano, S., 2002, Phys. Rev. D **66**, 111301.
Lai, H. L., *et al.*, 1997, Phys. Rev. D **55**, 1280.
Lai, H. L., *et al.* (CTEQ), 2000, Eur. Phys. J. C **12**, 375.
Larin, S. A., and J. A. M. Vermaseren, 1991, Phys. Lett. B **259**, 345.
Leader, E., and E. Predazzi, 1996, *An Introduction to Gauge Theories and Modern Particle Physics* (Cambridge University Press, Cambridge).
Leung, W. C., *et al.*, 1993, Phys. Lett. B **317**, 655.
Levelt, J., P. J. Mulders, and A. W. Schreiber, 1991, Phys. Lett. B **263**, 498.
Londergan, J. T., 2005, AIP Conf. Proc. **747**, 205.
Londergan, J. T., S. A. Braendler, and A. W. Thomas, 1998, Phys. Lett. B **424**, 185.
Londergan, J. T., G. T. Carvey, G. Q. Liu, E. N. Rodionov, and A. W. Thomas, 1994, Phys. Lett. B **340**, 115.
Londergan, J. T., G. Q. Liu, E. N. Rodionov, and A. W. Thomas, 1995, Phys. Lett. B **361**, 110.
Londergan, J. T., D. P. Murdock, and A. W. Thomas, 2005,

Phys. Rev. D **72**, 036010.
Londergan, J. T., D. P. Murdock, and A. W. Thomas, 2006, Phys. Rev. D **73**, 076004.
Londergan, J. T., A. Pang, and A. W. Thomas, 1996, Phys. Rev. D **54**, 3154.
Londergan, J. T., and A. W. Thomas, 1998, Prog. Part. Nucl. Phys. **41**, 49.
Londergan, J. T., and A. W. Thomas, 2003a, Phys. Lett. B **558**, 132.
Londergan, J. T., and A. W. Thomas, 2003b, Phys. Rev. D **67**, 111901.
Ma, B.-Q., 1992, Phys. Lett. B **274**, 111.
Ma, B.-Q., A. Schafer, and W. Greiner, 1993, Phys. Rev. D **47**, 51.
Macfarlane, D. B., *et al.* (CCFRR), 1984, Z. Phys. C **26**, 1.
Martin, A. D., R. G. Roberts, W. J. Stirling, and R. S. Thorne, 1998, Phys. Lett. B **443**, 301.
Martin, A. D., R. G. Roberts, W. J. Stirling, and R. S. Thorne, 2002, Eur. Phys. J. C **23**, 73.
Martin, A. D., R. G. Roberts, W. J. Stirling, and R. S. Thorne, 2004, Eur. Phys. J. C **35**, 325.
Martin, A. D., R. G. Roberts, W. J. Stirling, and R. S. Thorne, 2005, Eur. Phys. J. C **39**, 155.
Martin, A. D., W. J. Stirling, and R. G. Roberts, 1990, Phys. Lett. B **252**, 653.
Martin, A. D., W. J. Stirling, R. S. Thorne, and G. Watt, 2007, Phys. Lett. B **652**, 292.
Mason, D., *et al.*, 2007, Phys. Rev. Lett. **99**, 192001.
Melnitchouk, W., and M. Malheiro, 1997, Phys. Rev. C **55**, 431.
Melnitchouk, W., and J. C. Peng, 1997, Phys. Lett. B **400**, 220.
Melnitchouk, W., A. W. Schreiber, and A. W. Thomas, 1994a, Phys. Rev. D **49**, 1183.
Melnitchouk, W., A. W. Schreiber, and A. W. Thomas, 1994b, Phys. Lett. B **335**, 11.
Melnitchouk, W., and A. W. Thomas, 1993, Phys. Rev. D **47**, 3783.
Melnitchouk, W., and A. W. Thomas, 1996, Phys. Lett. B **377**, 11.
Meyers, P. D., *et al.*, 1986, Phys. Rev. D **34**, 1265.
Miller, G. A., B. M. K. Nefkens, and I. Slaus, 1990, Phys. Rep. **194**, 1.
Miller, G. A., A. K. Opper, and E. J. Stephenson, 2006, Annu. Rev. Nucl. Part. Sci. **56**, 253.
Miller, G. A., and A. W. Thomas, 2005, Int. J. Mod. Phys. A **20**, 95.
Mishra, S. R., 1990, *Proceedings of Workshop on Hadron Structure Functions and Parton Distributions* (World Scientific, Singapore), p. 84.
Mishra, S. R., and F. Sciulli, 1989, Annu. Rev. Nucl. Part. Sci. **39**, 259.
Moreno, G., *et al.*, 1991, Phys. Rev. D **43**, 2815.
Navasardyan, T., *et al.*, 2007, Phys. Rev. Lett. **98**, 022001.
Niskanen, J. A., 1999, Few-Body Syst. **26**, 241.
Oltman, E., *et al.*, 1992, Z. Phys. C **53**, 51.
Opper, A. K., 2008, Few-Body Syst. **44**, 23.
Opper, A. K., *et al.*, 2003, Phys. Rev. Lett. **91**, 212302.
Paschos, E. A., and L. Wolfenstein, 1973, Phys. Rev. D **7**, 91.
Peng, J. C., and D. M. Jansen, 1995, Phys. Lett. B **354**, 460.
Peng, J. C., *et al.* (E866/NuSea), 1998, Phys. Rev. D **58**, 092004.
Piller, G., and A. W. Thomas, 1996, Z. Phys. C **70**, 661.
Porsev, S. G., K. Beloy, and A. Derevianko, 2009, Phys. Rev. Lett. **102**, 181601.
Prescott, C. Y., *et al.*, 1978, Phys. Lett. **77B**, 347.
Pumplin, J., *et al.*, 2002, J. High Energy Phys. **07**, 012.
Rabinowitz, S. A., *et al.*, 1993, Phys. Rev. Lett. **70**, 134.
Reimer, P. E., 2007, Eur. Phys. J. A **31**, 593.
Rodionov, E. N., A. W. Thomas, and J. T. Londergan, 1994, Mod. Phys. Lett. A **9**, 1799.
Ross, D. A., and C. T. Sachrajda, 1979, Nucl. Phys. B **149**, 497.
Saito, K., A. Michels, and A. W. Thomas, 1992, Phys. Rev. C **46**, R2149.
Sather, E., 1992, Phys. Lett. B **274**, 433.
Schael, P., *et al.* (ALEPH), 2006, Phys. Rep. **427**, 257.
Schreiber, A. W., A. I. Signal, and A. W. Thomas, 1991, Phys. Rev. D **44**, 2653.
Seligman, W. G., 1997, Ph.D. thesis (Columbia University).
Seligman, W. G., *et al.*, 1992, *Particles and Fields 92: Seventh Meeting of the Division of Particles Fields of the APS (DPF 92)* (Fermilab, Chicago).
Seligman, W. G., *et al.*, 1997, Phys. Rev. Lett. **79**, 1213.
Signal, A. I., and A. W. Thomas, 1987, Phys. Lett. B **191**, 205.
Signal, A. I., and A. W. Thomas, 1989, Phys. Rev. D **40**, 2832.
Souder, P., 2008, *Proceedings of the 16th International Workshop on Deep Inelastic Scattering and Related Subjects (DIS 2008)* (Sciencewise, London).
Speth, J., and A. W. Thomas, 1997, Adv. Nucl. Phys. **24**, 83.
Stephenson, E. J., *et al.*, 2003, Phys. Rev. Lett. **91**, 142302.
Sterman, G., *et al.* (CTEQ), 1995, Rev. Mod. Phys. **67**, 157.
Sutton, P. J., A. D. Martin, R. G. Roberts, and W. J. Stirling, 1992, Phys. Rev. D **45**, 2349.
Thomas, A. W., 1983, Phys. Lett. **126B**, 97.
Thorne, R., 2008, private communication.
Thorne, R. S., and R. G. Roberts, 1998, Phys. Lett. B **421**, 303.
Towell, R. S., *et al.* (FNAL E866/NuSea), 2001, Phys. Rev. D **64**, 052002.
Tung, W. K., *et al.*, 2007, J. High Energy Phys. **02**, 053.
van der Steenhoven, G., 1996a, NIKHEF Report No. nIKHEF-96-026.
van der Steenhoven, G., 1996b, *Workshop on Future Physics at HERA* (DESY, Hamburg).
van Kolck, U., J. A. Niskanen, and G. A. Miller, 2000, Phys. Lett. B **493**, 65.
Whitlow, L. W., E. M. Riordan, S. Dasu, S. Rock, and A. Bodek, 1992, Phys. Lett. B **282**, 475.
Whitlow, L. W., S. Rock, A. Bodek, E. M. Riordan, and S. Dasu, 1990, Phys. Lett. B **250**, 193.
Yang, U.-K., *et al.* (CCFR/NuTeV), 2001, Phys. Rev. Lett. **86**, 2742.
Young, R. D., R. D. Carlini, A. W. Thomas, and J. Roche, 2007, Phys. Rev. Lett. **99**, 122003.
Zeller, G. P., *et al.* (NuTeV), 2002a, Phys. Rev. Lett. **88**, 091802.
Zeller, G. P., *et al.* (NuTeV), 2002b, Phys. Rev. D **65**, 111103.
Zhu, L. Y., *et al.* (FNAL E866/NuSea), 2008, Phys. Rev. Lett. **100**, 062301.